

# Characterisation of Regional Fluxes of Methane in the Surat Basin, Queensland

Phase 2: A pilot study of methodology to detect and quantify methane sources

Stuart Day, Cindy Ong, Andrew Rodger, David Etheridge, Mark Hibberd, Eva van Gorsel, Darren Spencer, Paul Krummel, Steve Zegelin, Robyn Fry, Mark Dell'Amico, Stephen Sestak, David Williams, Zoë Loh and Damian Barrett

EP 15369

May 2015

Report for the Gas Industry Social and Environmental Research Alliance (GISERA), Project No GAS1315

## Citation

Stuart Day, Cindy Ong, Andrew Rodger, David Etheridge, Mark Hibberd, Eva van Gorsel, Darren Spencer, Paul Krummel, Robyn Fry, Mark Dell'Amico, Stephen Sestak, David Williams, Zoë Loh and Damian Barrett (2015) Characterisation of regional fluxes of methane in the Surat Basin, Queensland: Phase 2: A pilot study of methodology to detect and quantify methane sources. CSIRO, Australia.

## Copyright and disclaimer

© 2015 CSIRO To the extent permitted by law, all rights are reserved and no part of this publication covered by copyright may be reproduced or copied in any form or by any means except with the written permission of CSIRO.

## Important disclaimer

CSIRO advises that the information contained in this publication comprises general statements based on scientific research. The reader is advised and needs to be aware that such information may be incomplete or unable to be used in any specific situation. No reliance or actions must therefore be made on that information without seeking prior expert professional, scientific and technical advice. To the extent permitted by law, CSIRO (including its employees and consultants) excludes all liability to any person for any consequences, including but not limited to all losses, damages, costs, expenses and any other compensation, arising directly or indirectly from using this publication (in part or in whole) and any information or material contained in it.

# Contents

Acknowledgments .....	ii
Executive Summary.....	iii
1 Introduction.....	1
2 Preferred Methodologies .....	3
2.1 Ground Surveys.....	5
2.2 Flux Chambers .....	6
2.3 Remote Sensing .....	7
2.4 Top-Down Atmospheric Monitoring .....	8
2.5 Gas Geochemistry .....	8
3 Ground Surveys .....	11
3.1 Experimental Methods.....	11
3.2 Results.....	14
4 SCIAMACHY Satellite .....	35
4.1 Instrumentation.....	35
4.2 Methane Retrieval Algorithms and Data Used for Analysis.....	35
4.3 Additional Data Analysis.....	36
4.4 Results from SCIAMACHY Data Analysis .....	36
5 ALMA G2 Airborne Survey .....	41
5.1 Instrumentation.....	41
5.2 Experimental Design.....	41
5.3 Results.....	42
6 Fixed Monitoring Network.....	45
6.1 Site Selection for Monitoring Stations .....	45
6.2 Simulated Concentration Signals.....	46
6.3 Installation of Ironbark Greenhouse Gas Monitoring Facility.....	55
7 Discussion .....	62
8 Future Work.....	67
References .....	69
Appendix.....	76

# Acknowledgments

This project is supported by the Gas Industry Social and Environmental Research Alliance (GISERA). GISERA undertakes publicly-reported independent research that addresses the socioeconomic and environmental impacts of Australia's natural gas industries. For further information visit [www.gisera.org.au](http://www.gisera.org.au).

The SCIAMACHY WFM-DOAS methane data products were produced by the Institute for Environmental Physics, University of Bremen and the IMAP-DOAS methane data products were produced by the Space Research Organization Netherlands (SRON) and Jet Propulsion Laboratory (JPL), NASA. We thank these institutions for providing access to these data.

UNSW Australia (Associate Professor Bryce Kelly and Charlotte Iverach) and Royal Holloway, University of London (Dr Dave Lowry, Dr Rebecca Fisher, Dr James France and Professor Euan Nisbet), are acknowledged for coordinating and participating in some of the near surface atmospheric methane surveys around Dalby, Cecil Plains, the Broadwater CSG developments and cattle feedlots discussed in Section 3. These surveys were undertaken in March 2014. UNSW Australia and Royal Holloway, University of London were funded by the Cotton Research and Development Corporation, and the National Centre for Groundwater Research and Training.

We are also grateful several landholders in the region who provided access to their properties where some measurements were made. Various personnel from gas companies provided information and valuable information and helpful discussions throughout the project. In particular, we thank Brad Pinder of Arrow Energy for providing a detailed geological map of the study region and Matt Kernke for facilitating access to the Origin Energy property where the first of the fixed monitoring station is located.

Finally, we thank the reviewers of this report for their valuable feedback and constructive comments.

# Executive Summary

The Surat Basin is one of Australia's largest coal seam gas regions and currently supplies a large proportion of Queensland's domestic gas requirements. Gas production is set to increase significantly over the coming years as several liquefied natural gas facilities under construction near Gladstone come on line. To assess the greenhouse impact of the CSG industry, it is important to understand the level of fugitive emissions of CH<sub>4</sub> from gas production and processing. However, it is also necessary to account for other sources of methane (CH<sub>4</sub>) contributing to overall regional emissions. The Surat Basin, like many other sedimentary basins, is known for seeps of CH<sub>4</sub> and other hydrocarbons and these along with other sources such as agriculture, must be determined before a proper assessment of CSG related emissions can be made. Methane emissions from these seeps are very small and pose no health concern to humans but measuring their concentration is important for locating sources and hence emission rates of methane from these seeps into the atmosphere.

At present there is relatively little quantitative CH<sub>4</sub> emission data for the Surat Basin. Hence the purpose of the project reported here, which was undertaken as part of the Gas Industry Social and Environmental Alliance (GISERA), was to develop appropriate methodology to characterise CH<sub>4</sub> emissions within the Surat Basin and to commence a programme to establish background CH<sub>4</sub> concentrations and emission rates (fluxes) and their changes over time in the region. In this report, we present the results of the pilot study aimed at developing and refining the different methods for measuring methane seeps. Implicit in this aim is to determine methane emissions from all contributors, including ground seeps, CSG operations and agriculture, which will ultimately allow the scale of emissions from CSG production to be placed into perspective.

The project was designed to be conducted in three phases:

- Phase 1 – a literature review of existing methods for detecting and quantifying natural CH<sub>4</sub> seeps. This phase of the project was completed in December 2013 (Day et al., 2013).
- Phase 2 – field trials of suitable methodology identified during Phase 1 at selected locations within the Surat Basin.
- Phase 3 – deployment of suitable atmospheric monitoring and other systems, based on the results of Phase 2 to conduct long-term monitoring of emissions at sites in the Surat Basin.

Present in this report are the findings of Phase 2 where several methods for detecting CH<sub>4</sub> emission sources and estimating the emission rates were examined during field trials conducted within the Surat Basin. It is important to note that Phase 2 was about proving different methods for detecting and quantifying emission rates. Consequently, this report does not provide detailed emissions estimates for the region; Phase 3, which will be conducted over a three-year period, is aimed at providing quantitative regional baseline data for the Surat.

One of the key methods identified during Phase 1 for locating CH<sub>4</sub> sources was mobile surveys, where a vehicle equipped with a suitable CH<sub>4</sub> analyser is driven throughout the study area to detect elevated concentrations of ambient CH<sub>4</sub>. This method was used extensively throughout Phase 2, covering more than 7,000 km on public and private roads. A large number of CH<sub>4</sub> sources, both anthropogenic and natural, were located and identified. These included agricultural sources (especially cattle and intensive feedlots), CSG infrastructure, wetlands, biomass burning and abandoned boreholes.

Although mobile surveys are effective at locating many sources, the primary limitations of the technique are that surveys are mostly confined to formed roads thus limiting the area that can be covered, and only provide snapshots in time rather than continuous monitoring. Moreover, the surveys must be made downwind of sources. Surveys provide concentration data that by themselves do not indicate the CH<sub>4</sub> emission flux from the source. In some circumstances, emissions fluxes may be estimated by combining the measured concentration in the downwind CH<sub>4</sub> plume with meteorological data and plume dispersion

methods. However, this is not always possible and uncertainties associated with flux estimates made with ground based traverses may be high.

Surface flux chambers are suitable for directly measuring emission rates from many ground surfaces, although this approach is really only suited to characterising sources over relatively small areas; it is unlikely that surface flux chambers could be used for high resolution surveys at regional scales. During this study, the method was applied to measure emissions rates from numerous natural surfaces and abandoned coal exploration boreholes.

During Phase 2, the feasibility of using remote sensing systems to detect CH<sub>4</sub> emissions was investigated. In one approach, historical data from the satellite-based SCanning Imaging Absorption spectroMeter for Atmospheric CHartographY (SCIAMACHY) sensor with a spatial resolution of 30 km (along track) by 60 km (across track) were analysed to detect any change in average CH<sub>4</sub> concentrations within the Surat Basin compared with the rest of Australia. The data examined spanned the years 2003 to 2009, which includes a period of early growth in CSG production in the Surat Basin. The present analysis of the data indicated that the satellite-derived average atmospheric CH<sub>4</sub> concentration trends across the Surat Basin during this period were similar to those across the rest of Australia. However, it must be noted that there are uncertainties attached to this approach that require further investigation to allow quantitative use of these data. Data from the SCIAMACHY sensor are no longer available but if it is important to track regional scale trends and impacts after the establishment of the CSG industry, it may be useful to acquire longer term data of this nature from other satellite atmospheric sounding missions, such as ACE-FTS, GOSAT, AIRS, TROPOMI and IASI.

The spatial resolution of current satellite sensors is generally too coarse to be able to identify localised emission sources so an airborne system with much higher resolution was used to assess its suitability for locating CH<sub>4</sub> seeps. The system trialled was the Airborne Laser Methane Assessment Generation 2 (ALMA G2), developed by Pergam, which uses a diode laser sensor. This system, which has only recently become available in Australia, was developed for pipeline inspection applications and has not previously been used for determining atmospheric CH<sub>4</sub> concentrations from other sources.

The ALMA G2 system was found to have sufficient sensitivity to locate many CH<sub>4</sub> sources previously located by ground surveys. However, because of the narrow swath of the instrument, detailed surveys require many passes of the aircraft to adequately cover the survey area. Moreover, airborne surveys with the ALMA G2 must be made at low altitude (< 50 m) and at low speed so the system is not suited to rapidly surveying at the regional scale. The system may have applications to efficient surveying of smaller areas or monitoring emissions from infrastructure. During the proposed Phase 3 of this research programme, consideration will be given to conducting a field trial of an imaging FTIR system that may be better suited to rapid landscape surveys and monitoring of terrestrial seeps.

The third component of work in Phase 2 was the assessment of 'top-down' atmospheric background monitoring of CH<sub>4</sub> emissions in the Surat Basin. Preliminary modelling and site visits have identified two sites for the location of the fixed monitoring stations required for this work. The selection of monitoring site locations was based on the following criteria. (1) To allow measurement of CH<sub>4</sub> concentrations of both the background (air arriving at the Surat Basin) and the signal resulting from the CSG source emissions (total CH<sub>4</sub> concentration minus background). (2) To optimise the size and frequency of concentration signals from the broader CSG source area without being overly influenced by individual sources close to the measurement site. (3) To differentiate as much as possible the emissions from non-CSG sources such as livestock, power stations, coal mines, vehicles, biomass burning and cities from CSG sources. (4) To take into account characteristics such as land cover and topography. (5) Practical considerations such as access, power and security. (6) Potential assistance by land owners and/or operators. (7) Future gas development possibilities which could affect the site. (8) Characteristic emission rates of sources found by other tasks.

The first of these stations is now established and operating at an Origin Energy property, Ironbark, which is approximately 57 km southwest of Chinchilla. A second site to the northeast of Chinchilla has been identified and the monitoring equipment is soon to be installed. Measurements of CH<sub>4</sub> and CO<sub>2</sub> concentration commenced at the Ironbark site during November 2014 and early results and model simulations suggest that the Ironbark facility, combined with the proposed Site #2 facility to the north, will

be well suited to monitoring potential emissions from CSG activities in their present state and as they are projected to grow. The combined concentration, meteorology and turbulence data will be used as input to test the ability of inverse modelling to infer sources across the CSG area in the proposed next phase of the project, which aims to develop a viable background CH<sub>4</sub> monitoring system for the Surat Basin.

### ***Key Findings Summary***

- Mobile ground surveys using a vehicle equipped with a CH<sub>4</sub> analyser to measure ambient CH<sub>4</sub> concentration are effective for detecting many emission sources. However, the main limitation is that surveys are only possible in areas with vehicle access. Remote sensing methods, especially using airborne sensors, may provide a rapid method for conducting landscape surveys, especially in areas inaccessible to vehicles. At present, however, there are limited airborne systems available in Australia and further work is required to demonstrate this approach.
- Ground surveys made between Dalby and Roma over about an 18-month period showed that ambient CH<sub>4</sub> concentrations in the region were generally consistent with normal seasonal background concentrations, averaging between about 1.75 to 1.80 ppm CH<sub>4</sub> (dry basis). However, there were many instances where elevated levels of CH<sub>4</sub> were detected. The peak concentration perturbations in these regions ranged from less than 20 parts per billion (ppb) to almost 20 parts per million (ppm) or more than 10 times background levels. The sources of these CH<sub>4</sub> peaks were identified as CSG infrastructure, agricultural activities, natural biogenic sources and ground seeps.
- While ground surveys and some remote sensing systems can detect even low level emissions, the concentration data produced are not necessarily indicative of the rate of CH<sub>4</sub> emission from a particular source. Concentration is highly dependent upon prevailing atmospheric conditions and can vary significantly throughout the day. In some cases, emission rates may be estimated from concentration measurements using plume dispersion methods combined with local meteorological data. This approach, however, requires suitable atmospheric conditions and access to the plume. The uncertainty of these estimates may also be significant, especially when ground level concentration measurements are made a long way downwind of the source.
- One of the most versatile and accurate methods for measuring CH<sub>4</sub> emission rates from ground sources is by static surface flux chambers. This method has high sensitivity and can reliably measure even low fluxes encountered in natural systems but also has the capacity to measure high flux rates. By making a series of closely spaced flux measurements on surfaces emitting CH<sub>4</sub> the spatial distribution of the emission source can be accurately mapped. In contrast to ambient concentration measurements, surface flux chambers yield emission flux data for ground sources. However, this technique requires a relatively large number of individual measurements, which may be time consuming and labour-intensive. Consequently, the method is generally suited to assessing localised sources rather than landscape scale surveys.
- A number of abandoned or 'legacy' boreholes were found to be leaking CH<sub>4</sub>. The leakage rate from some of these boreholes was significant (~100 L min<sup>-1</sup>), while for others the rate was very low. It was also apparent that there are other abandoned boreholes that do not emit CH<sub>4</sub>. It is unlikely that the small sample of boreholes identified during Phase 2 is representative of all legacy boreholes; a detailed investigation is required to determine the extent to which they are contributing to the regional CH<sub>4</sub> budget.
- One of the leaking abandoned boreholes located during the project was partially filled with concrete to mitigate gas emissions. While this reduced any safety hazard associated with an open borehole, CH<sub>4</sub> continued to be emitted via diffusion through the soil around the concrete plug, although at a considerably reduced rate.
- Top-down atmospheric monitoring using fixed stations to measure ambient CH<sub>4</sub> concentration and local meteorological data coupled with a suitable inverse model is being trialled to provide near continuous emission flux data at the regional scale. Initial results from a station located south west of Chinchilla confirm that the system has sufficient sensitivity to detect emissions from CSG operations approximately 30 km from the station and preliminary model simulations suggest that the technique has considerable promise. One of the main challenges with the top-down approach

will be discriminating between the numerous CH<sub>4</sub> sources that contribute to overall emissions within the monitoring region.



# 1 Introduction

CSIRO through the Gas Industry Social and Environmental Research Alliance (GISERA) is currently conducting a study to characterise regional methane emissions within the Surat Basin in Queensland. The overall aim of this study is to develop a better understanding of non-anthropogenic methane sources, or methane seeps, that occur as a result of natural connectivity between coal seams and coal bearing aquifers and the atmosphere. Although the primary focus is on methane seeps, other sources of non-CSG methane emissions are also being considered since these contribute to the overall greenhouse gas budget of the region. Moreover, a detailed understanding of all sources is essential for the development of an accurate baseline greenhouse gas emissions inventory.

This project is designed to operate over a number of years and is divided into three separate phases as detailed below.

- Phase 1: The purpose of this phase was to assess the applicability of various methodologies for detecting and quantifying methane emissions from seeps in the Surat Basin. During this phase, scientific and technical literature were reviewed and analysed with the view to developing a detailed proposal for a pilot scale trial at selected locations within the Surat Basin using a range of preferred techniques.
- Phase 2: During the second phase it was intended to conduct field pilot-scale trials of a range of methodologies identified in Phase 1 as promising techniques for measuring methane sources. These trials were to include (a) a remote sensing pilot, and (b) a ground based detection and monitoring pilot. The remote sensing approach was to test new methodologies (e.g. Differential Absorption Lidar) and imaging methods. Ground based detection was to test the use of atmospheric concentration and other measurements as inputs to assess the capability of atmospheric transport modelling to determine fluxes of methane on a defined spatial scale.
- Phase 3: The final stage of the project is aimed at deploying broad scale monitoring based on methods trialled in Phase 2 over an extended period to assess regional methane sources within the Surat Basin. Ongoing ground based monitoring will provide a baseline of methane seepage and other natural as well as anthropogenic source fluxes and their seasonal variations as the basis of a longer term monitoring programme.

Phase 1 of the project was completed in late 2013 and identified a number of prospective methods for both detecting methane sources and estimating their emissions rates (Day et al., 2013). As a result of the analysis undertaken during Phase 1, two general recommendations for the Phase 2 pilot study were made. Firstly, it was suggested that a field survey combining ground-based and remote sensing methods be made to establish the location and approximate magnitude of seeps in the Walloon coal measures outcrop/subcrop areas of the Surat Basin, and secondly, that an atmospheric measurement station be established to measure background methane fluxes from seeps and other sources within the region. Based on these broad recommendations, a detailed work plan for Phase 2 was developed with the aim to produce four specific outputs, which are detailed below.

1. Product 1: A high resolution map of Surat Basin methane sources based on surveys made with an instrumented vehicle. Similar systems have been used in the United States and elsewhere to locate methane emissions sources from urban gas reticulation networks (Phillips et al., 2013) and CSG infrastructure and seeps (LTE, 2007). When the methane concentration data are combined with location (provided by a GPS receiver), detailed maps of the methane source may be developed.
2. Product 2: A coarse resolution map of Queensland atmospheric methane concentrations using historical satellite data. In this component, dry air atmospheric column average methane concentration from the European Space Agency's Scanning Imaging Adsorption Spectrometer for Atmospheric Chartography (SCIAMACHY) satellite sensor were analysed for methane anomalies in the Surat Basin relative to other parts of Australia over a seven-year period.

3. Product 3: A high resolution map of methane sources based on laser diode sensor observations. Laser diode sensors mounted on aircraft have been used to detect methane leaks in gas infrastructure such as high pressure pipelines but to date have not been applied to the problem of locating natural seeps.
4. Product 4: An operating prototype background methane monitoring station. The location of the monitoring station was to be guided by the results of the mobile and remote sensing surveys to provide the ability to discriminate between the larger potential methane sources such as seeps, feedlots, CSG activities.

In this report we present the findings of Phase 2 of the project, i.e. the field trials of the preferred methods identified in the review of methodology undertaken as part of Phase 1. Section 2 of the reports provides a brief description of the various methods examined while in Section 3, Section 4, Section 5 and Section 6 we present the results of the experimental measurements of the ground surveys, satellite remote sensing, airborne surveys and establishment of the fixed monitoring stations, respectively. Finally, in Section 7, the implications of the results of this work are discussed and a summary of the proposed programme for Phase 3 is presented in Section 8.

## 2 Preferred Methodologies

The Surat Basin is well known for CH<sub>4</sub> seeps (Day et al. 2013). Soil gas surveys conducted over a number of years through the 1980s and 1990s indicated significant quantities of CH<sub>4</sub> and other hydrocarbons in various regions across the Surat and other Queensland sedimentary basins (Gasfields Commissions 2013). There have also been reports of gas outbursts associated with artesian bores dating back to the early 20<sup>th</sup> century (Gray, 1967). More recently, vigorous gas seeps have been observed in the Condamine River downstream of the Chinchilla weir near Chinchilla in Queensland. Subsequent measurements made along the river indicated that almost 700 L CH<sub>4</sub> min<sup>-1</sup> was being released as a result of these seeps (Sherman et al., 2014).

Large CH<sub>4</sub> seeps associated with artesian bores or rivers are generally relatively easy to detect; however, locating and quantifying emissions from less vigorous sources presents a significant challenge, especially over large areas such as the Surat Basin. Moreover, there are many other sources of CH<sub>4</sub> apart from ground sources that also contribute to overall CH<sub>4</sub> emissions. In particular, CSG activities and intensive agriculture are potentially significant sources that must be considered when developing regional emission inventories.

One of the principal aims of Phase 1 of the current GISERA project, therefore, was to identify techniques that may be suitable for both locating and determining the emission rates of CH<sub>4</sub> sources within the Surat Basin. In particular, the challenge was to identify CH<sub>4</sub> that has migrated from a coal seam to the surface via seepage and separate these emissions from other sources such as biogenically derived CH<sub>4</sub>. A summary of the methods investigated and suitability to this application is provided in Table 2.1.

Of these methods, a number were identified as being potentially suitable and practical for the problem of identifying potentially low emissions sources such as seeps and measuring their emissions rates. The most promising methods were selected for trialling during Phase 2 of the GISERA project. The methods investigated were:

- Mobile ground surveys using a vehicle equipped with a suitable CH<sub>4</sub> analyser to locate emission sources.
- Flux chambers to directly measure CH<sub>4</sub> emission rates and map the spatial extent of ground sources
- Remote sensing to detect emissions over wide areas.
- Top-down atmospheric methods to provide long-term continuous emission monitoring at the regional scale.

Each of these methods is discussed briefly in the following sections.

**Table 2.1. Summary of CH<sub>4</sub> detection and quantification methodologies considered during Phase 1.**

Method	Comments	Suitability
Soil gas surveys – analyses of gas within soil voids	Simple method to deploy locally. Expensive and difficult to deploy on large scale. May identify diffuse CH <sub>4</sub> seeps. Does not provide flux estimates. May be combined with isotopic measurements to distinguish source.	Too expensive and difficult to deploy at large scale. However, existing data should be exploited.
Terrestrial flux chambers	Established and proven method. Straightforward to deploy. Can provide accurate flux estimates over limited areas. Requires intensive field campaigns of limited duration.	Suitable for estimation of CH <sub>4</sub> flux from localised seeps but impractical at regional scales.
Mobile surveys using instrumented vehicle	Can potentially cover large areas, provided vehicle access is possible. Modern instruments provide very good sensitivity. When combined with plume dispersion models, suitable for estimation of CH <sub>4</sub> flux from localised sources.	Suitable for survey of CH <sub>4</sub> seep locations.
Vegetation surveys	Has potential to locate high flux CH <sub>4</sub> seeps. Not suitable for diffuse large scale and low flux seeps.	The dry climate vegetation in the Surat is generally not suitable for locating seeps.
Geological surveys	Has potential to locate coal resource where outcropping occurs or from geomorphological features in remote regions.	Not suitable due to high level of stratigraphic knowledge for this region already.
Airborne concentration measurements	Expensive and complex method for accurately measuring plume CH <sub>4</sub> concentrations which, when combined with boundary layer meteorology data can yield emission flux.	Possibly suitable but not practical within the timeframe of the project. May be useful during longer term monitoring phase.
Atmospheric trace gas concentration and transport modelling	Cost effective method of accurate CH <sub>4</sub> concentration measurement. Requires careful positioning of sample point with respect to seeps and other sources, and prevailing wind direction. Has significant setup costs at start but yields benefits in long term monitoring. When combined with atmospheric transport modelling can provide information on spatial location and flux of CH <sub>4</sub> in landscape. Isotope sampling may yield information on CH <sub>4</sub> source.	Suitable for deployment subject to locating seeps via survey methods. Requires access to power and location. This approach is one of very few that potentially offers continuous monitoring, provided the wind direction is suitable.
Isotopic analyses	Potentially important information to identify CH <sub>4</sub> source. Relatively simple and cheap measurements for some isotopes ( <sup>13</sup> C) but expensive and complicated for others (e.g. <sup>14</sup> C). However, isotopic signatures from some sources may partially overlap (e.g. Surat CSG and typical aquatic systems, e.g. see range of isotopic values of Walloon CSG in Hamilton et al., 2014) thus making positive identification difficult. Further complications arise from the numerous strata containing coal and the need to discriminate between strata.	Suitable for strategic sampling in pilot stage, subject to limitations stated.
Aquatic flux chambers, bubble traps and flow meters.	Established and proven method for measuring emissions from aquatic systems. Straightforward to deploy. Can provide accurate flux estimates over limited areas. Requires intensive field campaigns of limited duration.	Suitable for estimation of CH <sub>4</sub> flux from localised aquatic high flow seeps.
Hydroacoustic	Relatively new techniques with potential for quantifying distribution function of bubble size.	Not suitable as insufficiently developed for application in Surat Basin.
Thin boundary layer estimation	Established method for application in lakes and ocean. Only applies to diffusive CH <sub>4</sub> emissions (i.e. dissolved CH <sub>4</sub> flux from water to atmosphere). Not suited to bubbles or plumes.	Not suited as it is peripheral to the primary task.
Hyperspectral imaging and spectroscopy	Established theoretical basis. The spectral resolution of satellite and airborne hyperspectral imagers is too coarse to locate low flux diffuse CH <sub>4</sub> seeps. Spectroscopic sensors (high spectral resolution)	Potentially suitable spectroscopy methods are available. Requires proof of

	potentially useful and may provide ability to differentiate CH <sub>4</sub> flux from a heterogeneous background.	application.
Differential absorption LIDAR (DIAL)	Airborne systems are a new technology for methane surveys. Expensive, limited duration and not widely available. Needs to be developed/proven for low flux diffuse seeps with heterogeneous background. Ground based systems can be combined with mobile survey methods to yield accurate concentrations of plumes. Can be combined with micrometeorology techniques to yield fluxes. Limited duration and dependent on wind direction.	Potentially most suitable technology for surveys of CH <sub>4</sub> seeps. Requires proof of application.
Fourier transform infrared spectroscopy (FTIR)	Mature methodology and potentially useful. Needs development and proof of application for low flux and diffuse seeps as potentially close to detection limit.	Potentially suitable but requires proof of application.
Space borne sensors	Spectral and spatial resolution too coarse for this task.	Not suitable to detect specific seeps but may be useful to look at regional trends.

## 2.1 Ground Surveys

The simplest of the selected methods was the use of mobile ground surveys where a vehicle fitted with a suitable methane analyser is driven across the landscape to continuously measure ambient methane concentrations. This system has been used previously to locate methane sources both in Australia and overseas (LTE, 2007; Phillips et al., 2013; Maher 2014). Recent advances in gas analysers have resulted in commercially available systems with sensitivity of around 1 ppb and high levels of stability so that the instruments can be used routinely in a mobile arrangement (Crosson, 2008). Moreover, the concentration data may be combined with spatial data and processed in GIS software to yield detailed maps of methane concentration as a function of location. Care must be taken when interpreting the data, however, since the concentration is dependent upon prevailing atmospheric conditions and is not necessarily an indicator of the emission rate of the source.

While the concentration alone does not yield information on emission rates, when combined with micrometeorological data and knowledge of plume dispersion characteristics, it is possible in some circumstances to estimate emission rates. By traversing across a methane plume downwind of the source, the emission flux,  $F$ , may be estimated by integrating the CH<sub>4</sub> concentration enhancement,  $C$ , of the plume in the horizontal,  $y$ , and vertical,  $z$ , directions and multiplying by the average wind velocity,  $u$ .

$$F = u \int_{-y}^y \int_0^z C(y,z) dy dz \quad (2.1)$$

Because concentration measurements are usually made only at ground level, the vertical dispersion must be estimated by reference to plume dispersion models such as the Pasquill-Gifford curves of  $\sigma_z$  (i.e. the standard deviation of the distribution of CH<sub>4</sub> concentration in the vertical direction) as a function of downwind distance under given atmospheric turbulence conditions (Hanna et al., 1982). The vertical concentration profile of CH<sub>4</sub> within the plume may be assumed to decrease from the ground level concentration with height according to a Gaussian distribution through the plane. Other plume dispersion models such as the backward Lagrangian stochastic model may also be used to estimate emission fluxes from ground level concentration measurements (Loh et al., 2009).

In carefully designed experiments, ground based plume measurements can yield high levels of accuracy (e.g. Loh et al., 2009; Humphries et al., 2012). However in some cases, estimating the vertical extent of the plume introduces a significant source of uncertainty because the vertical concentration profile must be estimated from information on the spatial distribution of the source (i.e. an area or point source), downwind distance and prevailing atmospheric stability. Often these data are not well defined.

The uncertainty may be reduced by measuring the methane concentrations at various heights through the plume rather than attempting to estimate it; however, there are practical problems associated with measuring methane concentrations at elevated heights from a moving vehicle. A prototype system has been developed and demonstrated by the U.S. instrument manufacturer Picarro Inc. where samples from four points on a 5 m high mast attached to a vehicle enables the spatial distribution of the plume to be measured in both the horizontal and vertical axes simultaneously (Tsai et al., 2013). The emission rate from the source is calculated from the product of the resultant concentration profile and wind data using proprietary software.

Although this system does not require modelling to estimate vertical distribution, it does rely on most of the plume being within the 5 m vertical swath, so is not suited to distant or large sources, where the plume is substantially higher than 5 m.

An alternative approach is to use tracer gases to determine emission rate. Here, a stable gas unrelated to the source such as acetylene is released at a known rate,  $F_{Tracer}$ , from the same location as the methane source. Simultaneous downwind concentration measurements of both the tracer,  $C_{Tracer}$ , and methane,  $C_{CH4}$ , are made and the emission rate of methane,  $F_{CH4}$ , calculated according to Equation 2.2.

$$F_{CH4} = F_{Tracer} \times \frac{C_{CH4}}{C_{Tracer}} \quad (2.2)$$

The tracer method avoids the need to estimate the vertical methane profile in the plume and can yield accurate results (e.g. Lamb et al., 1995; Allen et al., 2013) but does require additional analytical capability to measure the tracer gas with sufficient accuracy and precision.

In Phase 2 of the current study, mobile ground surveys were used extensively to locate methane emission sources within the Surat Basin. In some instances, downwind traverses of methane plumes were used to estimate emission rates from some sources. At the time these measurements were made, we did not have suitable instrumentation available to use tracer gas methods. However, this approach is being examined for future work in this area.

## 2.2 Flux Chambers

Flux chambers are often used to measure emissions of gases from soils (Denmead, 2008). There are various designs available but essentially, all operate by enclosing an area of soil,  $A$ , by placing a chamber of known volume,  $V$ , on the ground surface and measuring the concentration of  $CH_4$  (or other gas) within the chamber over time. Flux chamber measurements are mostly made in the 'static' mode where the gas concentration within the chamber is measured over a period of time. Since there is no exchange of air with the outside atmosphere, the methane concentration increases as gas flows from the soil into the chamber during the course of the experiment. By measuring the rate of change of concentration,  $dC/dt$ , the gas flux per unit area,  $F$ , can be calculated according to Equation 2.3.

$$F = \frac{dC}{dt} \times \frac{V}{A} \quad (2.3)$$

For high flow situations, flux chambers may also be operated in a flow through mode where a stream of diluent gas is passed through the chamber at a known rate,  $f$ . In this mode, the steady state concentration of the gas is measured and the flux is calculated by Equation 2.4.

$$F = (C_{out} - C_{in}) \times \frac{!}{A} \quad (2.4)$$

where  $C_{out}$  is the gas concentration in the outlet flow from the chamber and  $C_{in}$  is the gas concentration in the inlet flow.

Flux chambers may also be used in aquatic environments such as the Condamine River (Sherman et al., 2014).

During this study, flux chambers were used to map and measure emission rates from numerous ground sources located by mobile surveys. They were also applied to measure CH<sub>4</sub> emission rates from natural surfaces.

## 2.3 Remote Sensing

Remote sensing is the practice of acquiring data from the Earth's land and water surfaces using sensors on remote platforms such as aircraft or orbiting satellites. The sensors measure reflected or emitted radiation across the electromagnetic spectrum (Campbell, 2002). The remote sensing of gases relies on the acquisition of spectral data across the spectral regions containing narrow absorption features specifically related to each gas. For CH<sub>4</sub> the spectral absorption features usually used are located around 1.65 µm, 2.3 µm, 3.3 µm and 7.6 µm.

Remotely sensed data specifically for gases can be obtained from a range of platforms, namely, satellite, airborne and ground/field. During Phase 2 of this study, we investigated the feasibility of using two systems for providing baseline methane levels at the Surat Basin. The first was the satellite-based SCanning Imaging Absorption spectroMeter for Atmospheric CHartographY (SCIAMACHY) (Burrows et al., 1995) data. The second system was an airborne diode laser sensor, Airborne Laser Methane Assessment Generation 2 (ALMA G2) developed by Pergam (<http://www.pergam-suisse.ch/en/application/airborne-gas-leak-detection/>). These techniques were selected for investigation during Phase 2 because of their ability to provide spatially comprehensive measurements and the ability to access these data.

The SCIAMACHY satellite data are available over a long time period thus offering the potential to provide an indication of trend over time, albeit at fairly coarse spatial resolutions. This system has been used recently to estimate total CH<sub>4</sub> emissions associated with oil and gas production and seeps in the United States (Schneising et al., 2014; Kort et al., 2014).

The airborne laser sensor has recently been made commercially available in Australia. It was developed for airborne pipeline leakage applications and has low detection limits but has never been applied for determining baseline levels. This study was the first time the ALMA G2 was deployed for such an application (see Section 5).

### 2.3.1 SCIAMACHY SATELLITE

Although Stage 1 of the study concluded that satellite data was unsuitable for detecting seeps due to its coarse spatial resolution (Day et al., 2014), it is possible that on a regional scale, temporal variations may be apparent. The SCIAMACHY satellite sensor is a passive spectrometer acquiring backscattered, reflected, transmitted or emitted radiation from the atmosphere and Earth's surface, which operates between the wavelength range of 240 and 2380 nm. The main objective of SCIAMACHY system was to provide global measurement of various trace gases in the troposphere and stratosphere (Burrows et al., 1995).

The typical footprint of SCIAMACHY is 30 km (along track) by 60 km (across track) at nadir and the maximum swath width is 960 km. The spectrometer was launched on board the European ENVISAT satellite (Bruzzi et al., 1995) operating at an altitude of 790 km ± 10 km and was operational from March 2002 to April 2012.



The sensor characteristics for SCIAMACHY are discussed in more detail in Section 4.2. The channels that are used for the retrieval of methane are channels 6 and 8 depending on the retrieval algorithm used.

### 2.3.2 ALMA G2 AIRBORNE DATA

The Airborne Laser Methane Assessment Generation 2 (ALMA G2) is a laser diode sensor developed by Pergam Suisse AG primarily for gas pipeline inspection. The ALMA G2 is based on a pulsed beam from a diode laser tuned to the 1.65  $\mu\text{m}$  methane absorption feature. The laser beam aimed downwind of the pipeline, is reflected and the scattered reflection collected by a receiving mirror. A photo-detector receives the signal which is compared to the signal from a reference channel. This reference consists of a laser beam projected through a cuvette containing a reference methane sample. When methane is present the laser light will be absorbed, and the attenuation of the signal is proportional to the concentration of methane along the laser beam path.

Whereas most gas analysers measure the concentration of a particular component in a sample, open path monitors, like the ALMA G2, measure the total amount of a specific gas in the path of the laser beam between the transmitter unit and reflector (i.e. the ground in the case of the ALMA G2). This is a 'total path' measurement and the units of the measurement are parts per million metres, or  $\text{ppm}\cdot\text{m}$ . Thus the integrated concentration within the air column is obtained by dividing the measurement (in  $\text{ppm}\cdot\text{m}$ ) by the path length.

Since the ALMA G2 was designed for natural gas pipelines monitoring it is usually mounted on a helicopter flying along known locations of pipeline and operated at an altitude of 25-150 m. The detection range is dependent on the altitude and is quoted as 25-20,000  $\text{ppm}\cdot\text{m}$  at 50 m and 100-20,000  $\text{ppm}\cdot\text{m}$  at 100 m while the instrument accuracy is quoted at 1 %.

Additional instrumentation acquiring data include three digital cameras (operating in the visible ranges) mounted to view 50 m to both sides and forward of the line being flown. A laser range finder is also included in the suite of instrumentation and is used in the processing of the ALMA G2 data.

## 2.4 Top-Down Atmospheric Monitoring

Atmospheric methods were chosen to monitor the net methane emissions across the broader Surat Basin. Measurements of atmospheric methane concentrations and meteorology from fixed stations combined with transport modelling (taking into account wind trajectories and turbulent dispersion) can be used to infer the net emissions strength and source locations across a wide region. The measurements can be continuous and long term and so can provide an early baseline and continue into the years of planned substantial growth in CSG activity. Shorter term variations in emissions caused, for example, by the different phases of the production process or by sporadic releases are more likely to be monitored in this way than by intermittent measurement surveys. Atmospheric methods are particularly suited to monitoring emissions distributed across a wide area. Point sources within an area can also be potentially resolved if sufficiently strong.

A review of top down atmospheric methods suitable for geological source monitoring is given by Leuning et al. (2008) and their relevance to monitoring CSG emissions is outlined in Day et al. (2012).

## 2.5 Gas Geochemistry

### 2.5.1 GAS COMPOSITION

Molecular composition of gas is widely used to differentiate the origin of natural gases (biogenic versus thermogenic, e.g. Scott et al., 1994, Golding et al., 2013), the maturity of their source rocks (e.g. Rezniko, 1969; Stahl, 1974; Connan and Cassou, 1980) and elemental composition of the organic matter in coal, especially hydrogen/carbon ratio (Rice et al., 1989). Coal seam gas in the Surat Basin consists of mainly  $\text{CH}_4$



but may also contain small quantities of light hydrocarbons such as ethane, CO<sub>2</sub>, and in some cases small amounts of N<sub>2</sub> (Smith et al., 1985, Smith and Pallasser, 1996) H<sub>2</sub>, He (Clayton, 1998) and H<sub>2</sub>S (Clayton, 1998). By comparison, coal seam gas from the adjacent Bowen basin is more thermogenic and contains higher chain hydrocarbons (Kinnon et al., 2010). The presence of 'wetter' components (i.e. hydrocarbons apart from CH<sub>4</sub>, typically ethane through to pentanes) tends to be a reflection of coal rank and pure microbial gases are characterised by low concentrations of ethane and heavier hydrocarbons. For desorbed gases from coal, the composition of gases analysed at different stages of desorption also varies (Hamilton et al., 2014).

## 2.5.2 CARBON AND HYDROGEN ISOTOPES OF GASES

The isotopic compositions of natural gases has long been used to help identify its origins (e.g. Stahl, 1977; Schoell, 1980; Rice et al., 1989; Whiticar, 1994), and the thermal maturities of their source rocks (e.g. Stahl and Carey, 1975; Dai and Qi, 1989; Berner and Faber, 1996). Thermogenic gases are generated from organic matter and oil by cracking at high temperature (Burruss and Laughrey, 2010). Methane also forms as a product of anaerobic microbial metabolism. Methane carbon isotope values between -20 to -50 ‰ relative to Vienna Pee Dee Belemnite (VPDB) typically indicate thermogenic gas and values lower than -50 ‰ are indicative of biogenic influences (Schoell, 1980, 1988; Strapoc et al., 2011). Intermediate values (-50 to -60 ‰) may be the result of mixing of thermogenic and secondary biogenic gases. Because variable contributions of the end members can result in a wide variety of carbon isotope values, distinguishing between thermogenic and biogenic contributions can be problematic on the basis of  $\delta^{13}\text{C}$  signatures alone. The use of hydrogen isotope ratios in addition to the carbon isotopes may provide further insight into the source as shown in Figure 2.1 (Whiticar, 1999; Golding et al., 2013).

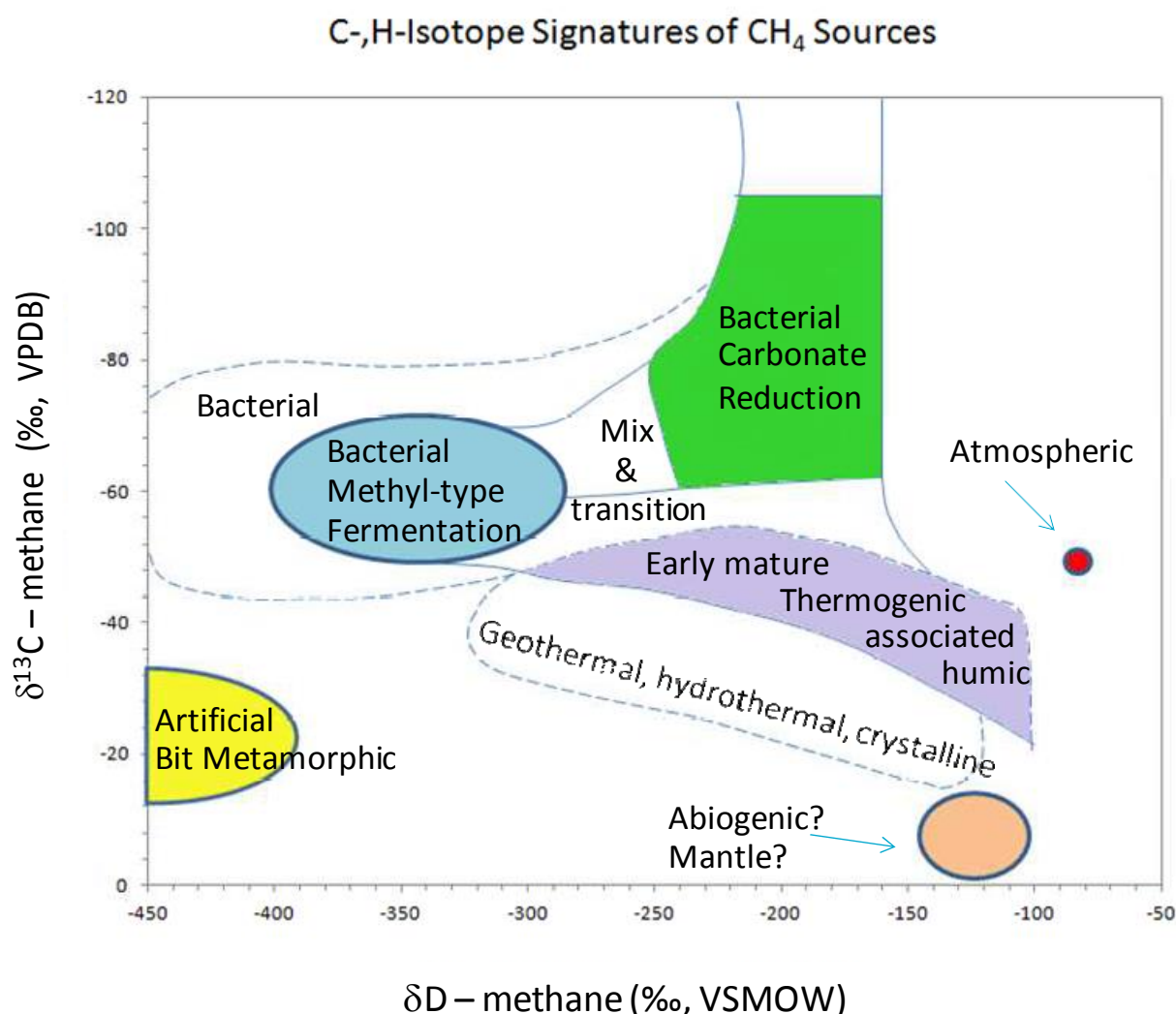


**Figure 2.1. Cross plot of carbon and hydrogen isotopes (adapted from Whiticar, 1999).**

Although this study focusses on methane fluxes in the Surat Basin, the isotopic analyses of carbon dioxide which is ever present in all gas samples ranging from CSG to atmospheric samples can in specific situations provide crucial supporting evidence for the origin of methane. The most pronounced example occurs in CSG areas dominated by significant secondary biogenic methanogenesis with carbon isotope values for CO<sub>2</sub> gas and DIC on CSG production water ranging from 0 to +33 ‰ (pronounced <sup>13</sup>C enrichments).

The isotopic values for atmospheric carbon dioxide tend to range from -8 to -12 ‰ depending on air pollution levels (Longinelli et al., 2005; Clark-Thorne and Yapp, 2003) and values for carbon isotopes of CO<sub>2</sub> in coal seams worldwide range between -28 ‰ and +19 ‰ (Golding et al., 2013, Smith et al., 1985; Rice, 1993; Koartarba and Rice, 1995; Clayton, 1998) but does overlap biogenic (photosynthetic origin) CO<sub>2</sub> which has carbon isotope values from about -10 to -30 ‰. Anaerobic bacterial reduction of CO<sub>2</sub> to form methane leads to isotopically heavier C isotopes in the residual CO<sub>2</sub> gas, in most cases positive values (Emery and Robinson, 1993; Golding et al., 2013; Kinnon et al., 2010). Carbon isotopic values of CO<sub>2</sub> between -5 to -28 ‰ are indicative of thermogenic sources (Irwin et al., 1977, Chung and Sackett, 1979, Clayton, 1998). Isotopic values of endogenic CO<sub>2</sub> are close to the main value for elemental C in the upper mantle and vary from -10 to -5 ‰ (Smith et al., 1985; Javoy et al., 1986; Hoefs, 1987; Jenden et al., 1993).

In the present study analyses of the isotopic compositions of carbon and hydrogen for CH<sub>4</sub> were used to provide insight into the possible origin of gases collected at some locations within the study region.

## 3 Ground Surveys

In this section we describe the methods and results of the mobile ground surveys and flux chamber measurements made during Phase 2. Also included in this section are the results of chemical and isotopic analyses of gas samples collected from a variety of sites.

### 3.1 Experimental Methods

#### 3.1.1 GAS COMPOSITION AND STABLE ISOTOPIC ANALYSES

During the project gas samples were collected from some seep sites. These were then analysed for chemical and carbon and hydrogen isotopic composition in the CSIRO Organic and Isotope Geochemistry laboratory in North Ryde.

##### *Sampling*

Samples were collected in evacuated 2.7 L stainless steel canisters. In the case of ground seep sites, a chamber was placed over the seep location to allow the gas to accumulate. After a suitable period of up to several minutes, the canister was connected to the chamber using a nylon tube and the canister valve opened to allow the canister to fill to atmospheric pressure.

##### *Gas Composition*

A gas sample was connected to the vacuum manifold on the Agilent GC to evacuate the air dead-volume. Then the gas sample was introduced through the vacuum manifold into a sample loop (0.25 mL) at atmospheric pressure for GC analysis on an Agilent 6890N Natural Gas Analyser, with a thermal conductivity detector (TCD). Four packed columns with Valco valve column switching are used to separate the gases, a 2 foot 12% UCW982 on PAW 80/100 mesh (pre-column), a 15 foot 25% DC200 on Paw 80/100 mesh, a 10 foot HaysepQ 80/100 mesh and a 10 foot Molecular Sieve 13X 45/60 mesh column. The oven was isothermally maintained at 90°C throughout the 20 minute run. The amount of separated gas components was determined against an external standard calibration. The molecular composition of gas components was corrected to air free values, assuming atmospheric ratios for the oxygen+argon/nitrogen peaks. At 90°C, oxygen and argon co-elute on the 13X molecular sieve column.

##### *Carbon Isotope Composition*

The carbon isotopic composition of gases was measured by GC-C-IRMS (gas chromatography/combustion/isotope-ratio mass spectrometry). The GC-C-IRMS system consisted of a GC unit (6890N, Agilent Technologies, USA) connected to a GC-C/TC III combustion device coupled via open split to a Delta V Plus mass spectrometer (ThermoFisher Scientific, Germany). The analytes of the GC effluent stream were oxidised to CO<sub>2</sub> and H<sub>2</sub>O in the combustion furnace held at 1000°C on a CuO/Ni/Pt catalyst. Water was removed on-line by a Nafion membrane and the CO<sub>2</sub> was transferred to the mass spectrometer to determine carbon isotope ratios. 20 -100 µL of sample gas was injected to the split/splitless inlet system (Agilent Technologies, USA), working in split mode (20:1 ratio). The inlet was held at a temperature of 200 °C. The gas components were separated on a fused silica capillary column (PoraPlot Q, 25 m x 0.32 mm ID, Varian). The GC was held isothermally at 40 °C. Helium was the carrier gas, set to a constant pressure of 14.3 psi. All gas samples were measured in duplicate with a standard deviation of ≤0.5 ‰ for the standards and samples. The quality of the carbon isotope measurements was checked regularly by measuring secondary standards of pure CH<sub>4</sub> and CH<sub>4</sub>/CO<sub>2</sub> mixtures with known isotopic composition as determined by inter-comparison on dual bellows inlet mode on a Finnigan MAT 252 against international primary carbonate standards prepared by the phosphoric acid method.

## Hydrogen Isotope Composition

The hydrogen isotopic composition of gases was measured by GC-TC-IRMS (gas chromatography/temperature conversion/isotope-ratio mass spectrometry). The GC-TC-IRMS system consisted of a GC unit (6890N, Agilent Technologies, USA) connected to a GC-C/TC III interface device coupled via open split to a Delta V Plus mass spectrometer (ThermoFisher Scientific, Germany). After passing through the GC, hydrocarbons were reduced to H<sub>2</sub> and elemental carbon in the pyrolysis reactor held at 1440 °C. H<sub>2</sub> was transferred on-line to the mass spectrometer to determine hydrogen isotope ratios. 20–200 µL of sample gas was injected to the split/splitless inlet system (Agilent Technologies, USA), working in split mode (20:1 ratio). The inlet was held at a temperature of 200°C. The gas components were separated on a fused silica capillary column (PoraPlot Q, 25 m x 0.32 mm ID, Varian). For CH<sub>4</sub> analysis, the GC was held isothermally at 40 °C. Helium was the carrier gas, set to a constant pressure of 14.3 psi. All gas samples were measured in duplicate with a standard deviation of ≤3 ‰ for most of the compounds and samples. The H<sup>3+</sup>-factor was determined daily by measuring 10 reference gas peaks with increasing amplitude. This factor had an average value of 2.487 ± 0.056 ppm/nA. The quality of the hydrogen isotope measurements was checked regularly by measuring secondary standards of pure H<sub>2</sub> and pure CH<sub>4</sub> with known isotopic composition as determined by inter-comparison on a TC-EA against international primary solid hydrogen isotope standards.

### 3.1.2 MOBILE SURVEYS

Mobile ambient methane concentration measurements were made using a Picarro Model 2301 CH<sub>4</sub>, CO<sub>2</sub>, H<sub>2</sub>O cavity ring-down spectrometer fitted into a four-wheel-drive vehicle. The gas analyser has a rapid response time and the high resolution (1 ppb for CH<sub>4</sub>) and low drift characteristics (Crosson 2008) necessary to detect small perturbations in methane concentration against background levels.

The instrument was operated with a Picarro Mobile Kit that included an inverter so that the system could be operated continuously off the vehicle's 12 V power supply. The Mobile Kit also includes a GPS receiver and software so that concentration data can be processed and displayed in GIS software. The nominal operating ranges of the analyser are CH<sub>4</sub> 0–20 ppm, CO<sub>2</sub> 0–1000 ppm and H<sub>2</sub>O 0–7 ‰. However, we have previously found that the actual operating ranges for CH<sub>4</sub> and CO<sub>2</sub> exceed these specifications, and provided that the instrument is calibrated against suitable standards, can reliably quantify significantly higher concentrations (Day et al., 2014).

The instrument can be operated in either 'three gas' mode or 'methane locator' mode. In the three gas mode, CH<sub>4</sub>, CO<sub>2</sub> and H<sub>2</sub>O are analysed simultaneously with the rate of data acquisition about 0.3 Hz. More rapid (about 2 Hz) data acquisition can be achieved by operating the analyser in the CH<sub>4</sub> locator mode; however, CO<sub>2</sub> and H<sub>2</sub>O are not measured in this mode.

The calibration of the analyser was regularly checked against a standard gas mixture containing 10.8 ppm CH<sub>4</sub> (BOC Gases Australia). The results of the calibration checks showed that the indicated concentration was within about 0.7 ‰ of the nominal concentration of the standard. This difference is less the uncertainty of the calibration standard of ±0.5 ppm. Periodic multipoint reference checks were also performed using this standard mix along with another containing 103 ppm CH<sub>4</sub> and a reference air sample containing 1.732 ppm CH<sub>4</sub> and 383 ppm CO<sub>2</sub> prepared by the CSIRO Marine and Atmospheric Research, now Oceans and Atmosphere, GASLAB (Francey et al., 2003). In the case of the reference air sample, the indicated CH<sub>4</sub> concentration was within about 0.2 ‰ of the nominal concentration, reflecting the higher precision of this reference sample.

During mobile surveys, the spectrometer was operated continuously while the vehicle was travelling but also for extended periods when stationary (an auxiliary battery system allowed the instrument to be operated for up to two hours without the engine running). Air was sampled via a ¼" nylon tube from the front of the vehicle about 1 m above ground level. The normal flow rate of sample air to the spectrometer is approximately 100 mL min<sup>-1</sup>; however, to minimise the lag time between air entering the inlet tube and reaching the analyser, an auxiliary pump in the Mobile Kit was used to increase the flow rate to about 5 L

$\text{min}^{-1}$ . When used for flux chamber measurements (Section 3.5), the auxiliary pump was bypassed using a three-way valve.

Surveys were made by driving the vehicle on public and sometimes private roads at speeds up to about  $100 \text{ km h}^{-1}$ . The rate of measurement of the instrument was such that relatively small methane anomalies could be detected at highway speed (i.e.  $\sim 100 \text{ km h}^{-1}$ ) although the response time of the instrument, which was about 14 s, resulted in an offset of several hundred metres at this speed. Usually, where elevated levels of methane were detected lower speed passes were made to identify and locate the source of the emissions.

Wind speed and direction were measured while the vehicle was stationary (to avoid the contribution of wind caused by motion of the vehicle) using a 2-dimensional sonic anemometer (Climatronics Sonimometer) mounted on the roof of the field vehicle.

### 3.1.3 SURFACE GAS FLUX

Emissions from the ground surface were made at locations where elevated  $\text{CH}_4$  concentrations measured during the mobile surveys indicated that surface emissions were present. Similar measurements were also made on unaffected surfaces throughout the study region to assess natural soil emission rates. Surface methane flux measurements were made using one of two systems, both of which are based on a closed accumulation chamber method. The first measurement system comprised a plastic cylindrical chamber 37.5 cm in diameter and 40 cm high with a total volume of about 45 L and an area of coverage of  $0.11 \text{ m}^2$ . The chamber was placed on the ground and connected to the Picarro analyser in the field vehicle via a  $\frac{1}{4}$ " nylon tube with a sample flow rate of approximately  $100 \text{ mL min}^{-1}$ . The  $\text{CH}_4$  concentration within the chamber,  $C$ , was continuously measured over a period of several minutes while a small fan inside the chamber ensured that the sample was well mixed during each measurement. Emission flux was calculated according to Equation 2.3.

This arrangement is capable of measuring very low gas fluxes normally encountered in natural systems (Day et al., 2014). However, at a number of sites, the emission rates were too high for the Picarro instrument to be used. Instead, a portable flux meter (West Systems srl, Italy) was used at these locations. The West Systems flux meter uses a 6 L chamber covering  $0.03 \text{ m}^2$  and is connected to a tuneable diode laser methane analyser with an operating range of 0-10 %  $\text{CH}_4$  and a resolution of 100 ppb (cf. 0-20 ppm range and 1 ppb resolution of the Picarro instrument). The instrument also measures soil  $\text{CO}_2$  emissions simultaneously. The West Systems flux meter is shown in Figure 3.1.

In both cases, measurements were made at multiple points within the emission zone to determine the spatial extent of the seep.

At a number of seep locations, samples of gas were collected to determine their isotopic and chemical composition. These samples were collected by placing a chamber over the source to capture gas seeping from the surface, then extracting a sample into an evacuated stainless steel canister which was then analysed at the CSIRO North Ryde laboratories.



**Figure 3.1. West Systems portable flux meter in use at a site in the Surat Basin. The CH<sub>4</sub> and CO<sub>2</sub> analysers and battery are mounted in the backpack.**

## 3.2 Results

### 3.2.1 GAS GEOCHEMISTRY

Samples of gas were collected from two ground seeps located during the project (Sites 2 and 3; see Section 3.2.4 for details), which were subsequently analysed for their chemical and isotopic compositions. The results of the analyses are summarised in Table 3.1. For comparison, two samples of production CSG from the Surat Basin, previously analysed in this laboratory are also shown. The CSG samples were analysed under a CSIRO strategic project (previously unpublished).



**Table 3.1. Molecular, carbon and hydrogen isotopic composition of gas samples analysed**

Sample	CO <sub>2</sub> (%)	CH <sub>4</sub> (%)	C <sub>2</sub> H <sub>6</sub> (%)	N <sub>2</sub> (%)	O <sub>2</sub> + Ar	δ <sup>13</sup> C CO <sub>2</sub> (‰ VPDB)	δ <sup>13</sup> C CH <sub>4</sub> (‰ VPDB)	δ <sup>2</sup> H CH <sub>4</sub> (‰ VSMOW)
CSG 1	0.78	96.3	0.02	2.34	0.53	+9.1	n.a.	-210.1
CSG 2	0.38	95.1	0.01	3.98	0.57	+6.2	-50.9	-216.3
Seep, Site 2	0.04	3.05	-	77.8	19.1	-9.5	-56.9	-202.8 *
Seep, Site 3	0.10	3.18	-	77.7	19.0	n.a.	-50.1	-210.2 *

*Note: \*Data needs to be treated with caution as gas sample in the canister was below atmospheric pressure at time of hydrogen analyses. Pressure drops below atmospheric pressure cause isotopic fractionation to occur.*

*n.a. : not available, in part due to a lack of sufficient gas pressure or concentration in the sample container.*

Variations in the concentration of CH<sub>4</sub>, CO<sub>2</sub> and nitrogen for the two CSG samples (CSG 1 and CSG 2 in Table 3.1) are typical of those obtained from Surat Basin coal in general and are influenced by variations in the inherent CSG properties (Golding et al., 2013, Hamilton et al., 2015, Hamilton et al., 2014). Some of the variations in gas composition that can occur are due to a myriad of factors such as: coal type, coal rank (thermal maturity due to burial), presence of intrusive volcanics (contact zones have localised high CO<sub>2</sub>), fracture/cleat system (permeability to gases and formation water flow), connectivity to meteoric water and nutrients (possibility for microbes to thrive), stratigraphy, outcropping at basin margins, gas fractionation (depending on the stage of coal desorption, i.e. CH<sub>4</sub> vs CO<sub>2</sub> have different coal diffusion/absorption coefficients) as well as variations in gas sampling (e.g. air contamination, leaks, sample container stability, etc.). For most CSG samples the dominant gases are methane, carbon dioxide and nitrogen, with the concentration of CO<sub>2</sub> mostly below 1 %. In the case of samples CSG1 and CSG 2, there are also traces of ethane (C<sub>2</sub>H<sub>6</sub>). Biogenically derived gases (marsh gas, biogas, sewage treatment plant, anaerobic digester gas, some CSG) which are strongly dominated by methanogenesis produce CH<sub>4</sub> and CO<sub>2</sub> almost exclusively; however there can be traces of ethane but usually no detectable heavy hydrocarbons and the CO<sub>2</sub> is usually in significant proportions (~10-30 %). Many of the samples can have variable amounts of nitrogen, largely due to air contamination during sampling but a representative CSG sample from the Surat Basin with minimal air contamination typically has nitrogen in the ~2-3 % range or lower (Hamilton et al., 2014).

In contrast to the Surat Basin CSG samples, the bulk molecular composition for the gas samples from the Surat Basin seeps (Site 2 and Site 3) are dominated by atmospheric ratios (high O<sub>2</sub>+Ar, high N<sub>2</sub>, low CO<sub>2</sub>) found normally in air, over-printing the CH<sub>4</sub> escaping from the ground. This is largely due to these samples being collected in surface flux chambers (see Section 3.2.4) which often results in high levels of air being entrained with the sample.

The molecular and isotopic values of the samples when used in conjunction sometimes allow a chemical signature to be developed, which may allow some degree of source contribution to be made.

Carbon isotopic compositions of CH<sub>4</sub> in the CSG gas samples range from ~-50 to -60 ‰ (Table 3.1).

Traditionally, δ<sup>13</sup>C values of CH<sub>4</sub> less than -55 to -60 ‰ are regarded as indicative of biogenic origin (Hunt, 1979, Burruss and Laughrey, 2010, Stopler et al., 2014), however, biogenic methane derived from carbonate reduction can have isotopic values ranging from less than -100 to -39‰ (Jenden, 1986, 1988; Valentine, D.L., 2011, Strapoc et al., 2011) indicating that biogenic and thermogenic methane cannot be necessarily distinguished from each other on the basis of δ<sup>13</sup>C CH<sub>4</sub> values alone (Scott et al., 1994).

Additionally, oxidation of CH<sub>4</sub> by aerobic or anaerobic bacteria selectively removes <sup>12</sup>C, thus shifting toward more positive values (Whiticar et al., 1986). However, the combination of the δ<sup>13</sup>C and δ<sup>2</sup>H data for CH<sub>4</sub> in a cross-plot generally provides greater insight into their origins (Whiticar, 1999, Golding et al., 2013). As shown in Figure 2.1 the results shown in Table 3.1 would plot in the early mature thermogenic field, close to the transition area.

In contrast, gas produced in a feedlot, anaerobic digester, freshwater swamp and landfill (Table 3.2) all utilise bacterial methyl-type fermentation. The carbon isotopic compositions of the CH<sub>4</sub> generated ranges

from -49 ‰ to -53 ‰ which is outside the generally accepted carbon isotope values for biogenic methane (i.e. <50 ‰; Schoell, 1980, 1988). However biogenic CH<sub>4</sub> can have a wide range in  $\delta^{13}\text{C}$  values (-40 ‰ to -110 ‰) depending on the isotopic composition of the original substrate, partial pressure of hydrogen in the system, the methanogenic pathways and the species of methanogens involved (e.g. Games and Hayes, 1978; Jenden and Kaplan, 1986; Valentine et al., 2004; Conrad, 2005). The hydrogen isotopic composition of CH<sub>4</sub> generated from the samples ranges from -341 ‰ to -255 ‰. Taken together with carbon isotope values of CH<sub>4</sub>, the feedlot and anaerobic digester values are generally consistent with bacterial origins and methyl type fermentation (Figure 2.1); while the freshwater swamp and landfill values plot in the mix and transition area.

**Table 3.2. Examples of carbon and hydrogen isotopic composition of gas from various sources measured in the CSIRO Geochemistry Laboratory.**

Sample	$\delta^{13}\text{C CO}_2$ (‰ VPDB)	$\delta^{13}\text{C CH}_4$ (‰ VPDB)	$\delta^{13}\text{C C}_2\text{H}_6$ (‰ VPDB)	$\delta^{13}\text{C C}_3\text{H}_8$ (‰ VPDB)	$\delta^{13}\text{C}$ $n\text{C}_4\text{H}_{10}$ (‰ VPDB)	$\delta^2\text{H CH}_4$ (‰ VSMOW)	$\delta^2\text{H C}_2\text{H}_6$ (‰ VSMOW)	$\delta^2\text{H C}_3\text{H}_8$ (‰ VSMOW)
CSG, NSW	+25.3	-52.8	-29.1	-25.0	-22.1	-247.6	-202.4	-150.2 *
Feedlot biogas, QLD	+4.4	-49.0	-	-	-	-341.0		
Anaerobic digester, NSW	+10.4	-49.7	-	-	-	-326.2		
Commercial natural gas, NSW	-2.2	-39.4	-30.9	-29.1	-29.5			
Commercial LPG, NSW	-	-	-34.6	-31.7	-			
Freshwater swamp, NSW	-10.4	-51.2	-	-	-	-258.6	-	-
Landfill, NSW	+16.4	-53.0	-	-	-	-255.2	-	-

Note: \*Data needs to be treated with caution as gas sample was below atmospheric pressure at time of hydrogen analyses.

During bacterial CO<sub>2</sub> reduction, the formation water supplies the hydrogen, whereas during fermentation, up to three quarters of the hydrogen comes directly from methyl groups in the coal, which is already depleted in the heavier deuterium atoms. Most Surat basin coal samples have hydrogen isotope values -220 to -200 ‰ VSMOW, hence would sit squarely in the mixed gas portion of the carbon vs hydrogen isotope plot (i.e. mixture of thermogenic and biogenic gases from CO<sub>2</sub> reduction) (Golding et al., 2013, Strapoc et al., 2011)).

In summary, the Surat Basin CSG and seep samples are considered to have mixed source inputs from early mature thermogenic methane gas from the coal matrix mixed with some bacterial CO<sub>2</sub> reduction generated methane; classification is based on the combination of molecular, carbon and hydrogen isotopes (Hamilton, et al., 2014). Eastern Australian basin studies where coals locally contain more than 90 volume % CO<sub>2</sub> show that coal bed and natural gases with CO<sub>2</sub> contents greater than 10 vol % exhibit a narrow range of  $\delta^{13}\text{C}$  – CO<sub>2</sub> values between -3 and -10 ‰, and are derived largely from inorganic sources (Golding et al., 2013). For the sample from Site 2, the CO<sub>2</sub> value of -9.5 ‰ is indicative of an inorganic CO<sub>2</sub> input.



### 3.2.2 MOBILE SURVEYS

Surveys were made in the region of the Surat Basin generally between Dalby in the east and Roma to the west, roughly within the  $350 \times 200$  km area shown in Figure 3.2. The total area of the survey region was approximately 70,000 km<sup>2</sup> and included the major CSG production areas of the Surat. Mobile monitoring was conducted on public and private roads over seven separate field campaigns between January 2013 and July 2014, covering a total distance of more than 7,000 km along the routes shown in Figure 3.2. Many of these roads were traversed on numerous occasions to provide an indication of the temporal variation in the concentrations measured.

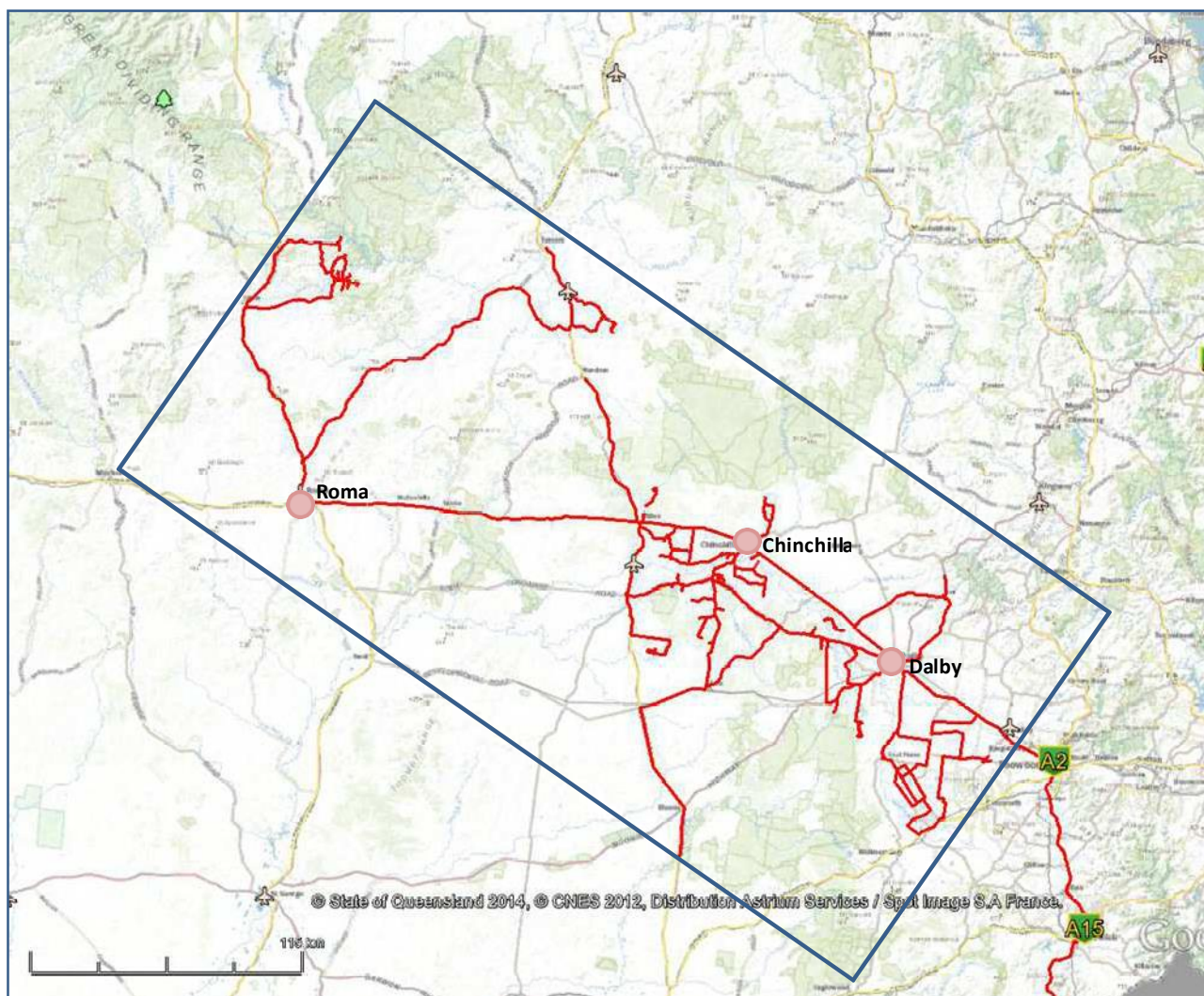
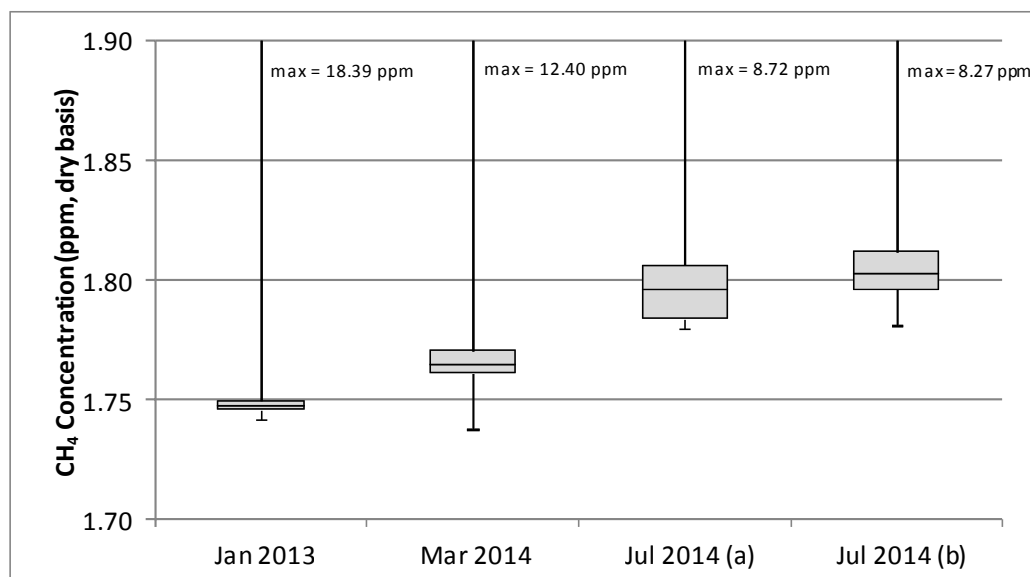


Figure 3.2. Survey area showing a composite of all routes travelled during the mobile surveys (red lines).

The methane concentrations measured over most the survey area were generally around background ambient levels, averaging between about 1.75 and 1.80 (dry basis), depending on the season. Carbon dioxide concentrations were also often measured during these surveys; however, the results were frequently affected by vehicle exhaust from traffic on the survey roads. Carbon dioxide concentrations are also likely to vary widely due to diurnal and seasonal variation in CO<sub>2</sub> flux associated with vegetation (Hutley et al., 2005). Although elevated ambient CO<sub>2</sub> concentrations have been suggested as an indicator of CSG related fugitive emissions (Maher et al., 2014), this seems unlikely given that CSG produced in this region contains less than 1 % CO<sub>2</sub> (Hamilton et al., 2014).

A summary of ambient CH<sub>4</sub> concentration data measured between Jan 2013 and July 2014 is plotted in Figure 3.3. The two July surveys were made between the 8<sup>th</sup> and 10<sup>th</sup> July (Jul 2014 a) and 21<sup>st</sup> to 24<sup>th</sup> (July 2014 b). The data are presented as box plots showing the median, 25<sup>th</sup> and 75<sup>th</sup> percentiles, minimum and maximum for each data set. Given the wide range of concentrations measured during these surveys the

median is considered to be the more representative ‘average’ because it is less affected by extreme values than the mean. Note also, the datasets have been filtered to include only data collected when the vehicle was travelling at greater than  $0.5 \text{ m s}^{-1}$ . This was to eliminate the contribution from flux chamber measurements where the methane concentration was measured inside the chamber rather than ambient air.



**Figure 3.3. Summary of CH<sub>4</sub> concentration data made during four surveys within the study region. Data are presented on a dry basis.**

The results shown in Figure 3.3 are reported on a dry basis, i.e. corrected for atmospheric moisture content to allow comparison of data measured under different levels of humidity. These measurements were made when the Picarro analyser was operating in the ‘three gas’ mode where CH<sub>4</sub>, CO<sub>2</sub> and water were analysed concurrently. The instrument was also operated in ‘CH<sub>4</sub> locator’ mode on many occasions to increase the speed of data acquisition. However, in this mode moisture is not measured hence dry basis data are not determined. Surveys made in this mode are not included in the data presented in Figure 3.3.

The median CH<sub>4</sub> concentrations varied between about 1.75 and 1.80 ppm. Some of the observed variability may be due to differences in the routes driven during each survey; however, most of the observed variation is likely to be due to normal seasonal effects where higher CH<sub>4</sub> concentrations occur during the winter months. The median CH<sub>4</sub> concentrations are consistent with ambient measurements made at the CSIRO Cape Ferguson monitoring station in northern Queensland (location 19.28°S, 147.05°E). A comparison of the survey data and monthly averages measured at Cape Ferguson during the same periods as the surveys is shown in Table 3.3 (World Data Center for Greenhouse Gases, 2015).

**Table 3.3. Median CH<sub>4</sub> concentrations (dry basis) measured during four surveys.**

Survey	Median CH <sub>4</sub> Concentration (ppm, dry basis)	Cape Ferguson CH <sub>4</sub> Concentration (ppm, dry basis)	Difference (%)
Jan 2013	1.7470	1.7530	0.30
Mar 2014	1.7649	1.7640	-0.05
Jul 2014 a	1.7961	1.7979	0.10
Jul 2014 b	1.8026	1.7979	-0.26

Although these data show that overall methane concentrations throughout the survey region were close to background levels, there were numerous occasions where elevated methane concentrations were detected. These ranged from less than 20 ppb above ambient to almost 20 ppm above background. While there are no exposure limits set for methane, it is classified as a 'simple asphyxiant' meaning that high concentrations will reduce the oxygen content of the atmosphere to below 18 % (NOHSC, 2001). The lower explosive limit of CH<sub>4</sub> is approximately 5 % (50,000 ppm) so it is unlikely that any ambient CH<sub>4</sub> concentrations measured during these surveys pose any human health or safety risks.

The range of elevated CH<sub>4</sub> concentrations detected during the surveys varied substantially depending on the time of day (higher levels are generally encountered during the early morning due to low mixing conditions in the near surface boundary layer) and prevailing wind conditions. This effect often resulted in significantly different ambient CH<sub>4</sub> concentrations being measured for the same region at different times of the day. Similar effects have been reported for surveys conducted in the same region by Iverach et al. (2014) who described some of the complexities of attempting to attribute sources of CH<sub>4</sub> based on ambient concentration measurements.

Some examples of the mobile surveys are shown in Figure 3.4 where the ambient CH<sub>4</sub> concentration is plotted in relation to the vehicle position. The location and source of some the elevated concentrations are also marked in Figure 3.4. The CH<sub>4</sub> sources are discussed in more detail in the following sections.

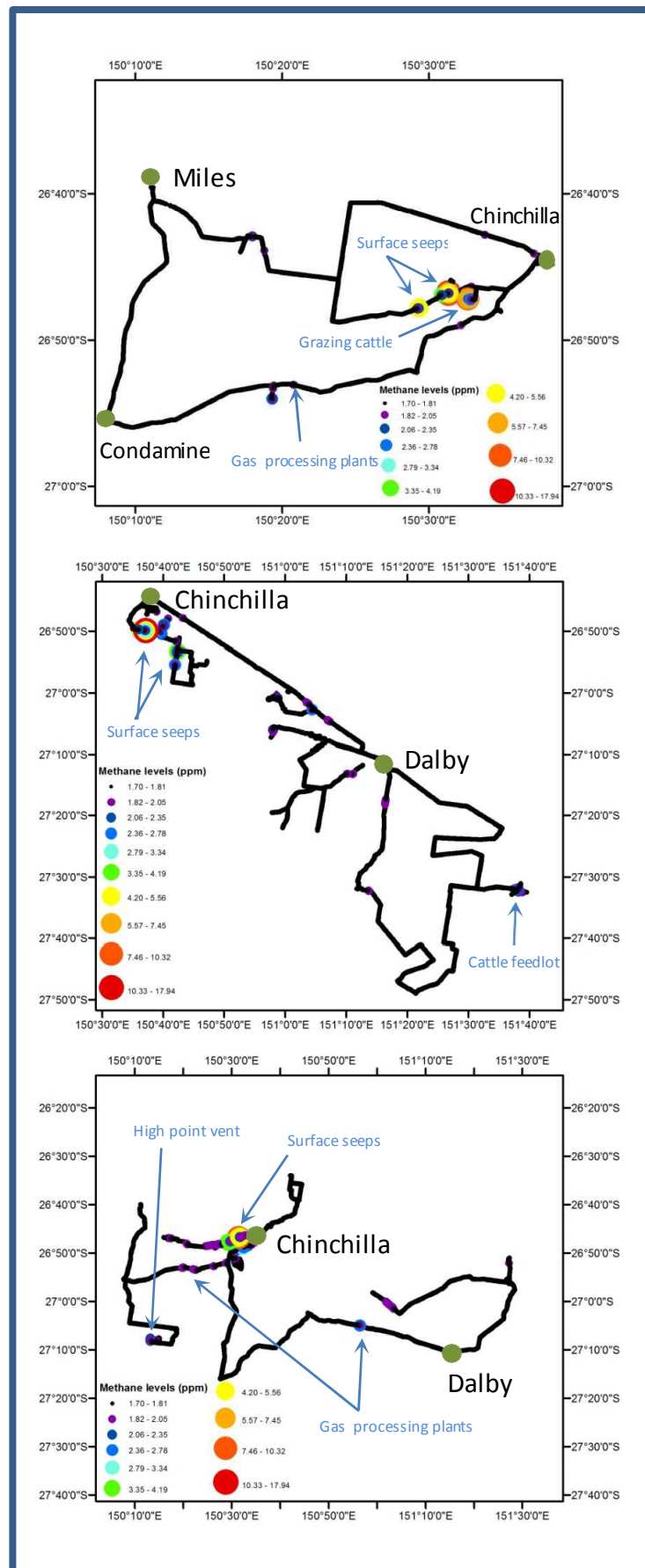


**Figure 3.4. Some examples of the data obtained during mobile surveys in the study region, with sources of elevated CH<sub>4</sub> levels identified. Top – route driven during January 2013; middle – route driven during March 2014 (accompanied by UNSW and RHUL researchers); bottom – route driven during July 2014.**



### 3.2.2 CATTLE AND OTHER BIOGENIC SOURCES

One of the most common sources of methane detected during the mobile surveys was cattle grazing near the edge of the road. During the March 2014 survey, CH<sub>4</sub> emissions from cattle were also recorded by the teams from UNSW Australia (Bryce Kelly and Charlotte Iverach) and Royal Holloway, University of London (Dave Lowry, Rebecca Fisher and James France). Cattle emissions from feedlots and individual animals were observed at many locations throughout the other surveys made during the study period.

The CH<sub>4</sub> concentrations associated with cattle depended on the proximity to and number of cows and the prevailing wind conditions. In one case, where the vehicle was driven slowly within a few metres of cattle on an unfenced roadside and under essentially still conditions, the measured concentration was more than 10 ppm. Usually, however, CH<sub>4</sub> concentrations from individual cattle were much lower. A typical example of the measured CH<sub>4</sub> concentration profile encountered in the vicinity of cattle is shown in Figure 3.5.



**Figure 3.5. Methane concentration (dry basis) profile near grazing cattle and a large cattle feedlot (the CSIRO data used in this plot were initially processed by Bryce Kelly of UNSW). Maximum plume concentration was 0.64 ppm greater than background atmospheric methane concentration of 1.77ppm.**

In this example, which was measured at the same time as the UNSW and RHUL researchers, cattle grazing in a paddock within about 50 m of the road resulted in several CH<sub>4</sub> peaks up to about 1.83 ppm (i.e. about 0.07 ppm above ambient). Figure 3.5 also shows the emission profile from a large cattle feedlot located south east of Dalby. Here, a broad plume with a peak CH<sub>4</sub> concentration of about 2.4 ppm was measured about 1,000 m downwind of the feedlot. McGinn et al. (2008) estimated average CH<sub>4</sub> emissions from a cattle feedlot in this region of Queensland to be equivalent to  $166 \pm 90 \text{ g CH}_4 \text{ day}^{-1} \text{ animal}^{-1}$ . Assuming that this feedlot was operating at its maximum capacity of 26,500 head of cattle (JBS, 2014), the total CH<sub>4</sub> emission rate from the facility is equivalent to approximately 4,400 kg of CH<sub>4</sub> day<sup>-1</sup> or about 4,500 L min<sup>-1</sup>.

On another occasion a CH<sub>4</sub> plume about 600 m wide and a peak concentration of 7.8 ppm was detected about 700 m downwind of another large cattle feedlot in the region.

South eastern Queensland is a major cattle producing region and consequently there are numerous intensive feedlots operating within the study area. Figure 3.6 shows the location of many of these feedlots

(DAFF, 2014). Although the size of feedlots varies considerably (the example shown in Figure 3.5 is probably among the largest) these facilities nevertheless represent significant sources of CH<sub>4</sub> throughout the region.

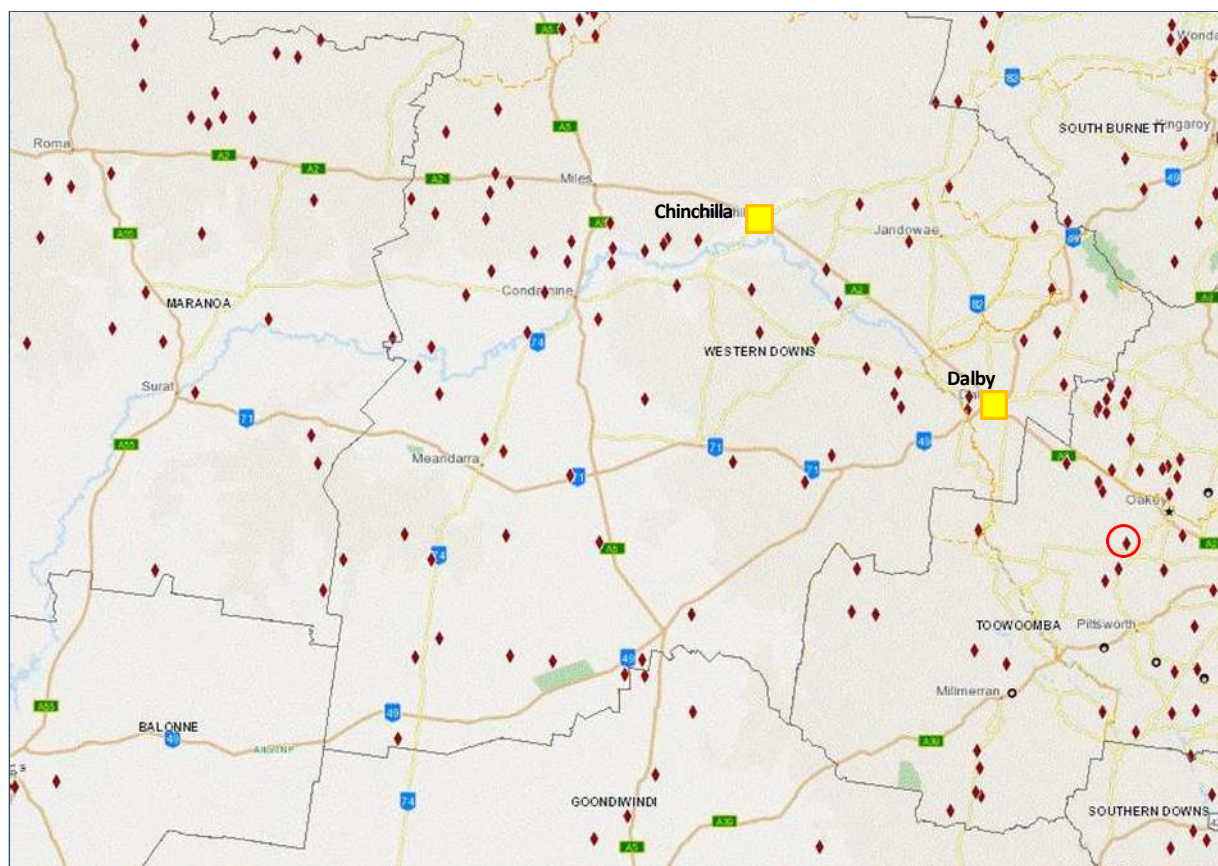


**Figure 3.6. Cattle feedlots, shown as red diamonds, within the study region (map generated from <http://wali.daff.qld.gov.au> on 10 Nov 2014). The location of the feedlot shown in Figure 3.3 is marked on the map by the red circle. © State of Queensland (Department of Agriculture, Fisheries and Forestry).**

Other biogenic sources included irrigation ponds and natural water bodies (Figure 3.7). In the example plotted in Figure 3.7, there is a significant increase in CH<sub>4</sub> concentration adjacent to a water storage impoundment and near the Condamine River. Although there are a number of well known CH<sub>4</sub> seepage sites along parts of the Condamine River that are believed to be derived from geological sources (Sherman et al., 2014), these are located much further downstream of the location shown in Figure 3.7. It is probable that the CH<sub>4</sub> measured at this location was produced by anaerobic microbial activity in the river. This tends to be supported by measurements of  $\delta^{13}\text{CH}_4$  in gas bubbles collected from upstream of the Condamine weir (Iverach et al., 2014). Keeling plots derived from measurements made at this site yielded  $\delta^{13}\text{CH}_4$  of -60 ‰ relative to Vienna Pee Dee belemnite (VPDB). While this is consistent with that associated with CH<sub>4</sub> derived from wetlands, it could also indicate a mixed CSG-aquatic system source. This ambiguity tends to highlight the difficulty of attributing CH<sub>4</sub> sources based on  $\delta^{13}\text{CH}_4$  alone.

Mobile ground surveys in the vicinity of the documented river CH<sub>4</sub> seep sites were not made during Phase 2 of this project because the land adjacent to the river seeps is privately owned; however, a separate study has determined that the total CH<sub>4</sub> flux from these sites is about 700 L min<sup>-1</sup> (Sherman et al., 2014). Airborne surveys were made over the river seeps during July 2014 as described in Section 5.



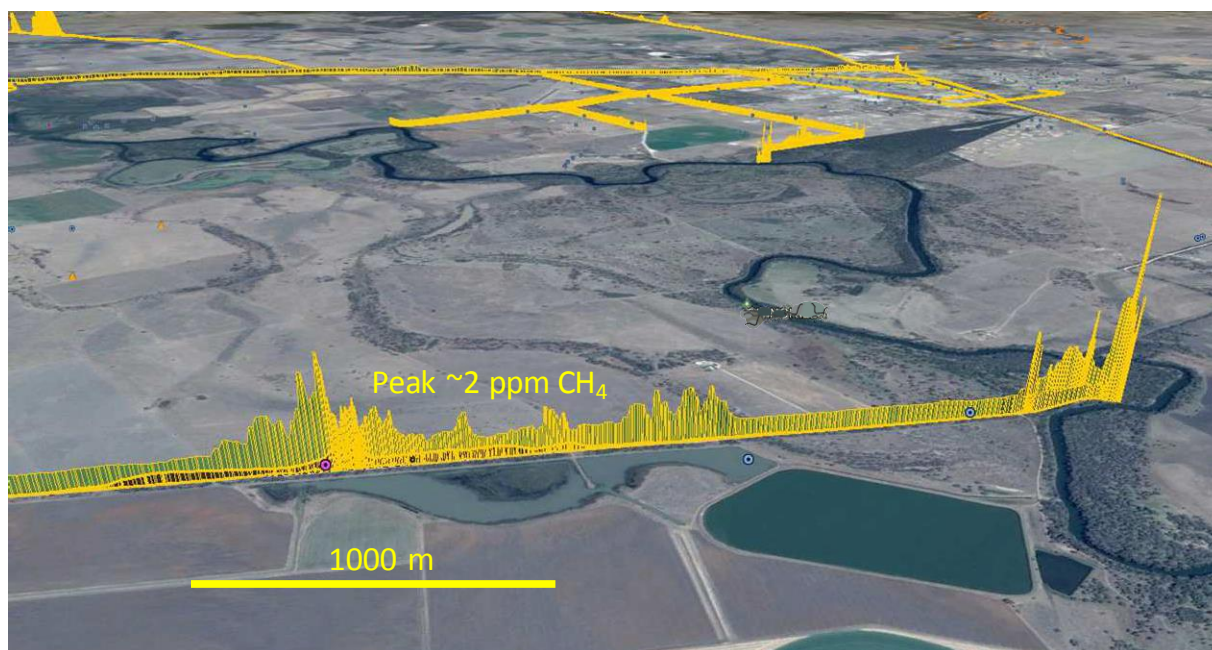


**Figure 3.7. An example of CH<sub>4</sub> detected near irrigation facilities and the Condamine River with a peak concentration about 0.23 ppm above the natural atmospheric background level of 1.77 ppm.**

Another occasional source of CH<sub>4</sub> was found to be bushfires. Bushfires are a significant source of CH<sub>4</sub> and it has been estimated that they contribute as much as 1502 Gg y<sup>-1</sup> in south eastern Australia (Wang and Bentley, 2002). During July 2014, a fire was burning near Chinchilla, probably as a result of hazard reduction activities ahead of the bushfire season. Methane levels of up to several ppm above ambient were detected when driving through the smoke plume.

Finally, landfills and sewerage treatment plants near population centres are also sources of CH<sub>4</sub>. There are numerous such facilities throughout the Surat, although it is expected that overall these would contribute relatively minor amounts of CH<sub>4</sub> compared to other sources within the region. During these surveys made as part of this study, elevated CH<sub>4</sub> concentrations were detected at landfill sites near Dalby and Macalister. At the Macalister site, a maximum CH<sub>4</sub> concentration of 2.4 ppm was recorded within 50 m of the tipping area.

### 3.2.3 CSG INFRASTRUCTURE

Some CSG facilities were found to be sources of CH<sub>4</sub> emissions. Occasionally slight perturbations in CH<sub>4</sub> concentrations were detected downwind of CSG wells located near roads. For example, a plume about 70 m wide with a maximum concentration of 1.82 ppm (i.e. 0.07 ppm enhancement above background) was detected about 100 m from a well located in a paddock.

Coal seam gas wells are likely to represent spatially distributed potential sources of CH<sub>4</sub> across large areas of the Surat Basin because of the large number of wells currently in operation and the expected increase in production over the coming years. Many of these wells are visible from public roads and the survey vehicle was driven past numerous CSG wells during the course of the project. Mostly, little or no CH<sub>4</sub> was detected from wells during these 'drive-bys'. This was because in many cases the wind direction was unfavourable (i.e. moving any plume away from the vehicle) but even under favourable wind conditions, CH<sub>4</sub> levels were low. On a few occasions, slightly elevated CH<sub>4</sub> concentrations of a few tens of ppb above background were observed when passing CSG wells within about 100 m of the road thus indicating that CH<sub>4</sub> was being emitted from these wells. Mostly, however, no CH<sub>4</sub> plume was detected downwind of CSG wells. Since many of these wells were several hundred metres from the road it is possible that any CH<sub>4</sub> emission occurring on the pad was too low to be detected at this distance. Closer monitoring would be required to confirm whether or not CH<sub>4</sub> was being released from these more distant wells.

To specifically examine the contribution of CSG wells to regional CH<sub>4</sub> emissions, we made a number of traverses near a gasfield west of Dalby in conjunction with researchers from the University of NSW and Royal Holloway University of London in March 2014. On this occasion, surveys were made along roads that enclosed a region about 10 × 10 km square containing around 100 CSG wells (Figure 3.8). Measurements were made during the morning over about three hours between 7 am and 10 am with a wind generally from the north east at between 1.5 to 3.5 m s<sup>-1</sup>.

As shown in Figure 3.8, CH<sub>4</sub> concentrations within the region were relatively constant and consistent with background levels, although there were several small peaks observed. Two of these peaks were from the exhaust of the vehicle while parked but there were two others on the eastern leg of the traverse. In both cases the CH<sub>4</sub> enhancement was approximately 50 to 60 ppb but did not appear to be derived from CSG operations within the survey area. One of these was a broad peak with a maximum concentration of 1.82 ppm. This may have been due to microbial activity occurring in the wetland within the Broadwater reserve. Another narrower peak of 1.83 ppm was also observed but in this case the source was not apparent since there were no CSG wells or other identifiable sources immediately upwind of the peak, although there were cattle in the region which may have been the source.

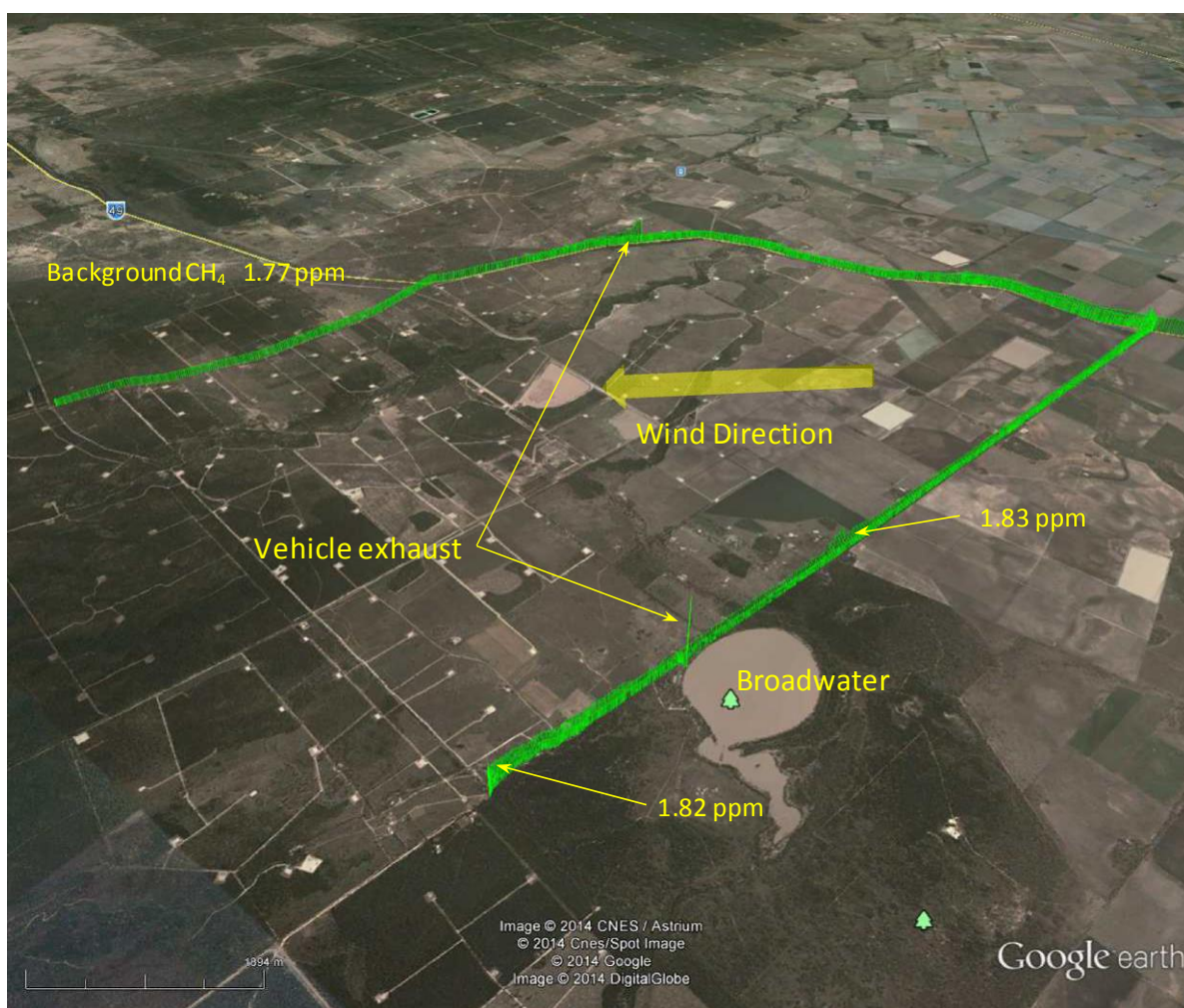


**Figure 3.8. Methane concentration (dry basis) profile measure around CSG wells near Dalby.**

Although mobile surveys did not locate significant emissions from CSG wells, it is nevertheless likely that wells do contribute to overall emissions in the region. Recent research (Day et al., 2014) has shown that most wells (albeit within a small sample of 43 wells) were emitting CH<sub>4</sub> to some extent. These emissions were found to be derived from equipment leaks, operation of vents and pneumatic equipment and exhaust from engines used to power dewatering pumps. Overall, the average emission rate from the 43 wells examined in that study was around 3.2 g CH<sub>4</sub> min<sup>-1</sup> (~5 L min<sup>-1</sup>); however, there was a wide range of emissions. Emissions from the CSG wells examined ranged from zero to 44 g min<sup>-1</sup> (67 L min<sup>-1</sup>). It is probable



that these relatively low emission rates would be difficult to detect during mobile surveys made several hundred metres or more downwind of the wells.

In addition to wells, high point vents were also found to be sources of methane within the study region. These vents are installed on water gathering networks to prevent gas locks from forming in the pipeline system and are designed to periodically vent gas to the atmosphere. During this study we noted a number of high point vents releasing gas which was indicated by the occasional audible ‘puff’ as the valves actuated. On one occasion when the vehicle was parked about 10 m from a vent, a CH<sub>4</sub> peak of 5.8 ppm was measured immediately after the vent operated (see Figure 6.12 in Section 6).

Other sources of CH<sub>4</sub> associated with CSG production that resulted in elevated ambient CH<sub>4</sub> concentrations were gas compression plants and water treatment facilities, which are distributed throughout the gas fields. An example of the CH<sub>4</sub> concentration profile along the Kogan-Condamine Road plotted as a function of the vehicle position is shown in Figure 3.9. This particular profile was measured during the early morning during the September 2013 field campaign.

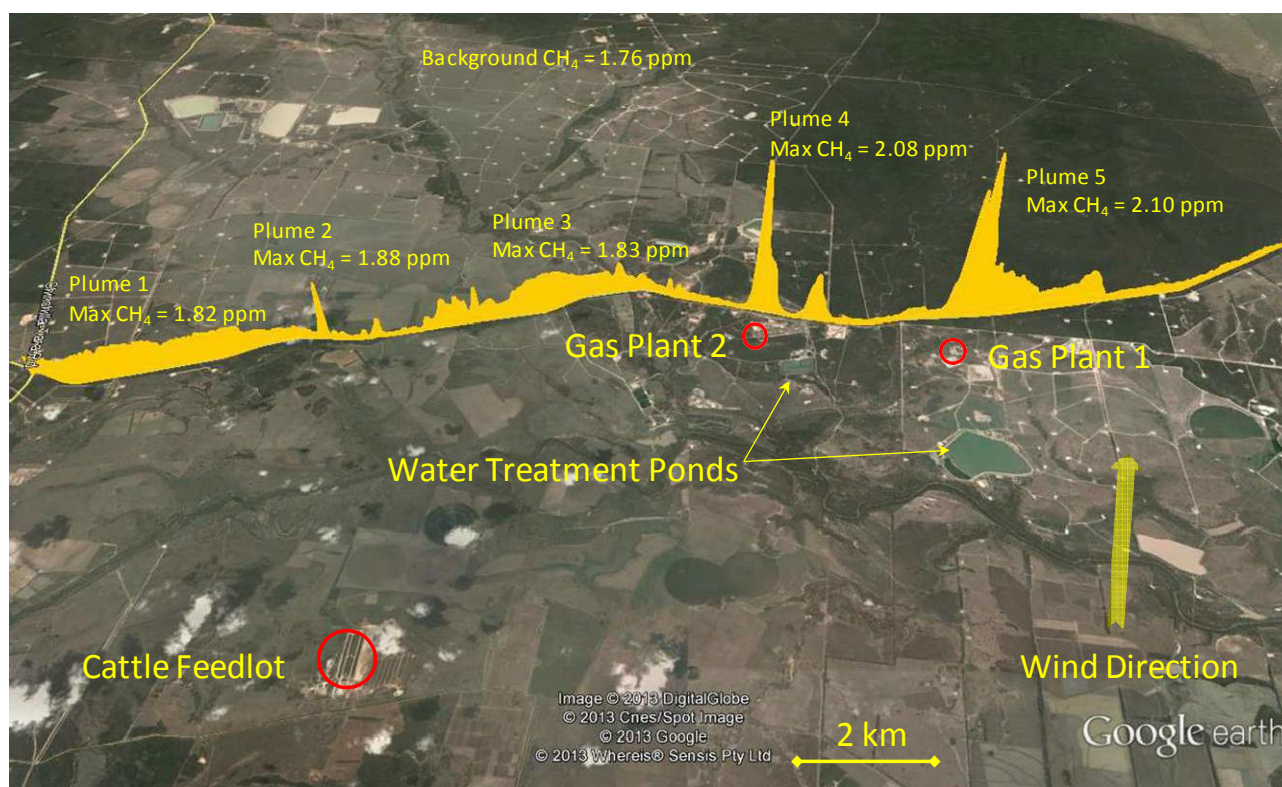


**Figure 3.9. CH<sub>4</sub> concentration profile on Kogan-Condamine Road. The scale of the CH<sub>4</sub> trace in this figure has been expanded to illustrate the location of the plumes detected; the maximum concentration detected was less than 0.35 ppm above the background concentration of approximately 1.76 ppm.**

A number of distinct plumes were identified during the traverses, two of which (Plumes 4 and 5 in Figure 3.9) were from two gas compression plants adjacent to the road. Both gas plants yielded double plumes with the larger peak in each case from the gas processing plant itself with a second smaller plume apparently derived from adjacent water treatment facilities. In the case of Gas Plant 1, there are a number of CSG wells upwind of the facility so some of the CH<sub>4</sub> in the plume detected during the traverse may have originated from these wells. The maximum concentration enhancement in these plumes was about 0.35 ppm above the background.

Emissions from gas processing facilities are not unexpected since they are known to emit CH<sub>4</sub> through vents and gas-actuated pneumatic devices (Clearstone Engineering, 2002). The engines that drive the compressors are also normally fuelled by CSG so it is probable that some unburnt CH<sub>4</sub> may be emitted in the exhaust. Water treatment plants and holding ponds are also likely to be sources as CH<sub>4</sub> degasses from the water. A recent study of CSG emissions in the Surat Basin also found elevated concentrations of CH<sub>4</sub> in

the vicinity of CSG infrastructure (Maher et al., 2014). Like the current GISERA study, the Maher et al. work was based on mobile surveys that were made on a route similar to that driven during the current study.

Several other CH<sub>4</sub> plumes besides those from the processing plants were detected during these traverses which are shown in Figure 3.9. The first (Plume 1) was about 4 km wide with a peak CH<sub>4</sub> enhancement of 0.07 ppm but the source of the methane is unclear. It may have originated from a number of leaking abandoned boreholes in the region that were found to be sources of CH<sub>4</sub> (see below) but other, as yet, unidentified sources may have also contributed. Plume 2 was from a small ground-level source adjacent to the road, also probably an old borehole. Plume 3 was most likely from a cattle feedlot located about 7.5 km upwind. The other two plumes (4 and 5) were from two gas compression plants and associated water treatment facilities.

During an initial traverse made during January 2013, only one plume was detected along this road which was attributed to Gas Plant 1, whereas in subsequent traverses, other sources were apparent. The reason for the absence of elevated methane levels during the January is probably related to the very hot conditions ( $T > 35\text{ }^{\circ}\text{C}$ ) at the time of the traverse. Under these conditions atmospheric mixing is high and consequently ambient CH<sub>4</sub> concentrations near the source are much lower than under more the stable conditions encountered during the September traverses.

### 3.2.3.1 Estimation of CH<sub>4</sub> Emissions Rates

The variation in the measured concentration of CH<sub>4</sub> illustrates the potential problems with attempting to assess the level of emissions by concentration data alone. It is more useful to report the emission rates from the sources. We therefore attempted to quantify the emissions from the sources detected on the Kogan-Condamine Road during an experiment conducted during September 2013. A number of traverses were made over two days along this road during the first two to three hours after sunrise when the mixing height was relatively low and ground level concentrations are enhanced. Due to the formation of a nocturnal inversion and the associated stable atmospheric conditions at the times of the traverses, it was necessary to estimate wind speed at higher levels than possible with the roof mounted anemometer. This was achieved by periodically releasing a helium-filled balloon and timing the duration of travel between two points about 200 m apart after the balloon had risen about 50-70 m above the ground. The direction of the balloon travel was also noted. Wind speed and direction were reasonably constant above tree height (~20 m). Background CH<sub>4</sub> concentrations were measured along the Leichhardt and Warrego Highways, upwind of the CH<sub>4</sub> sources examined.

Data from these traverses were used to estimate CH<sub>4</sub> emission rates from the two gas compression plants and the cattle feedlot using the general approach described in Section 2.1. However, because this methodology requires knowledge of the downwind distance from the emission source, we were unable to estimate the emission rate associated with Plume 1 because the location of the source was not known. Plume 2 was apparently from a ground based seep next to the road but the source appeared to be on both sides of the road. Hence the traverse passed through the centre of the emission source so downwind traverses could not be applied in this case. The emission rate from this source was estimated separately using surface flux chambers as discussed later in this report.

The emission rates estimated for the two gas processing facilities and feedlot are summarised in Table 3.4.

**Table 3.4. Emission rate estimates derived from plume traverses along the Kogan-Condamine Road during September 2013.**

	Source	Maximum CH Enhancement (ppm)	Wind Speed (m s <sup>-1</sup> )	Emissions Rate (kg day <sup>-1</sup> )
Day 1	Gas Plants 1 and 2	0.055	1	1650
	Feedlot	0.15	1	2300
Day 2	Gas Plant 1	0.36	3.1	850
	Gas Plant 2	0.40	3.1	650
	Feedlot	0.065	3.1	1200

During the Day 1 traverses, the plumes from the two gas plants were not fully resolved probably due to the low wind speed of about 1 m s<sup>-1</sup> and hence the emission rate is shown combined for both plants. Assuming that the plants each contribute half the emissions, the emission flux from each plant is equivalent to about 820 kg CH<sub>4</sub> day<sup>-1</sup>. This is in reasonable agreement with the results obtained during Day 2 of 850 and 650 kg CH<sub>4</sub> y<sup>-1</sup> for Gas Plants 1 and 2, respectively.

The feedlot emissions were estimated to be 2300 kg CH<sub>4</sub> day<sup>-1</sup> during the Day 1 traverses but only about half this figure on Day 2. While it is possible that the wide variation in these results was due to changes in the feedlot's operation (e.g. large changes in cattle population), it seems more likely that the variability is the result of the inherent uncertainty associated with the ground level traversing methodology used to estimate these emissions.

Although the ground level traverses provided an accurate measure of the CH<sub>4</sub> concentration profile in the horizontal plane of the plumes, the vertical extent had to be estimated based on knowledge of plume dispersion characteristics. Under some conditions, ground level plume measurement can provide accurate emission estimates. For instance, Loh et al. (2009) applied the method to measure emissions from a controlled release experiment to generally within 10 % of the actual emission rate. Humphries et al. (2012) reported uncertainties of 3 % for a similar experiment using a network of fixed monitors located around a controlled release of CH<sub>4</sub>. In a previous study of fugitive emissions from individual CSG wells, we used near field vehicle traverses (i.e. within 50 m of the source) to estimated emissions rates where controlled release experiments yielded uncertainties of around 30 % (Day et al., 2014).

However, all of these studies were made at much smaller scales where the plume rise was relatively small. In the measurements made on the Kogan-Condamine Road, the sources were much larger in area and more distant. Moreover, the emissions within these sources are likely to be distributed unevenly throughout the facility. Consequently there is likely to be a much higher level of uncertainty associated with determining the vertical dispersion of the plumes.

While it is difficult to quantify the uncertainty on these measurements, previous work suggests that the uncertainty may be of the order of a factor of two or more. Williams et al. (1994) used ground level traverses to estimate CH<sub>4</sub> emissions from open-cut coal mines in NSW and Queensland using essentially the same technique as used here. They estimated that the uncertainty was about a factor of two. More recently, Lilley et al. (2012) used a similar method (among others) to measure greenhouse gas emissions from self-heating in spoil at open-cut coal mines. In that case the traversing method yielded emission rates that varied by a factor of three. Some of this variability was attributed to seasonal effects, however, it was also noted that the largest source of uncertainty lay with determining the plume characteristics.

Because of the uncertainties associated with these emission rate estimates it is stressed that the data presented in Table 3.4 are indicative only and cannot be interpreted as accurate emission rates from these facilities. Further work is required to better define the emissions from these sources. The atmospheric 'top-



down' method using a network of fixed monitoring stations proposed for Phase 3 of this project (see Section 6) is likely to significantly reduce the uncertainty of flux estimates for CH<sub>4</sub> sources, including major CSG infrastructure such as gas processing facilities.

### 3.2.4 SEEPS

During the mobile surveys a number of localised CH<sub>4</sub> plumes were found that were not directly associated with CSG facilities, agriculture or other obvious sources. Many of the peaks detected were minor, with CH<sub>4</sub> concentration enhancements of only a few tens of ppb. Often when travelling near rivers and creeks small CH<sub>4</sub> peaks were observed, which as discussed above, were probably due to aquatic microbial activity. Figure 3.10, for example, shows a small peak with a maximum concentration of 1.77 ppm (i.e. ~20 ppb above background) on Charleys Creek near Chinchilla. However, there were numerous occasions when much higher methane concentrations were encountered. This is illustrated in Figure 3.10 where three significant but narrow peaks were found within a distance of less than 4 km on Greenswamp Road west of Chinchilla.

Where practical, when such peaks were observed, low speed (<1 m s<sup>-1</sup>) traverses were made to locate the source of CH<sub>4</sub>. Concentrations in excess of 20 ppm were sometimes observed during these traverses and at all locations, CH<sub>4</sub> was found to be seeping from the ground surface. In some cases where the wind conditions and access were favourable, downwind plume traverses were made to estimate the emission rate from these sources using the method described in Section 2.1.

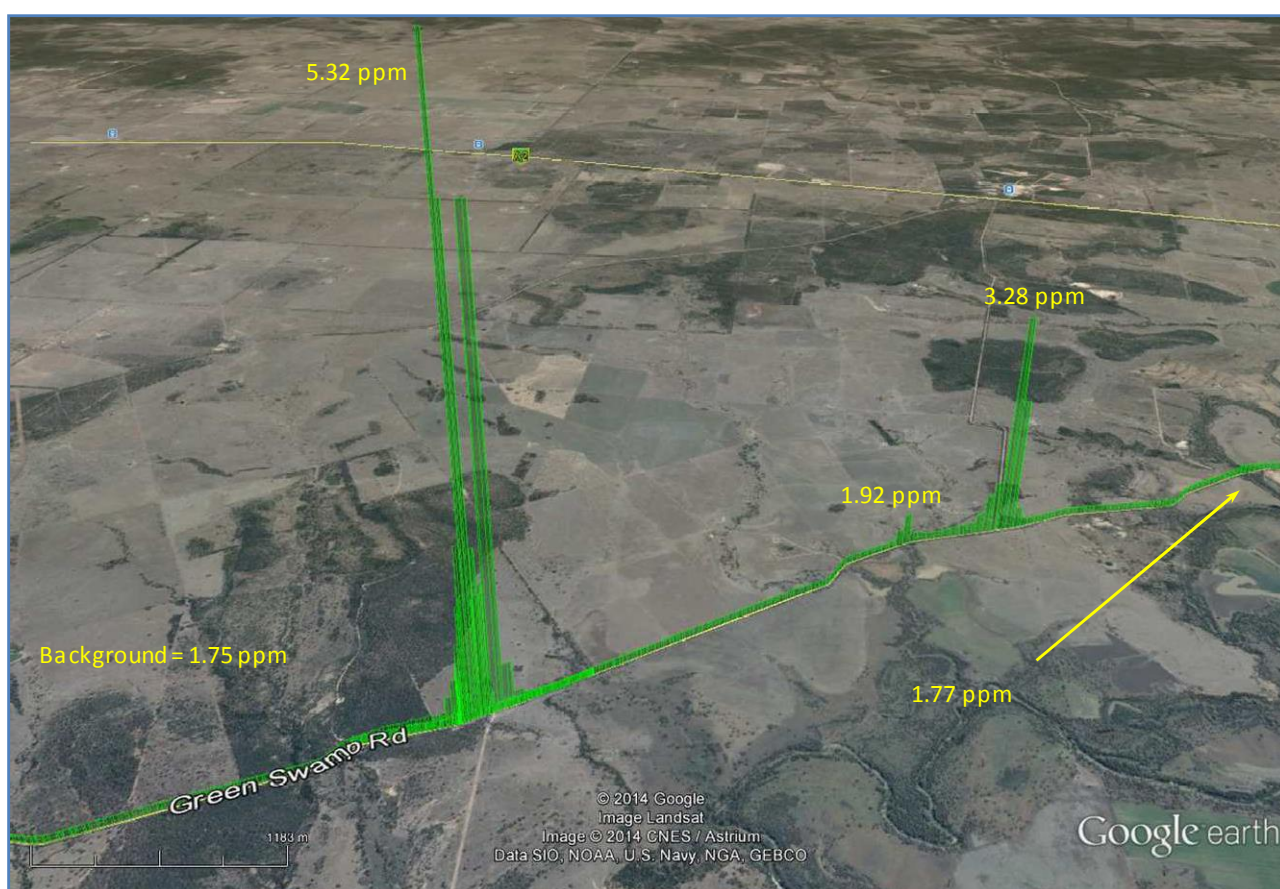


**Figure 3.10. CH<sub>4</sub> plumes associated with ground seeps. Peak of 3.28 ppm CH<sub>4</sub> is located at seep Site 1 and peak of 5.32 ppm CH<sub>4</sub> is at Site 2 (see Table 3.5). Note that the CH<sub>4</sub> concentrations are not corrected for atmospheric moisture content because the analyser was operating in 'locator' mode.**

An example of the results of traverses made at one site (Site 1) is shown in Figure 3.11 where the CH<sub>4</sub> concentration profile of the plume during four individual traverses is plotted as a function of distance across the plume.

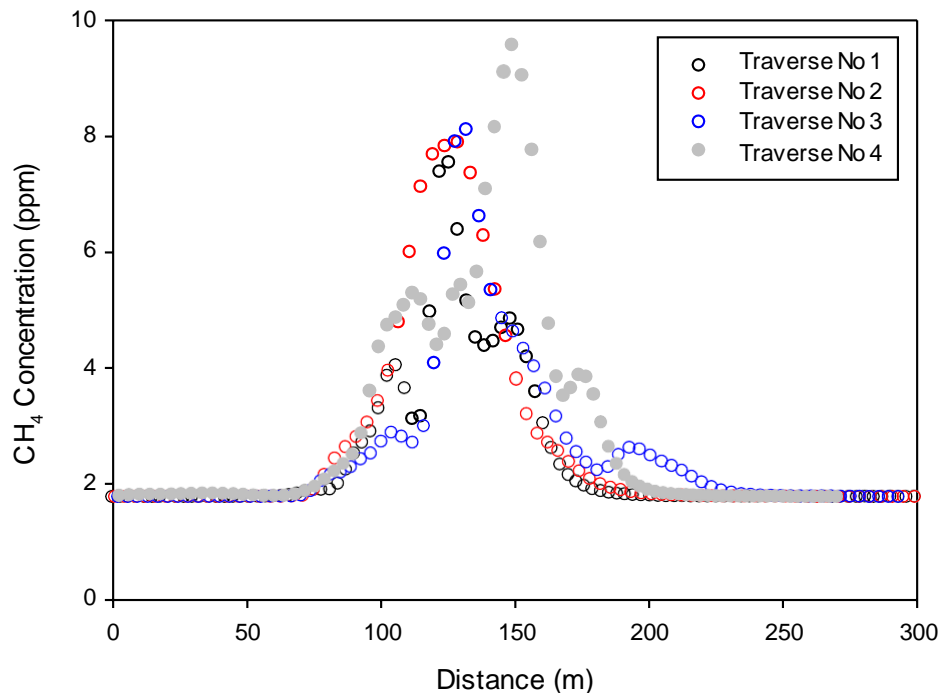


**Figure 3.11. Methane concentration as a function of distance across the plume originating from Site 1.**

In this example, measured during September 2013, the plume was reasonably constant in profile with a maximum concentration of around 10 ppm and a total width of approximately 100 m. Based on these traverses the emission rate from the site was estimated to be  $55 \text{ g CH}_4 \text{ min}^{-1}$  or about  $80 \text{ kg day}^{-1}$  (Table 3.5). An earlier set of traverses made during January 2013 yielded an emission rate of about  $49 \text{ kg day}^{-1}$ , which given the inherent uncertainty of this method is reasonable agreement. It is also possible that there is some temporal variation in emissions from the site which would also contribute to the difference.

Traversing measurements were made at two other ground seeps; Site 3 and Site 10 (Table 3.5). Like Site 1, Site 3 was also on the side of a public road and plume  $\text{CH}_4$  concentrations of up to 10 ppm were measured about 20 m downwind of the site, yielding an estimated emission rate of more than  $100 \text{ kg day}^{-1}$  (Table 3.5). Site 10, on the other hand, yielded much lower levels of  $\text{CH}_4$  emissions. Methane was detected within 10 m of the source but the maximum concentration observed was less than 0.05 ppm (50 ppb) above background. The emission rate from Site 10 was estimated to be less than  $0.1 \text{ kg CH}_4 \text{ day}^{-1}$ .

Site 10 was on private land and according to the property owner, was the site of an exploration borehole drilled about 30 years ago. The property owner also identified two other abandoned coal exploration boreholes drilled during the 1980s; however we found no sign of elevated  $\text{CH}_4$  at either of these locations.

A number of other known abandoned exploration boreholes were examined at another property. In this case the land holder had a detailed map showing the location of individual coal exploration boreholes drilled during 2008. These holes have since been covered and the sites rehabilitated. Only one of these sites (Site 9) yielded slightly elevated  $\text{CH}_4$  levels in the vicinity of the hole although we were unable to derive flux estimates from the ambient  $\text{CH}_4$  concentration data in this case (but surface flux measurements were made). No  $\text{CH}_4$  was detected at the other five locations identified as abandoned boreholes.

Surface flux measurements were made at all of the sites found to be seeping  $\text{CH}_4$  except Site 10 where thick vegetation cover precluded the use of the flux chamber. At Site 1, 50 individual flux chamber measurements were made within a  $40 \times 80 \text{ m}$  area to define the spatial extent of the source. Surface emission rates ranged from zero up to  $270 \text{ g day}^{-1} \text{ m}^{-2}$  with the highest emissions concentrated within an area less than  $20 \times 20 \text{ m}$  square (Figure 3.12). Measurements made at other sites yielded generally similar profiles in that emissions were concentrated within a very localised area, sometimes within only a few square metres. In all cases, the bulk of the  $\text{CH}_4$  emissions were centred on a relatively small region as

shown in the examples in Figure 3.12 where the surface emission rate is plotted as a function of the x and y distance (note the different scales in the vertical axes in each plot).

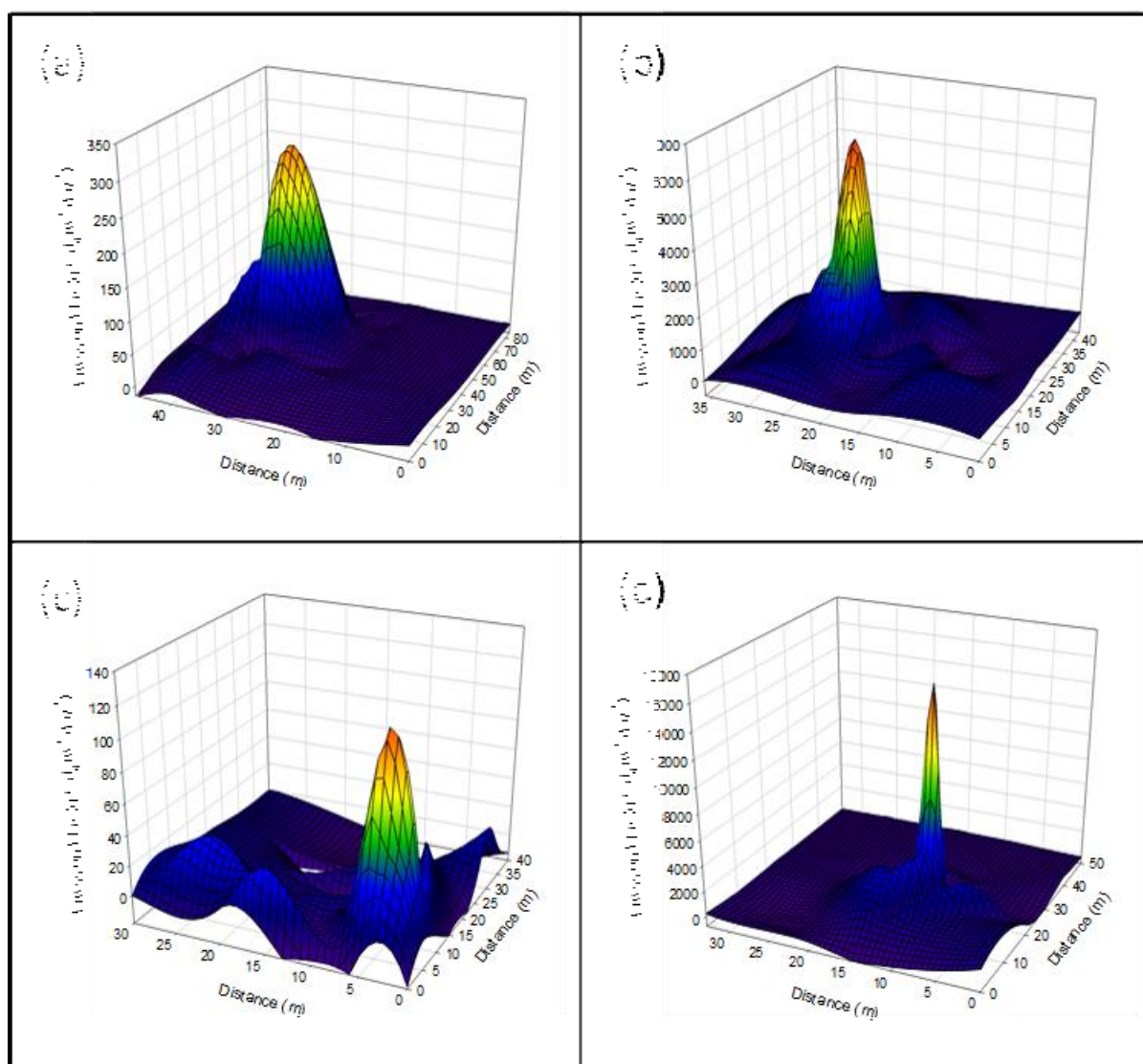


**Figure 3.12. Surface emission profiles measured by surface chambers at Site 1(a), Site 2 (b), Site 5 (c), and Site 6 (d). Note that the vertical scales vary significantly in each plot.**

While surface flux measurements confirmed that CH<sub>4</sub> emissions were generally localised at each site, the emission intensity varied considerably. At Site 5, for instance, the maximum emission rate was about 100 g m<sup>-2</sup> day<sup>-1</sup> whereas at Site 6, the highest emission rate measured was more than 14,000 g m<sup>-2</sup> day<sup>-1</sup> (Figure 3.12).

The total emission flux from each site was calculated by integrating the data presented in Figure 3.12 across the area of measurement; the results are summarised in Table 3.5 along with the emission rates determined by plume traverses, where available.

**Table 3.5. Summary of emission flux results made by the flux chamber and traversing methods at 10 ground surface sources. NA means measurements were not made.**

Site	Location	Emission Rate (kg day <sup>-1</sup> )	
		Traverse	Flux Chamber
Site 1 Jan 2013	26°46'48.51"S, 150°31'20.85"E	48.8	46.6
Site 1 Sept 2013	26°46'48.51"S, 150°31'20.85"E	79.8	na
Site 2	26.79670655°S, 150.48894°E	na	102
Site 3	26°48'59.49"S, 150°32'10.90"E	103	61.3
Site 4	26°52'45.36"S, 150°26'2.39"E	na	7.1
Site 5	26°49'46.15"S, 150°36'9.89"E	na	3.7
Site 6	26°49'53.58"S, 150°37'8.55"E	na	51.5
Site 7	26°53'18.09"S, 150°42'16.88"E	na	1.7
Site 8	26°55'21.92"S, 150°41'57.40"E	na	1.0
Site 9	26°32'44.37"S, 150°14'39.86"E	na	0.2
Site 10	27°01'04.50"S, 150°57'12.26"E	0.1	na

The emission rates estimated from these ground seeps ranged over three orders of magnitude from less than 0.1 kg CH<sub>4</sub> day<sup>-1</sup> at Site 10 up to more than 100 kg CH<sub>4</sub> day<sup>-1</sup> at Site 2.

The source of the emissions at most of the sites examined was not immediately apparent since there were no surface manifestations associated with the emissions (such as vegetation dieback, discolouration of the ground etc.). Gas samples collected from Sites 2 and 3 yielded  $\delta^{13}\text{CH}_4$  values of -56.9 ‰ and -50.1 ‰ VPDB, respectively (Table 3.1). This compares with  $\delta^{13}\text{CH}_4$  value of -50.9 ‰ VPDB measured for a sample of coal seam gas collected from a well in this region. The isotopic composition of the gas from Site 3 is very close to that of produced CSG tending to confirm its geological origin. However, the sample from Site 2 is somewhat depleted in <sup>13</sup>C compared to CSG suggesting a stronger biological component. Measurements made by Iverach et al. (2014) at Site 2 also yielded a  $\delta^{13}\text{CH}_4$  value of about -60 ‰ VPDB. Despite this, however, it seems likely that the gas being emitted from these ground seeps was in fact derived from coal seams. An informal conversation with a long-term resident in the region confirmed that exploration drilling occurred at Site 2 during the 1970s. Moreover, the emission profiles of these sites are consistent with those measured at abandoned oil and gas wells in the United States (Etiope et al., 2013), although natural seeps have also been found to occur over relatively small regions (Etiope, 2010). The presence of a borehole was confirmed at Site 3 when at the end of the measurements we attempted to mark the maximum emission point with a metal stake. When driving the stake into the ground, the overlying soil collapsed revealing a borehole about 200 mm in diameter. When the hole was cleared the gas flow appeared to increase with a discernible breeze at the opening of the hole.

The reason for relatively light  $\delta^{13}\text{CH}_4$  results obtained at Site 2 is unclear. One explanation is that there is a significant amount of biological activity occurring in the subsoil that is enriching the biogenic component of CH<sub>4</sub> in the gas reaching the surface. However, it is difficult to make a definitive conclusion in this regard because of the wide range of isotopic data that have been reported for the region. For instance Hamilton et al. (2014) found isotopic ratios in the Walloon coal measures range from -58.5 ‰ to -45.3 ‰ which clearly shows that there is a genuine substantial variation in isotopic makeup in the gas within the



coal. This therefore makes source attribution on stable carbon isotopes alone difficult. Sherman et al. (2014) has also noted high levels of variability in isotopic ratios of gas collected from the Condamine River seeps which complicates source attribution. When taken together with the other isotopic data the source of the gas seems to be similar in origin to other geological sources within the region which tends to support the notion that these sites are indeed leaking boreholes.

Because of the exposed open hole at Site 3, the Queensland Department of Natural Resources and Mines capped the hole with concrete about two weeks after the initial flux measurements in accordance with a policy to remediate abandoned boreholes (DNRM, 2013). During November 2013 about four weeks after the borehole at Site 3 was capped, a follow up visit was made to this site to remeasure surface emissions. The results are summarised in Figure 3.13.

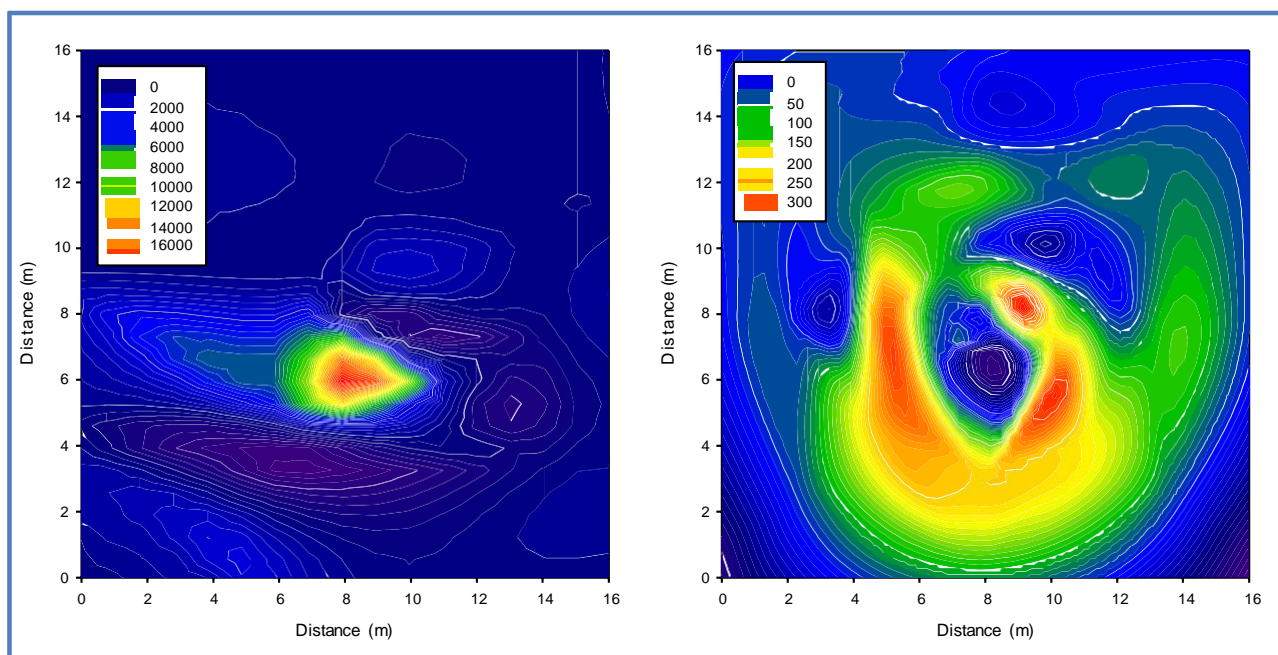


**Figure 3.13. Surface CH<sub>4</sub> emission profile at Site 6 before capping (left hand plot) and after the exposed borehole was filled with concrete (right hand plot). Units are kg CH<sub>4</sub> y<sup>-1</sup> m<sup>-2</sup>.**

The left hand image in Figure 3.13 shows the original measurements where the total flux from the site was estimated to be approximately 61 kg CH<sub>4</sub> day<sup>-1</sup>. After the hole had been capped, CH<sub>4</sub> emissions continued despite the presence of the concrete plug although the profile was substantially altered as shown in the right hand image in Figure 3.13. The reduction in emissions from the original hole is clearly evident; however, a significant amount of CH<sub>4</sub> has bypassed the concrete plug to find alternative routes to the surface. Integrating the data yielded an overall emission rate of 14 kg CH<sub>4</sub> day<sup>-1</sup>, i.e. about a quarter of the emission rate before capping.

It is understood that there are many 'legacy' boreholes drilled throughout Queensland although the exact number is unknown. Since these boreholes were drilled long before GPS was available, their locations are often poorly defined, if at all and consequently, they are difficult to locate. In this study leaking boreholes were located by their CH<sub>4</sub> signature. Most of the boreholes located to date have been in the Chinchilla region although it is certain that there are many boreholes spread over large areas of the Surat Basin. Some of these may also be leaking and further work is required to fully assess the extent to which legacy boreholes are contributing to the overall CH<sub>4</sub> emissions in the region.

While some of the boreholes found during this study individually had significant CH<sub>4</sub> emissions, it seems likely that many of the legacy boreholes are not leaking. In addition to the 10 sites where CH<sub>4</sub> was found to be leaking, there were eight others that were identified as old boreholes that showed no signs of CH<sub>4</sub> leakage. A key challenge is to undertake an audit of legacy boreholes to determine their contribution to the region's CH<sub>4</sub> budget.



The variation of emissions with time may also be an important aspect. It is not known when the boreholes started to emit CH<sub>4</sub>. It is possible that progressive reduction in the level of groundwater through extraction for irrigation or gas production may initiate gas flow that would otherwise not occur with higher water levels. The interaction of gas flow and hydrology is an important area of ongoing research.

### 3.2.5 NATURAL SURFACES

Surface flux chamber measurements were made at a six other locations throughout the study region. These sites ranged from dry compacted soil, pasture and moist soil along water courses. A brief description of each site is provided below. In addition to these sites, measurements were made at three other locations well outside the Surat Basin. These are also described below.

*Site A.* Dry largely bare surface in a lightly wooded area next to Greenswamp Road, approximately 10 km west of Chinchilla; approximate location: -26.798°S, 150.485°E. This site was several hundred metres west of the seep at Site 2.

*Site B.* Grassed surface adjacent to pasture on Greenswamp Road about 500 m east of Charley's Creek; approximate location: -26.773°S, 150.547°E. The ground at this site was moist from recent rain.

*Site C.* Dry compacted surface along the Chinchilla-Kogan Road. This site was within about 100 m of the seep at Site 4; approximate location: -26.879°S, 150.434°E.

*Site D.* Dry compacted surfaces within a CSG field. Measurements were made within about 500 m of several CSG wells; approximate location -26.955°S, 150.361°E.

*Site E.* Sandy beach at the Chinchilla Weir reserve; approximate location -26.801°S, 150.581°E.

*Site F.* Sandy bed of the Condamine River about 17 km west of Dalby; approximate location -27.122°S, 151.091°E.

*Other Sites.* Soil CH<sub>4</sub> flux was also measured at Yaegl Nature Reserve on the north coast of NSW (approximate location -29.453°S, 153.220737°E), Newcastle Energy Centre (approximate location -32.885°S, 151.727693°E) and Girraween National Park (approximate location -28.832°S, 151.938°E). Although each of the three sites are quite different, the results have been grouped together since only a small number of measurements were made at each site and differences in emissions rates between sites could not be discerned.

Because CH<sub>4</sub> fluxes associated with natural surfaces are usually very low, measurements on these surfaces were made during this study using only the Picarro system (i.e. not the West Systems portable flux meter with much lower sensitivity), which has sufficient sensitivity to measure concentration changes of less than a few parts per billion.

The results of the soil flux measurements from these sites are summarised in Table 3.6.

**Table 3.6. Summary of soil flux measurements made on natural surfaces. Units are in  $\text{mg CH}_4 \text{ m}^{-2} \text{ day}^{-1}$ .**

	Site A	Site B	Site C	Site D	Site E	Site F	Others
n	3	8	5	5	3	9	8
Minimum	-7.58	-4.19	-1.23	-0.52	1.94	-0.19	-1.00
25 <sup>th</sup> percentile	-3.81	-0.74	-1.06	-0.51	2.22	0.50	-0.59
Median	-0.05	0.26	-1.04	-0.19	2.50	5.76	3.49
25 <sup>th</sup> percentile	0.81	6.00	-0.25	0.03	3.42	275.89	0.19
Maximum	1.67	902.73	0.26	0.95	4.35	418.36	62.79

The soil  $\text{CH}_4$  fluxes measured at these sites were unsurprisingly very much lower than those measured at the seep sites described previously. At most sites where moisture was present, slight  $\text{CH}_4$  emissions were measured. The highest of these (Site B) was on muddy soil immediately adjacent to a large puddle amongst a stand of trees, with an emission rate of about  $900 \text{ mg CH}_4 \text{ m}^{-2} \text{ day}^{-1}$  (cf.  $> 14,000 \text{ g CH}_4 \text{ m}^{-2} \text{ day}^{-1}$  measured at the ground seep at Site 2). Methane emissions of up to about  $400 \text{ mg CH}_4 \text{ m}^{-2} \text{ day}^{-1}$  were also measured on wet sand at the edge of stagnant pool in the Condamine River while somewhat lower emissions were found at the water's edge upstream of the Chinchilla Weir. However,  $\text{CH}_4$  emissions dropped substantially even short distances from the wet areas. It is most likely that these  $\text{CH}_4$  emissions were a result of anaerobic microbial activity within the soil at the time the measurements were made.

While some of the sample sites with free water were found to be emitting small amounts of  $\text{CH}_4$ , most of the others sites yielded negative emissions, i.e. the soil was consuming  $\text{CH}_4$  from the atmosphere. This phenomenon is the result of certain microorganisms capable of oxidising  $\text{CH}_4$  in aerated soils. Methane uptake rates are dependent upon many factors including type of soil, temperature, moisture content, level of aeration and numerous others (Dalal et al, 2008). Published values therefore vary widely although Dalal et al. (2008) suggest that on average  $\text{CH}_4$  uptake is generally less than  $100 \mu\text{g CH}_4 \text{ m}^{-2} \text{ h}^{-1}$  ( $2.4 \text{ mg CH}_4 \text{ m}^{-2} \text{ day}^{-1}$ ). Kiese et al. (2008) reported a maximum  $\text{CH}_4$  uptake rate for a Queensland rainforest during the dry season of  $109 \mu\text{g CH}_4 \text{ m}^{-2} \text{ h}^{-1}$  ( $2.6 \text{ mg CH}_4 \text{ m}^{-2} \text{ day}^{-1}$ ) while Crill (1991) found  $4.9 \text{ mg CH}_4 \text{ m}^{-2} \text{ day}^{-1}$  in a hardwood forest in the United States.

Methane uptake rates at these sites ranged from approximately  $0.04$  to about  $7 \text{ mg m}^{-2} \text{ day}^{-1}$ , which are consistent with previous published studies.

The measurements made at these sites provide a basis for comparison but the spatial distribution is not sufficient to provide detailed information on natural sources and sinks in the region. It is however an important aspect in relation to overall regional methane fluxes and it is therefore anticipated that further surface flux measurements will be made throughout the region during Phase 3 of the project.

## 4 SCIAMACHY Satellite

### 4.1 Instrumentation

The satellite SCIAMACHY sensor is a passive remote sensing spectrometer acquiring backscattered, reflected, transmitted or emitted radiation from the atmosphere and Earth's surface, operating in the wavelength range between 240 and 2380 nm (Burrows et al., 1995). The typical footprint of SCIAMACHY is 30 km (along track) by 60 km (across track) at nadir and the maximum swath width is 960 km. The sensor characteristics for SCIAMACHY are tabulated on Table 4.1. Channels 6 and 8 are used for retrieving CH<sub>4</sub> data, depending on the retrieval algorithm used.

**Table 4.1. Spectral configuration of the SCIAMACHY instrument from Gottwald and Bovensmann (2013)**

Channel	Spectral Range (nm)	Resolution (nm)	Spectral Stability (nm)	Operating Temperature Range (K)
1	214 - 334	0.24	0.003	204.5 – 210.5
2	300 - 412	0.26	0.003	204.0 – 210.0
3	383 - 628	0.44	0.004	221.8 – 227.8
4	595 - 812	0.48	0.005	222.9 – 224.3
5	773 - 1063	0.54	0.005	221.4 – 222.4
6	971 - 1773	1.48	0.015	197.0 – 203.8
7	1934 - 2044	0.22	0.003	145.9 – 155.9
8	2259 - 2386	0.26	0.003	143.5 – 150.0
9	214 - 334	0.24	0.003	204.5 – 210.5

There is potential for the SCIAMACHY data to be used to understand regional scale impacts, as shown by Schneising, et al. (2014) and Kort et al. (2014), where the data were used to highlight underrepresentation of emissions values from the fossil-fuel extraction activities in the Bakken and Eagle Ford formations and Four Corners region in the USA, respectively. The size of the Surat Basin, at approximately 320,000 km<sup>2</sup>, is much smaller than the Four Corners region but with a spatial resolution of 30 × 60 km, the SCIAMACHY image still contains 177 pixels.

### 4.2 Methane Retrieval Algorithms and Data Used for Analysis

There have been quite a few algorithms developed for the retrieval of the different trace gases since the launch of SCIAMACHY. The ones specific to CH<sub>4</sub> include Weighting Function Modified DOAS (WFM-DOAS) developed by the Institute for Environmental Physics, University of Bremen (Buchwitz et al., 2000; Buchwitz et al., 2005; Buchwitz et al., 2006; Schneising et al., 2009), Iterative Maximum Likelihood Method (IMLM) developed by the Space Research Organization Netherlands (SRON) (Gloudemans et al., 2005) and Iterative Maximum A Posteriori-DOAS (IMAP-DOAS) developed by the University of Heidelberg (Frankenberg et al., 2005).

The WFM-DOAS and the IMAP-DOAS algorithms rely on channel 6, which is tuned for the 1.65  $\mu\text{m}$  methane absorption feature, while the IMLM algorithm uses channel 8, which is tuned for the 2.3  $\mu\text{m}$   $\text{CH}_4$  absorption feature (see Table 4.1).

Most of the data collected over the operational life of the SCIAMACHY have been processed to retrieve the column methane using the WFM-DOAS and IMAP-DOAS algorithms and are accessible to the general public. These retrieved column methane measurements, available for the time period 2003-2012 for the IMAP-DOAS and for 2003-2009 for WFM-DOAS, were acquired for further analysis for this project. Note that the latest version of WFM-DOAS (v3.7) covers the time period October 2002 to December 2011.

The WFM-DOAS methane data product that was used for this study was the level 3 product (version 2.02) containing the gridded quality filtered data at monthly time resolution. The monthly data are a composite of data flagged as good quality for the calendar month. These data provide the methane column-averaged mole fraction at the geolocation of the given grid cell, which is gridded at 0.5° spatial resolution. More information on the data products and algorithms used can be obtained from Schneising and Heymann (2012).

The level 3 IMAP-DOAS data (version 6.0) was also used to generate the methane product. Similar to the WFM-DOAS, this product also has been filtered for quality and provides the monthly average but was gridded at 2° spatial resolution. See Scheepmaker and Frankenberg (2007) for more information on these data products.

### 4.3 Additional Data Analysis

The analysis conducted on the SCIAMACHY data included calculation of the statistical maximum, minimum, mean and standard deviation. These statistics were calculated for each of the monthly average data for the areas defined as the Surat Basin and the whole continent of Australia without the Surat Basin. These data are intended to be used to determine if a trend can be observed through time for the Surat Basin and to compare this trend for the Basin against the rest of Australia.

### 4.4 Results from SCIAMACHY Data Analysis

Figure 4.1 shows the column methane product generated using the WFM-DOAS algorithm and produced by University of Bremen for the month of October in 2003, while Figure 4.2 shows the methane product generated using the IMAP-DOAS algorithm and produced by SRON/JPL for the same month in 2003. The outline of the Surat Basin, which was used for extracting the statistics, is shown on Figure 4.1 in the central eastern portion of Australia. Generally, the two images (and images of the same month produced from the two algorithms) show the same patterns. That is, Northern Australia and areas of population build up showing higher levels than Southern Australia. However, there are differences in the absolute column methane levels between the two algorithms.

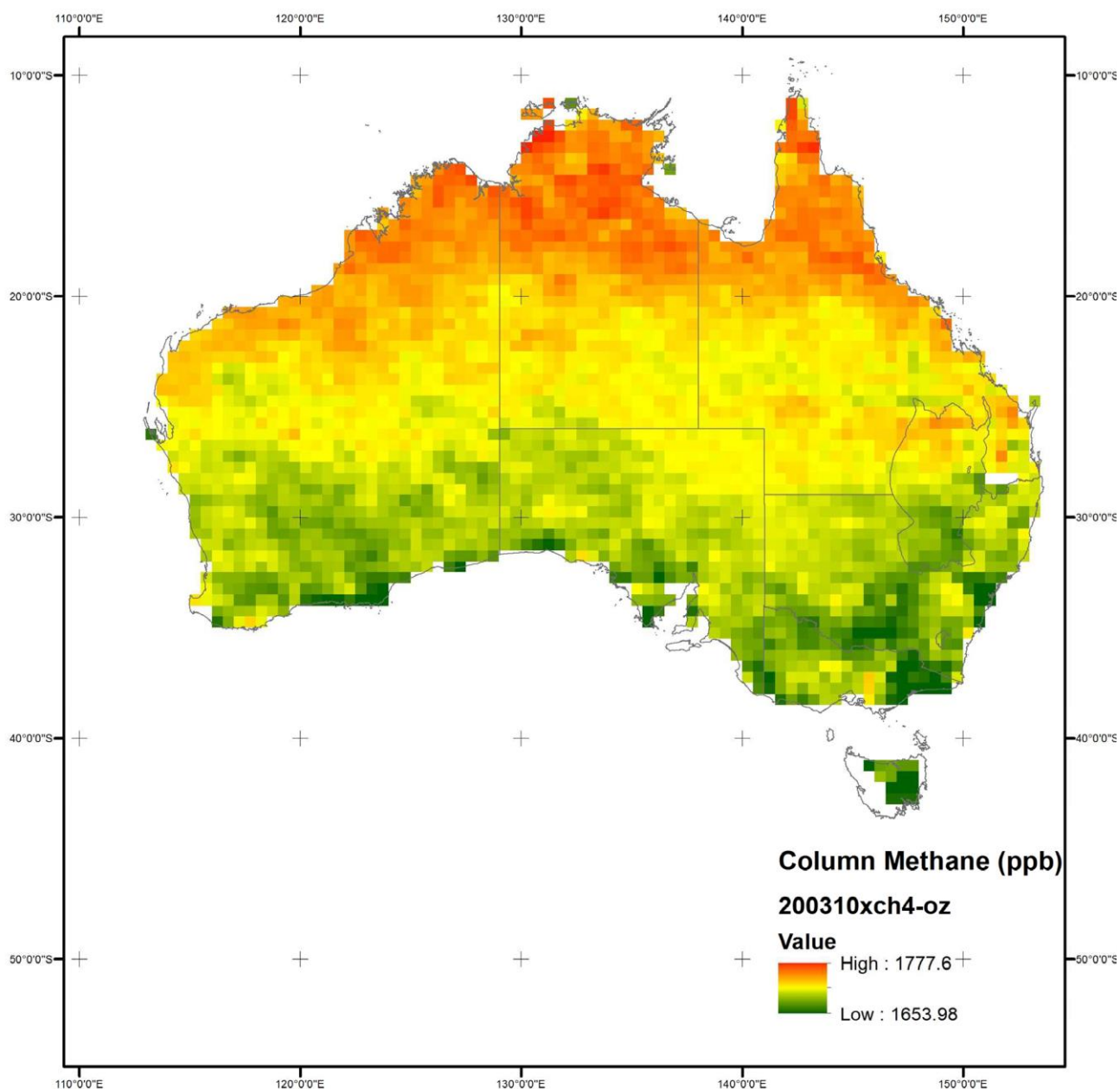
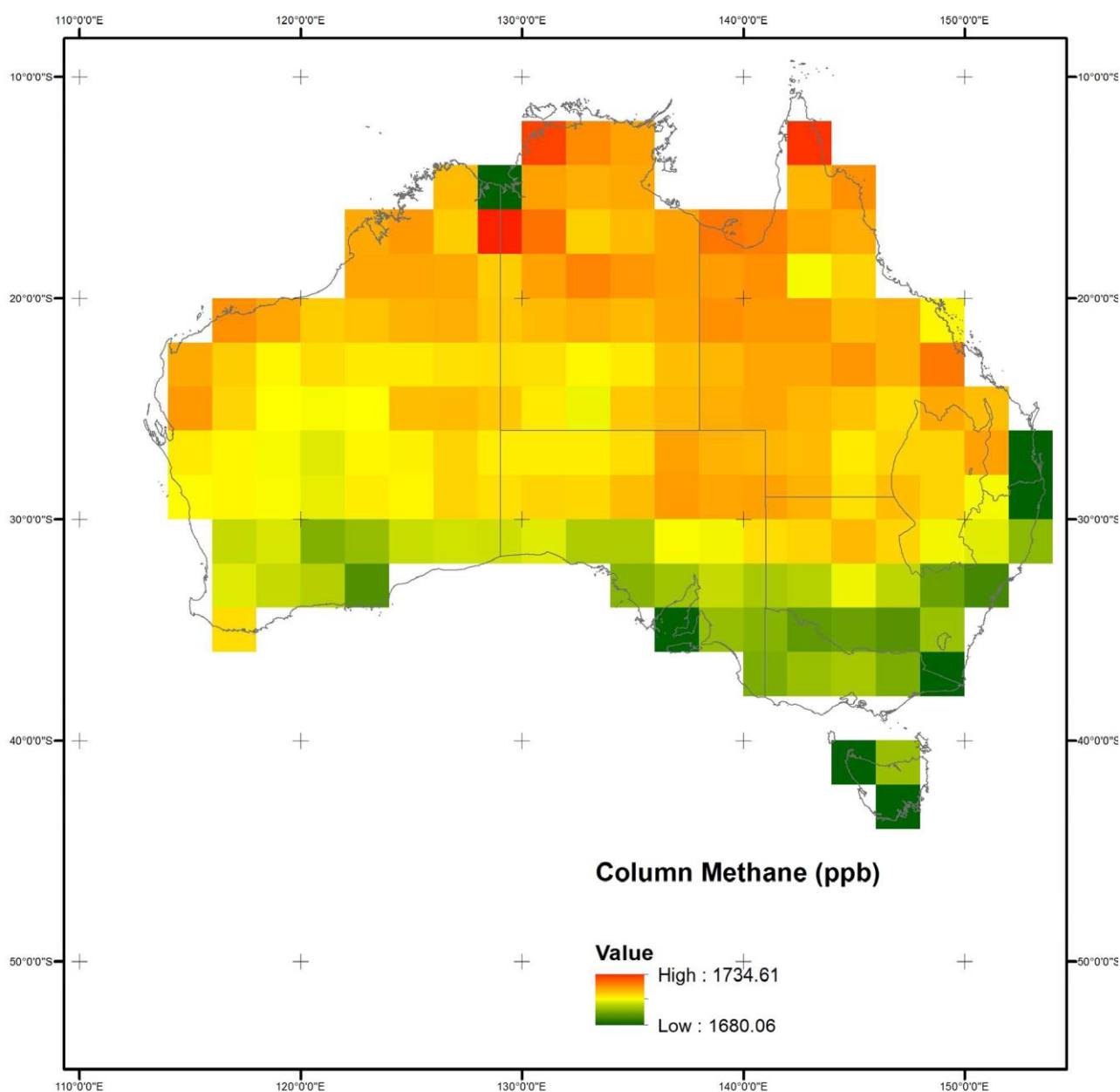


Figure 4.1. Total column methane measurement produced using the WFM-DOAS algorithm. The data were gridded at 0.5°. The Surat Basin outline can be seen in the central eastern portion of Australia.



**Figure 4.2. Total column methane measurements produced using the IMAP-DOAS algorithm. The data were gridded at 2°. The Surat Basin outline can be seen in the central eastern portion of Australia.**

Although the satellite derived column  $\text{CH}_4$  cannot be directly compared with surface measurements, with the WFM-DOAS product it was noted that the minimum values for some of the data such as those on Figure 4.1 appear to be much lower than those recorded from ground long term monitoring stations (CSIRO Oceans and Atmosphere GASLAB). Further analysis including acquiring additional ground validation data and processing of available ground validation data to more directly comparable products are required to better understand the differences. Additionally, both images show a trend of increasing  $\text{CH}_4$  concentration mapping towards the north of Australia with lower values towards the south. While it is known that  $\text{CH}_4$  concentrations increase towards the tropics in the southern hemisphere (Nisbet, et al., 2014), this effect nevertheless warrants further investigation. Further, with the data used for the Surat Basin and continental Australia, on closer examination of the WFM-DOAS product, the low values appear to be close to areas where no data were gridded, as the data did not meet the quality criteria (more information on the quality criteria can be found on Schneising and Heymann (2012)), and hence, there may be a higher level of uncertainty related to these data because of this. However, in the context of this study, the absolute values of the calculated methane levels are not the prime objective. Rather, the data product values are used as

relative indicators and will be used to observe trends over time periods. Therefore, the main statistics that may be useful to observe this trend are the averages over the time period of the SCIAMACHY observations.

These averages are plotted on Figure 4.3 for clarity. It is noted that there appear to be two peaks for the Surat Basin averages located on May 2005 and May 2006 on the IMAP-DOAS data. Further examination of the data indicates that these are likely to be outliers, as they are at the edge of pixels that were blank, meaning that it did not meet the quality criteria for inclusion. The fact that the WFM-DOAS product did not replicate these patterns tends to confirm this.

In addition to the major outliers, there are other differences observed between the two algorithms. The validation work which compared the satellite-derived measurements with ground-based FTIR data (Dils et al., 2014) provides an insight into why differences may be observed between the satellite-derived and ground observations. Specifically, the results of the Dils et al. (2014) research suggested that all algorithms exhibit a level of biases. Additionally, the biases, especially those of WFM-DOAS, are larger: “The differences between the algorithms are fairly distinct. Obvious is the far larger scatter in the WFM-DOAS data (overall 76 ppb compared to 50 ppb for IMAP)”, from Dils, et al. (2014).

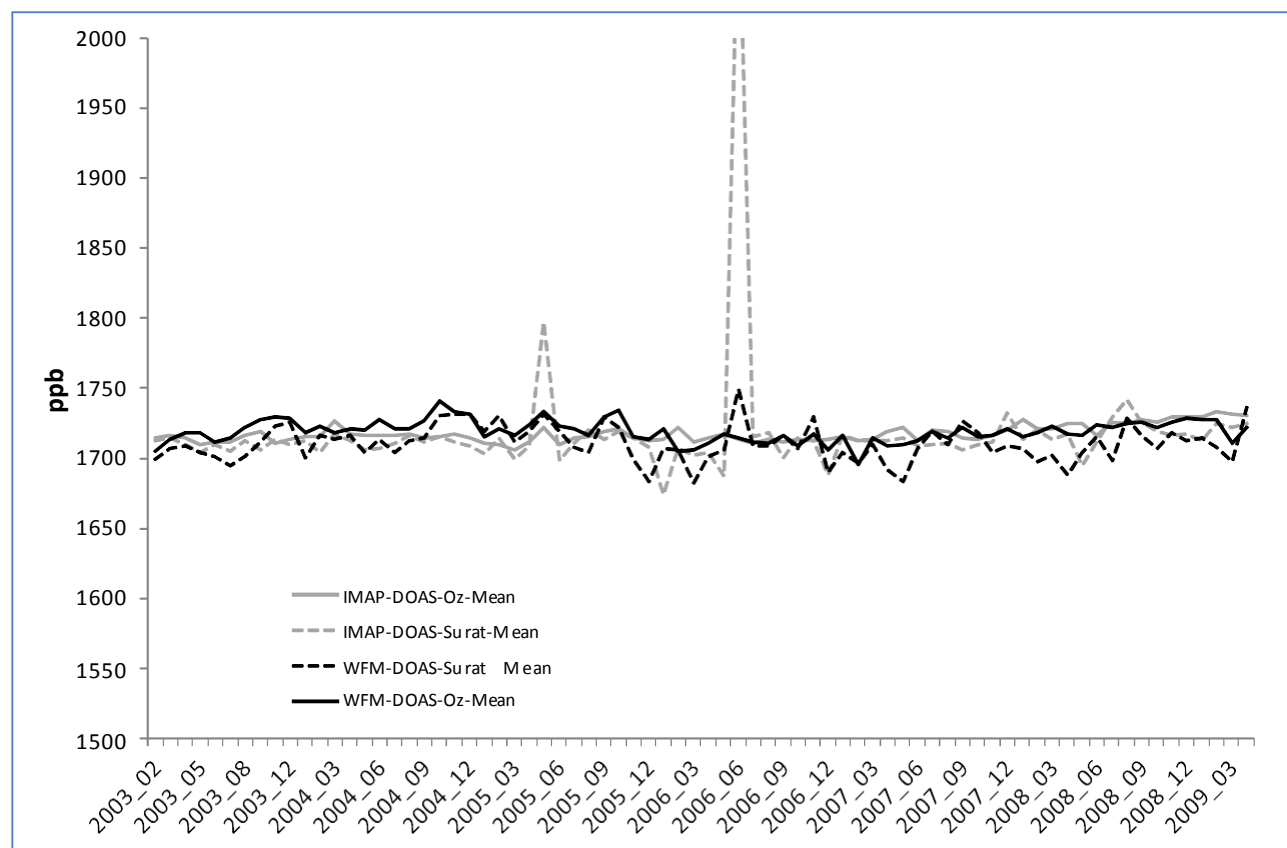


**Figure 4.3. Mean column CH<sub>4</sub> values across the Surat Basin and Australia extracted from data products generated using the WFM-DOAS and IMAP-DOAS algorithms.**

The investigation of SCIAMACHY data indicates that the data were able to provide an indication of the column CH<sub>4</sub> trends over time at a regional scale. The statistics show that the satellite-derived average trends across the entire Surat Basin was close to the average trends across the rest of Australia for the time period analysed (2003-2009). If it is important to track the regional scale trends after the establishment of the CSG industry or regional scale impacts, it may be useful to acquire longer term data of this nature. Although the SCIAMACHY instrument is no longer operational, there are other sensors that have provided continuity to this mission. Some of these are Atmospheric Chemistry Experiment-Fourier Transform Spectrometer (ACE-FTS) ([http://www.ace.uwaterloo.ca/instruments\\_acefts.html](http://www.ace.uwaterloo.ca/instruments_acefts.html)), Greenhouse gases Observing SATellite (GOSAT) ([http://www.gosat.nies.go.jp/index\\_e.html](http://www.gosat.nies.go.jp/index_e.html)), Atmospheric Infrared Sounder (AIRS) ([http://disc.sci.gsfc.nasa.gov/AIRS/documentation/airs\\_instrument\\_guide.shtml](http://disc.sci.gsfc.nasa.gov/AIRS/documentation/airs_instrument_guide.shtml)), Tropospheric Monitoring Instrument (TROPOMI) (<http://www.tropomi.eu/TROPOMI/Home.html>) and Infrared



Atmospheric Sounding Interferometer (IASI) (<http://wdc.dlr.de/sensors/iasi/>). It is possible that some of these spaceborne systems could be applied to longer term regional monitoring of the Surat Basin and other gas producing regions. However, it must be noted that these data yield regional scale trends and will not provide the ability to identify and separate local scale impacts such as the contributions from feedlots compared to a gas well, for example. Some sensors such as GOSAT have higher spatial resolutions than the SCIAMACHY sensor (10.5 km) but different systems may use different technology and spectral ranges. Therefore the combined use of data products from different sensors will require careful harmonisation and cross calibration. Additionally, further research and development is necessary to understand the uncertainties and constraints in using these data. These include:

1. Modelling the impacts of complicating factors such as the ground composition, land use, seasonal variations, sampling resolution, topography and other interferences such as atmospheric water vapour.
2. Determining the optimal option from the published algorithms for retrieving column methane for the Surat Basin. Ultimately, a tailored algorithm may be required, either by adapting the algorithms for the environment or developing new methods. This must be undertaken together with the acquisition of independent data for the calibration of the model as well as validation of the model. This is of course not possible with previous datasets but will be possible with sensors that are currently in orbit. The adapted or new algorithms may be transferable to the previous datasets but cross calibration studies would be required to validate the results.

A more detailed discussion of the uncertainties associated with SCIAMACHY is provided in Section 7 of this report.



## 5 ALMA G2 Airborne Survey

### 5.1 Instrumentation

The ALMA G2 instrumentation is described briefly in Section 2.3.2. More details can be found in the report of the Chinchilla trial prepared by the instrument's operator, Skyline Sensing, which is provided in the Appendix. Figure 5.1 shows the ALMA G2 sensor mounted on the underside of the Bell JetRanger helicopter used during the trial.



Figure 5.1. Photo showing the ALMA G2 (in circle) mounted on the underside of a Bell JetRanger 206 helicopter.

### 5.2 Experimental Design

The experimental setup was designed to test some of the unknowns with the application of the ALMA G2 instrument to determine the spatial distribution of the background  $\text{CH}_4$  levels. This is because the ALMA G2 was designed for the detection of pipeline leakages, that is, peak levels above background, not background. The experiment was designed to test:

1. the detection limit, and the required flying speed to achieve the optimal detection limit, and,
2. the line spacing required to understand the distribution of an anomalous gas plume.

To obtain the optimal detection limit, the flying height was set at 30 m. This was determined by advice from the instrument developer, who was present during the data acquisition. The flying speed determines the detection limit, that is, the lower the flying speed the better the detection limit. However, the low flying speed also limits the data acquisition and hence, a practical solution needs to be determined between amount of data and detection limit. To explore this, data were acquired several times at different speeds along a selected number of flight lines.

The flight plan was designed to assist in determining the line spacing required to understand the distribution of an anomalous gas plume. The flight lines are shown on Figure 5.2 in red. These flight lines

were selected based on known locations of seepages from old wells and feedlots identified by the ground-based surveys made using a Picarro 2301 cavity ring down spectrometer mounted on a four-wheel drive vehicle. The yellow circles in Figure 5.2 denote the locations of previously located CH<sub>4</sub> seeps; probably leaking abandoned boreholes (see Section 3.2.4). Additionally, the locations of natural seepages along the Condamine River were also used to select the flight lines and these are shown by the green polygons. The first flight line is drawn directly above the identified seepage locations, after which, additional flight lines are added adjacent to the first flight lines. The first four adjacent flight lines were spaced 50 m apart and the next four 100 m apart.

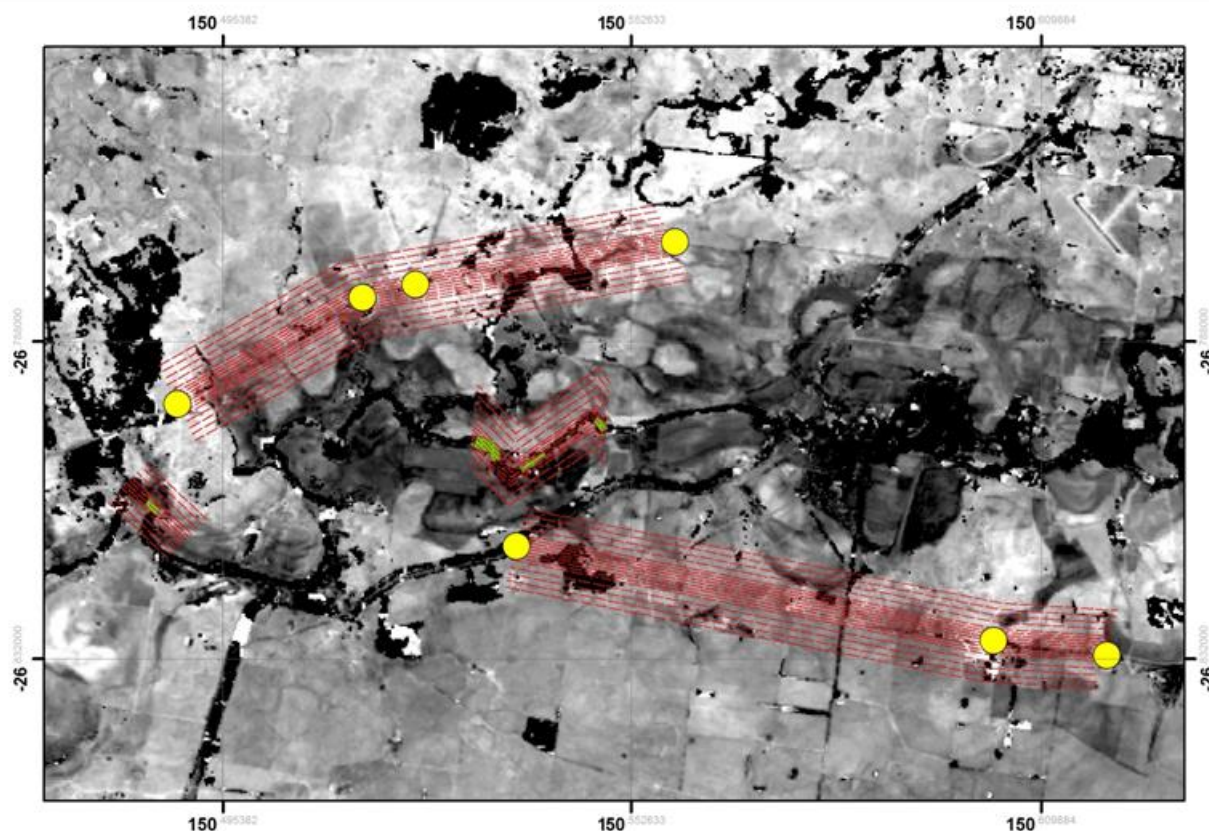


**Figure 5.2. Flight lines (in red) across the Chinchilla test area overlaid over a black and white satellite image. The yellow circle denotes the locations where leakage from abandoned boreholes has been detected using the ground surveys. The green polygons show areas where natural methane seepages have been identified along the Condamine River.**

## 5.3 Results

The initial data provided by the instrument operator consisted of a spreadsheet identifying the locations where peaks have been found across the survey area, Google Earth kmz files of the locations of these areas, a report documenting the peaks found and a set of 'raw' data (see Appendix). The former are standard products delivered as part of the service for pipeline inspection work. The latter were additional data requested to obtain the complete datasets acquired from the survey necessary to undertake further processing.

Figure 5.3 plots the peak data provided by the data operators. These peaks are plotted as circles with cool colours (starting with blue) depicting low column methane values to warm colours (ending with red) depicting high column methane values. Note that some of these peaks extend some distance along the flight lines but only the start of each peak has been plotted. The values range from the lowest peak detected by the ALMA 2 to the highest value. Additional data (beyond the planned flight lines) were acquired during the mobilisation of the helicopter to Miles where the aircraft was refuelled. These are

located towards the west of Figure 5.3. A number of peaks were identified and on further investigation, some of these appear to correspond to possible methane sources such as feedlots and/or water treatment plants, which are identified as green stars in Figure 5.3.

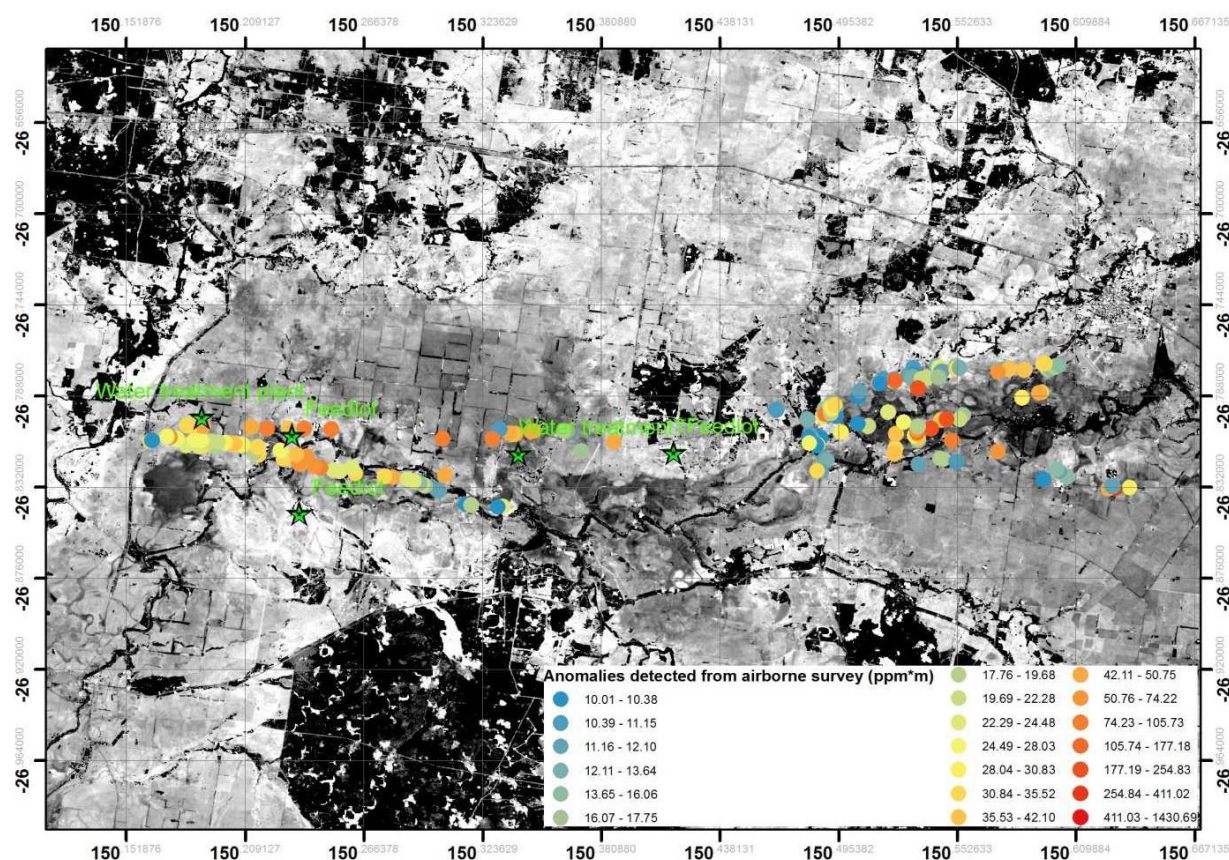


**Figure 5.3. Peaks detected from the ALMA G2. Note that the units are ppm\*m. The green stars denote locations associated with possible methane sources (e.g. feedlots).**

Figure 5.4 shows a zoomed in area of Figure 5.3 which included only the track flown for the planned flight lines. The peaks (large circles) generally identified areas of high values previously identified by the Picarro analyser during ground surveys and also areas of known natural seepages. Note that the colour coding is similar to Figure 5.3, that is, cool colours (starting with blue) depicting low column  $\text{CH}_4$  value detected to warm colours (ending with red) depicting high column methane values. The tracks acquired concurrently by the Picarro instrument during the airborne survey are also plotted (unbroken line with smaller circles). Note that although the same colour legend was used, the ALMA G2 is in different units than the mobile Picarro survey (i.e. ppm\*m for the ALMA; ppm for the Picarro). Therefore, only relative comparisons can be done between these measurements. At this stage, detailed investigation of the relationship between the ground-based Picarro measurements and the airborne ALMA G2 measurements has not been undertaken.



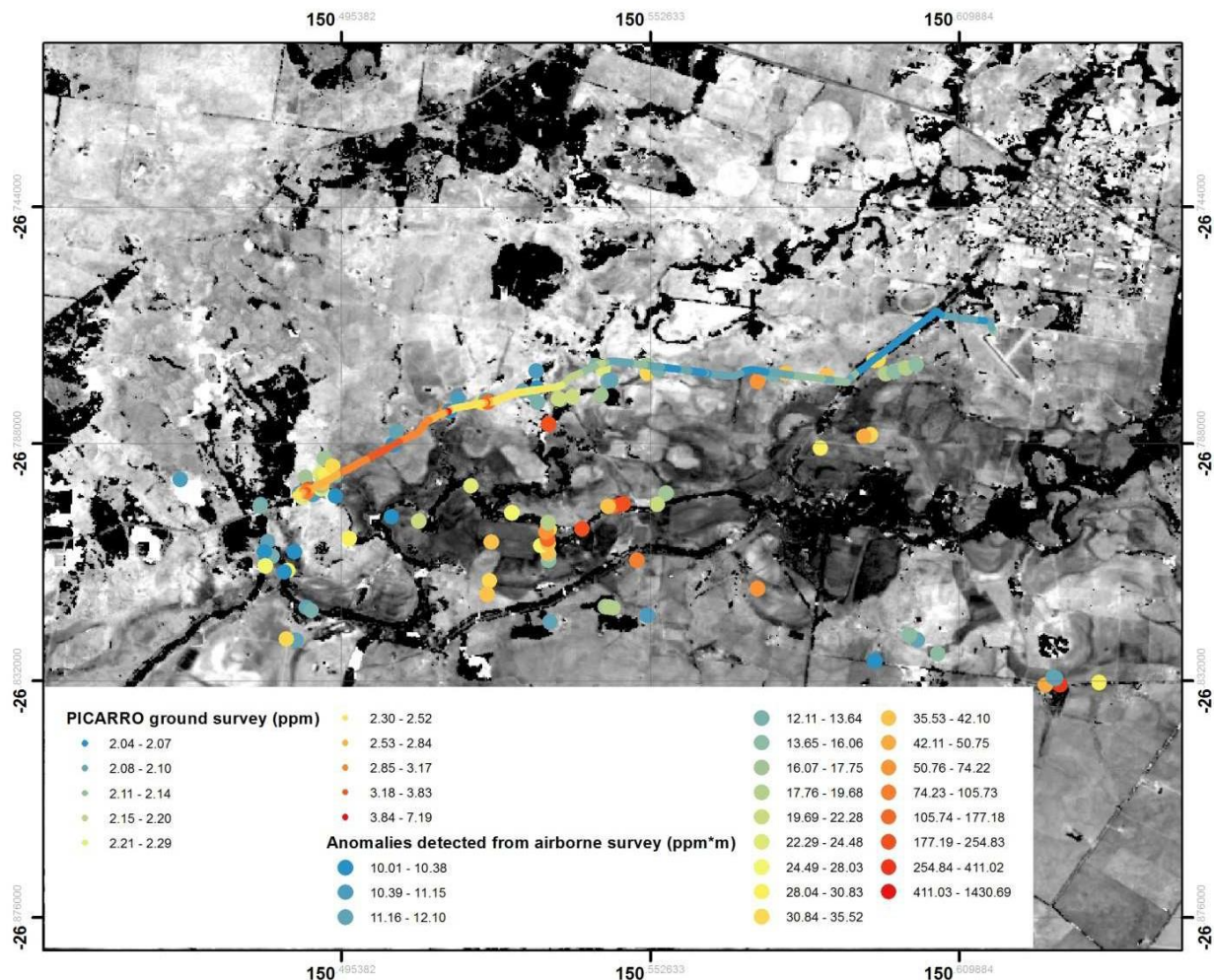


**Figure 5.4. Zoomed in area of Figure 5.3 showing only the planned flight lines. The large circles show the peaks detected from the ALMA G2. The methane levels recorded by the ground surveys, which were acquired concurrently with the ALMA G2 survey, are plotted with small circles showing a continuous unbroken line. Note that although the same colour legends were used, the ALMA G2 and the ground survey results do not have the same units. The ALMA G2's units are ppm\*m and the ground survey ppm.**

The survey conducted with the ALMA G2 represents the first time that this system has been tested for use to obtain baseline methane values. The standard products delivered provided an indication of the areas where peak levels of methane were detected. Many of these peaks correlated to known peaks previously identified using other methods. However, in the context of this study, the aim was to obtain a spatially comprehensive image of the distribution of all the CH<sub>4</sub> levels and not just the peaks. Therefore, it was necessary to negotiate access to all the 'raw' data for analysis. This request has not been made previously as the data were only ever used to determine 'hot spot' areas (i.e. leaks in pipelines). The next stage of work that will be undertaken will be to reprocess and analyse these data, specifically focussing on:

- collation of all the 'raw' data, GPS and laser range finder data;
- as data are not all synchronised, it will be necessary to manually aligning the raw data, GPS and laser finder data;
- plot and analyse the raw data to provide a spatial map; and,
- analysis and further processing to produce the final map.

It was initially envisaged that the digital camera data may be able to provide extra information, such as changes in vegetation that may be related to areas of emissions. Further investigation of these data and their acquisition details indicate that it will not be possible to generate quantitative, geo-located data of sufficient quality for further analysis.

## 6 Fixed Monitoring Network

In this section, we describe the progress to date on the fixed monitoring network for the ‘top-down’ atmospheric methods, including the selection of the monitoring sites and establishment of the facilities. Some preliminary results are also presented.

### 6.1 Site Selection for Monitoring Stations

The selection of monitoring site locations for the Surat Basin CSG field was based on the following:

- To allow measurement of CH<sub>4</sub> concentrations of both the background (air arriving at the Surat Basin) and the signal resulting from CH<sub>4</sub> emissions in the Surat Basin (total CH<sub>4</sub> concentration minus background).
- To optimise the size and frequency of concentration signals from the broader CSG source area without being overly influenced by individual sources close to the measurement site.
- To differentiate as much as possible the emissions from non-CSG sources such as livestock, power stations, coal mines, vehicles, biomass burning and cities from CSG sources.
- To take into account characteristics such as land cover and topography.
- Practical considerations such as access, power and security.
- Potential assistance by land owner or operator.
- Future gas development possibilities which could affect the site.

Potential CH<sub>4</sub> sources in the region include production and exploration wells, produced water, pipes, pumps and other infrastructure, processing plants, and sources existing before CSG production, such as seeps and agricultural bores and coal exploration wells.

CSG industry sources were assumed to be represented by the locations of CSG projects (DNRM 2014). The likely locations and strength of seeps were based on geological mapping (Gas Migration Region of Interest, B. Pinder, Arrow Energy, 2014). This shows a band extending about 300 km along a NW-SE axis and between about 30 and 100 km wide, centred approximately on Chinchilla. Other potential CH<sub>4</sub> and CO<sub>2</sub> sources related to CSG and to activities unrelated to CSG are also shown.

The original strategy of having only one measurement site was supplemented with plans for a second site to obtain more accurate and frequent downwind-upwind differences. Our experience of monitoring elsewhere is that the accuracy of background-subtracted concentrations (that is, the potential emission signal) is often limited by poorly quantified background. Measurement of the background is more accurate and in the end requires less effort than estimating it by other means (e.g. Luhar et al., 2009; Wilson et al., 2014).

A requirement for both measurement sites was to be 10-20 km away from the region of large CSG sources in order to integrate emissions across the region. They were also situated away from, or upwind of nearby individual sources, so that those emissions are not overly represented. Monitoring within the CSG belt by Origin Energy is also planned and measurements from those stations could be incorporated in the modelling. Methane measurements will be accurately inter-calibrated so that differences across the region (from which emissions are inferred) can be precisely found.

Two sites were identified on either side of the CSG belt that met many of the above requirements, subject to the outcomes of the gas source dispersion modelling described next.

## 6.2 Simulated Concentration Signals

The first step in identifying possible locations for atmospheric monitoring stations was to analyse the winds in the region. The meteorological model TAPM (e.g. Hurley et al., 2005) was used to generate an annual wind rose (i.e. a graphical representation of wind speed and direction in the region) for a central location in the Surat Basin at Miles. The model predicts the regional and local-scale meteorology such as terrain-induced flows and sea breezes given inputs of large-scale synoptic weather analyses, terrain, vegetation, etc. It was run for the three years 2011-2013 to generate robust annual and monthly wind roses. The annual wind rose in Figure 6.1 shows the predominance of easterly winds with a range from north-north-easterlies to east-south-easterlies. There are also periods with south-westerlies but very few winds along the main north-west to south-east axis of the Surat CSG region.

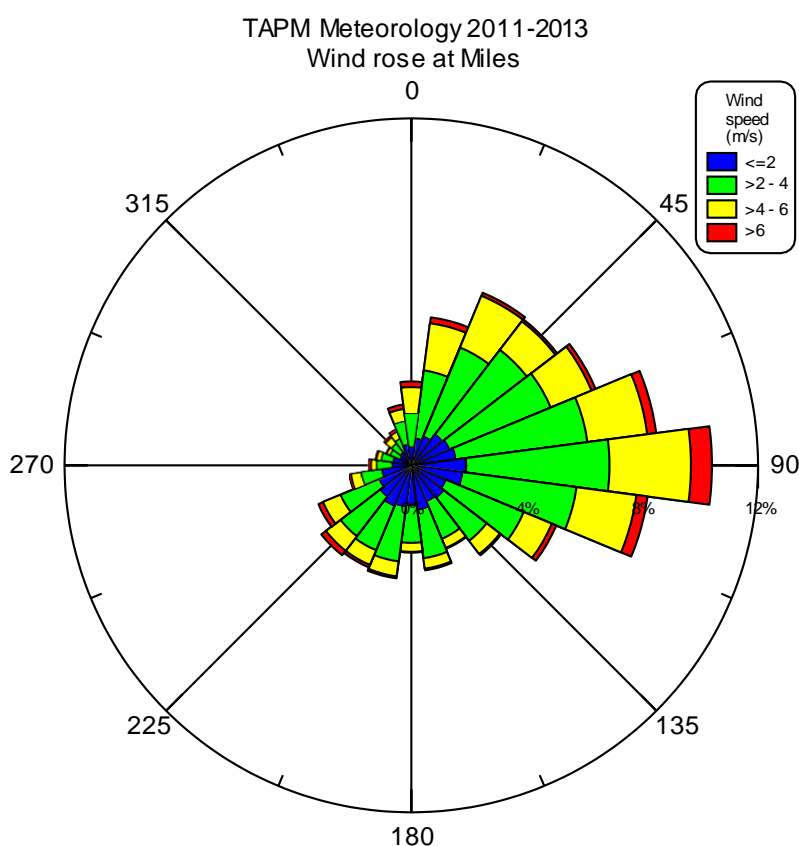


**Figure 6.1. Annual wind rose at Miles derived from TAPM meteorological modelling for the three years 2011-2013.**

The monthly break-down of the wind roses in Figure 6.2 shows significant variations in the wind patterns during the year. The key features can be seen by categorising them in (mainly) three-month blocks. The months from January to April are dominated by winds in a fairly narrow easterly sector. The following three months (May to July) have a mixture of roughly equal periods of easterly and south-westerly winds with almost no northerly component. Moving into spring (August to October), the north-easterly sector dominates the wind roses with a decreasing proportion of south-westerlies. November has a fairly narrow range of north-easterly winds, which broadens in December to include more easterlies as the wind roses move to the summer pattern dominated by easterlies.

The key features of this wind rose analysis are:

- Dominance of winds in the easterly sector
- Easterly to north-easterly winds significant in all months of the year
- South-westerly winds significantly from May to August but rare at other times of the year
- Very few winds along the north-west to south-east axis of the Surat basin CSG fields

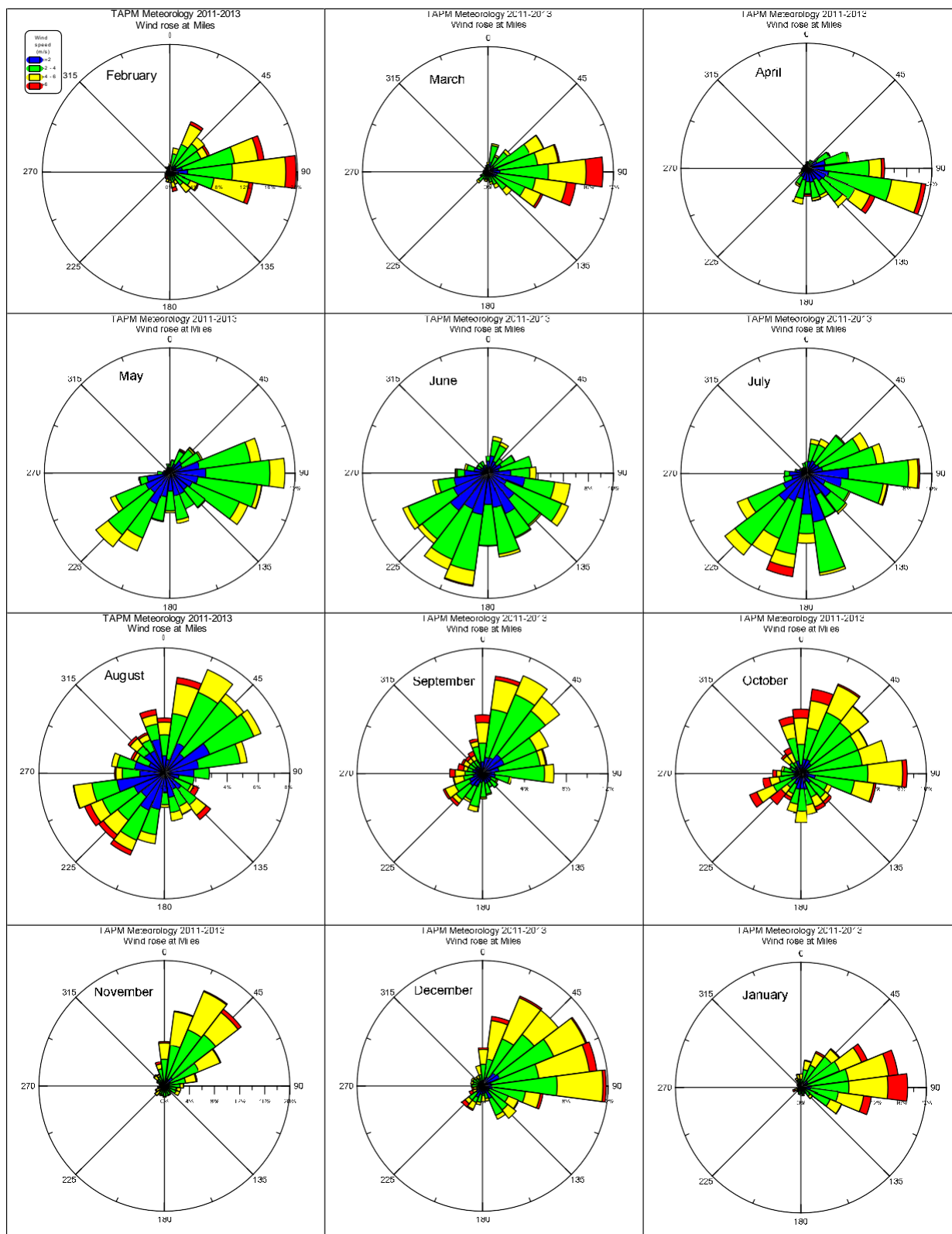


**Figure 6.2. Monthly wind roses at Miles derived from TAPM meteorological modelling for the three years 2011-2013.**

This wind analysis indicates that the most suitable locations for atmospheric monitoring stations are on the south-west and north-east edges of the Surat Basin CSG field. This analysis also shows that having a monitoring site on each side of the Basin would ensure that during much of the year, one of the sites would be able to provide upwind background measurements of methane concentrations. This would improve

interpretation of the measurements from the other downwind site by providing a better estimate of the impact of emissions from the region between the two monitoring sites.

The dispersion modelling was also undertaken using TAPM (Hurley et al., 2005) with the model grid shown in Figure 6.3. The grid size is 5 km × 5 km. The grid squares shaded green were modelled as sources of CH<sub>4</sub> at an assumed nominal emission rate of 10 L min<sup>-1</sup> km<sup>-2</sup>. This value was based on the ground-based monitoring (Section 3) and was used as the best available estimate for undertaking this preliminary modelling study. In practice the emission rate will vary from site to site and could differ significantly from this estimate.

Two separate scenarios were modelled – one with emission from grid squares containing an operating CSG project, the second including both operating and projected (under development) CSG projects. Both were derived from a recent coal seam gas overview for Queensland. The second scenario included emissions from all of the green-shaded grid squares in Figure 6.3. Modelling was undertaken for calendar year 2013.



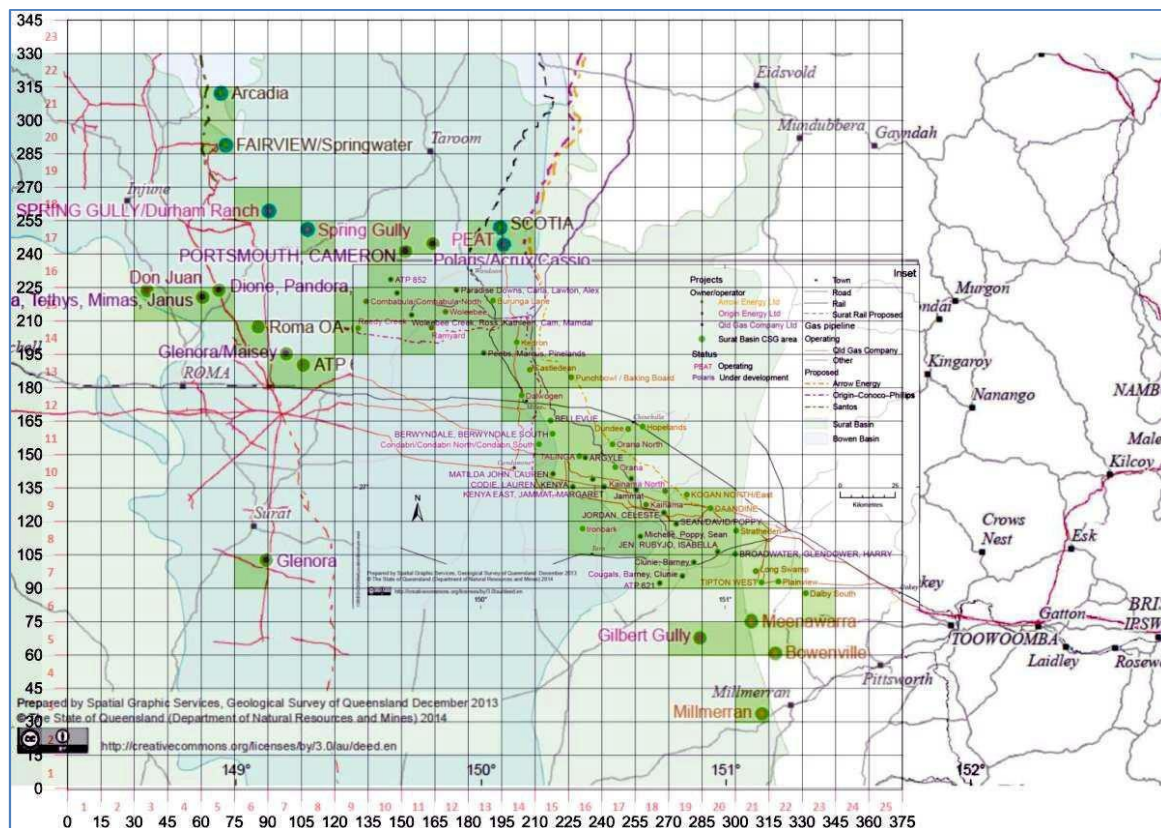


Figure 6.3. TAPM model grid overlaid on a Surat Basin CSG resource map (DNRM, 2014). The grid squares shaded green were modelled as sources of methane at an assumed emission rate of  $10 \text{ L min}^{-1} \text{ km}^{-2}$ . Two separate scenarios were modelled – one with emission from grid squares containing an operating CSG project, the second including both operating and projected (under development) CSG projects as given in DNRM (2014). The second scenario included emissions from all of the green-shaded grid squares.

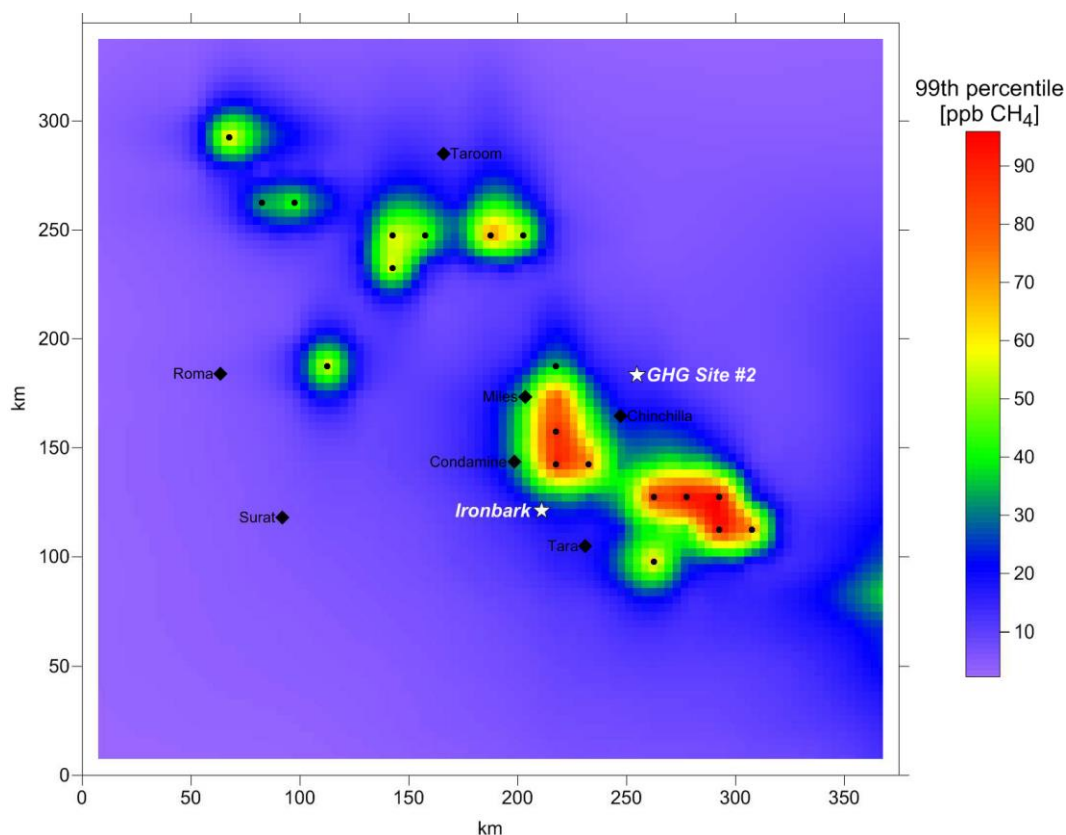
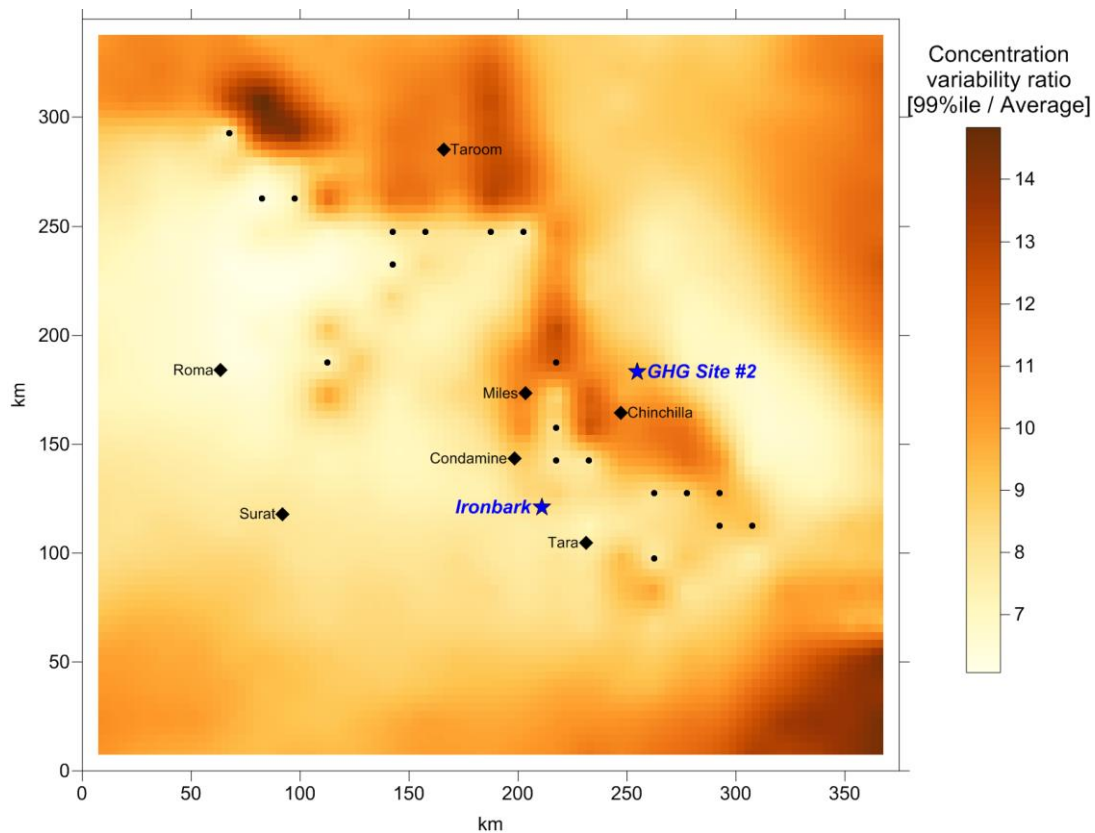


Figure 6.4. Modelled annual 99th percentile 1-hour average concentrations (above background) due to methane seepage



**Figure 6.5. Modelled concentration variability ratio due to methane seepage of  $10 \text{ L min}^{-1} \text{ km}^{-2}$  in areas of current CSG operations**

Figure 6.4 shows results of the TAPM modelling for nominal emissions from the current CSG operations. The modelled region covers an area of  $375 \times 345 \text{ km}$ , centred just west of Miles. The locations of some towns in the region are shown by labelled diamonds. The coloured shading shows the modelled 99th percentile 1-hour average concentrations of  $\text{CH}_4$  in ppb for the nominal emission rate of  $10 \text{ L min}^{-1} \text{ km}^{-2}$  from the grid squares containing a black dot. The results do not include the background methane concentration of 1780 ppb. Also shown are the locations of the two selected atmospheric monitoring sites: Site #1 – Ironbark, and GHG Site #2 (yet to be installed). As shown in more detail later (Figures 6.10 and 6.11), both sites are away from individual sources and measure the impact of emissions from a range of source areas.

Depending on the winds, the measured  $\text{CH}_4$  concentrations at the monitoring sites will vary depending on what sources are in the upwind trajectory. A measure of this variability is given by the ratio of the 99th percentile to the average concentrations shown in Figure 6.5. The average ratio is about 10. It is lower at Ironbark than at GHG Site #2 because of the more frequent winds in the easterly sector, which means that Ironbark is impacted more often by the modelled methane emissions.

Results for the second scenario with modelled emissions from both current and projected CSG areas are shown in Figure 6.6 and Figure 6.7. With the increase in the number of modelled emission sources, the 99th percentile concentrations at the monitoring sites are about double those from the first scenario (only current operating regions) and the impacted region is much larger. This impact is seen more clearly in the change in the modelled cumulative frequency distribution of concentrations at Ironbark in Figure 6.8, which shows the percentage of time that the concentration is below the value shown on the x-axis. These results show that the monitoring sites would be well placed to detect any significant increase in emissions related to the expansion in CSG operations in the Surat.

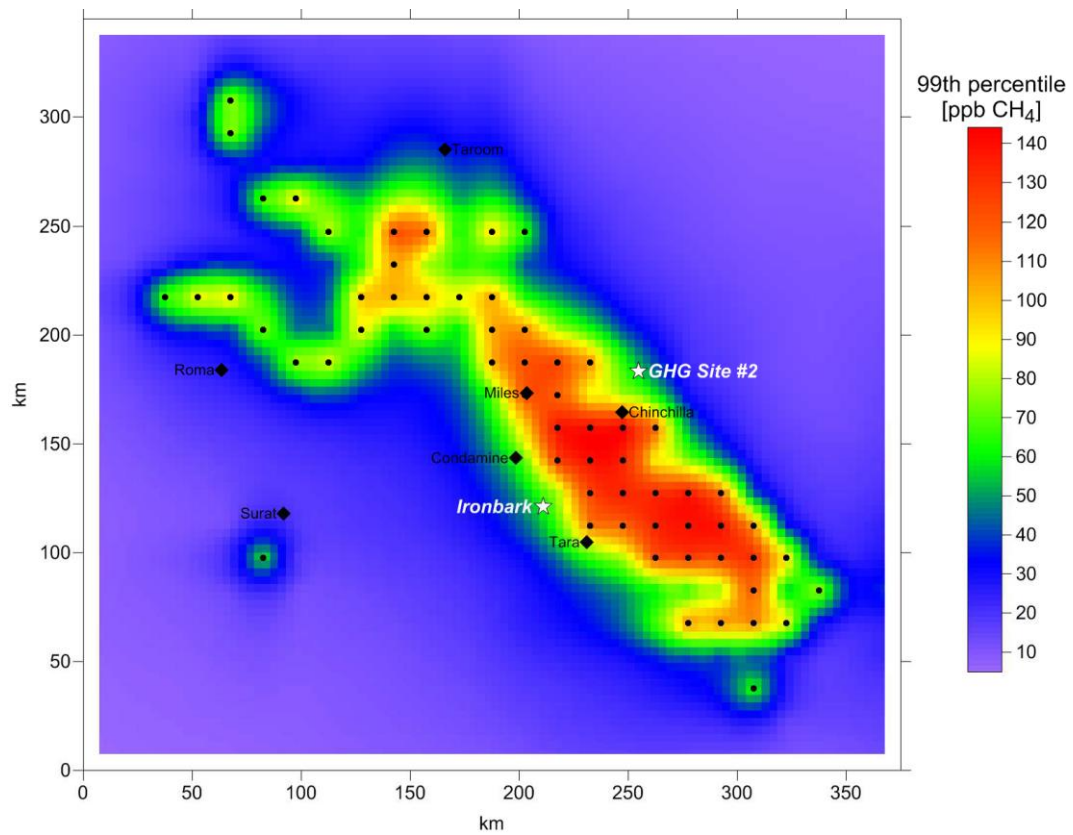


Figure 6.6. Modelled annual 99th percentile 1-hour average concentrations due to methane seepage of  $10 \text{ L min}^{-1} \text{ km}^{-2}$  in areas of current & projected CSG operations

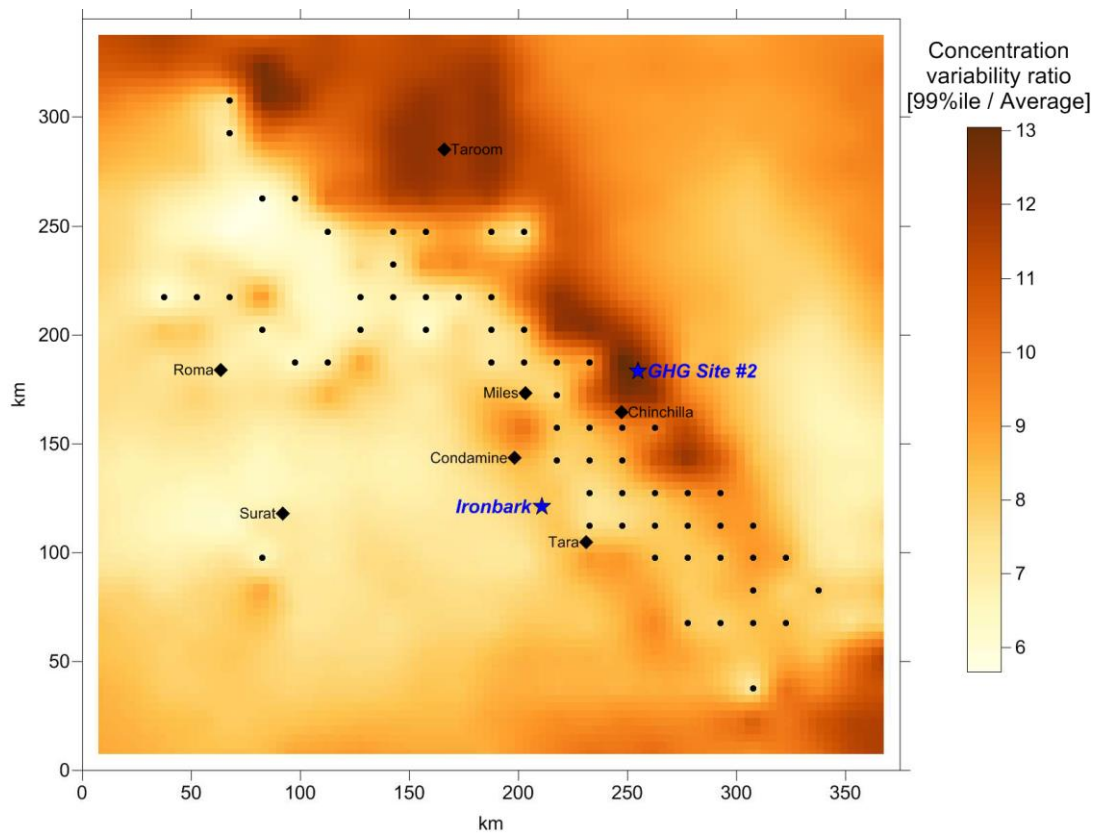


Figure 6.7. Modelled concentration variability ratio due to methane seepage of  $10 \text{ L min}^{-1} \text{ km}^{-2}$  in areas of current and projected CSG operations

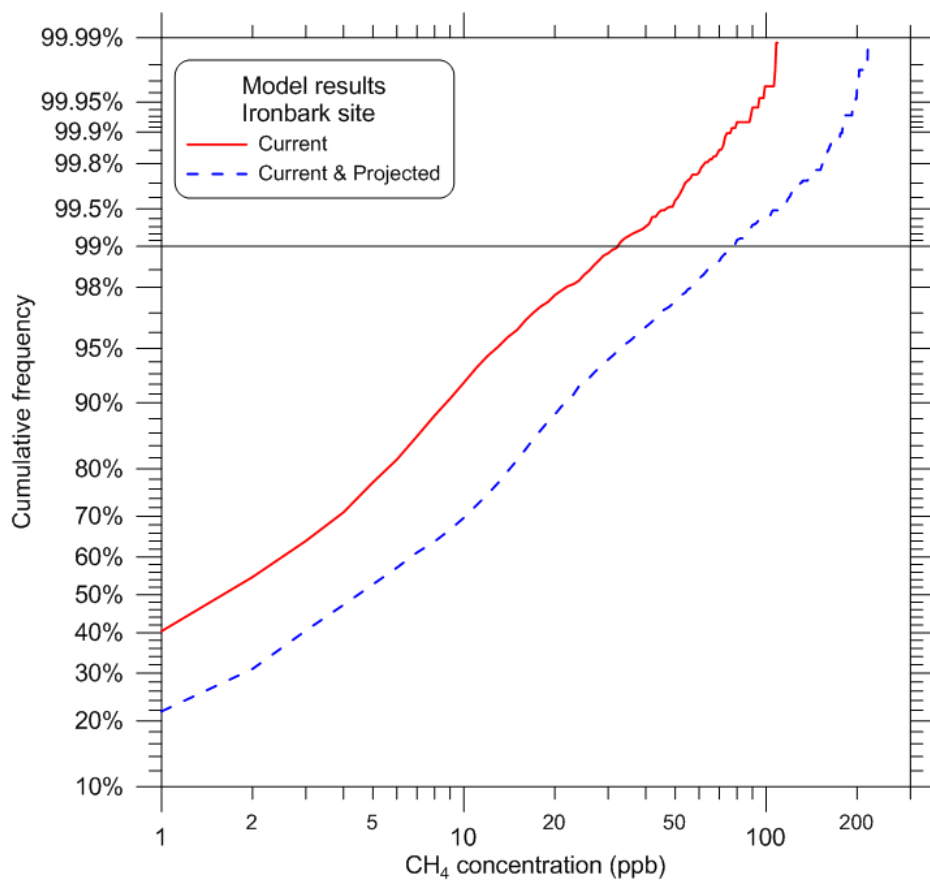
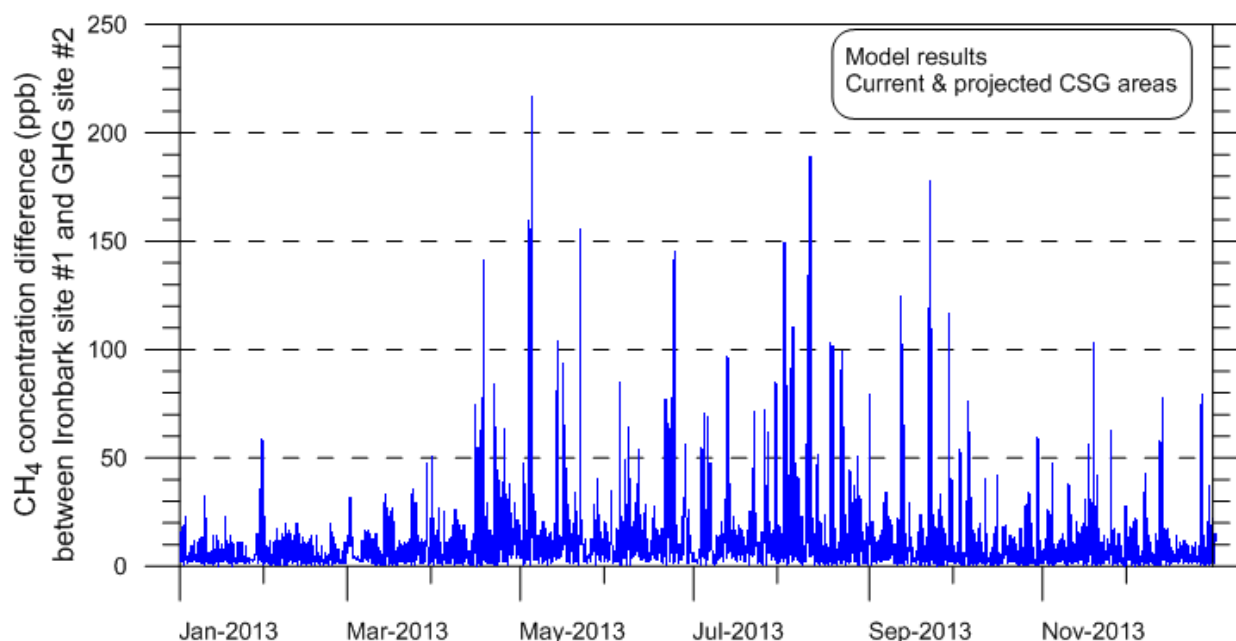


Figure 6.8. Annual cumulative frequency distribution of modelled concentrations at Ironbark monitoring site #1.





**Figure 6.9. Simulated time series of absolute difference between Ironbark and GHG Site #2 concentrations for modelled year 2013.**

The time series of the absolute difference between the modelled concentrations at the two sites is shown in Figure 6.9. This could be considered to represent an idealised case with one of the monitoring sites upwind and the other downwind for many of the hours of the year. The lower concentrations from January to March are related to the higher winds speeds (and hence greater atmospheric mixing) seen in the monthly wind roses in Figure 6.2.

These exploratory simulations for identifying fixed monitoring sites included nominal emission rates from regions with current or proposed CSG projects, but not detailed information about sources such as gas treatment or compression plants or power stations.

An estimate of the impact of methane emissions from Brisbane and Toowoomba was made using the above modelling system. The methane emissions were based on information in the South East Queensland Air Emissions Inventory (Queensland EPA, 2004), which showed the largest non-industrial source to be landfill emissions. Scaling these based on population, the CH<sub>4</sub> emission rate for Greater Brisbane was estimated to be 545 g s<sup>-1</sup> and for Toowoomba 38 g s<sup>-1</sup>. The impact of the Greater Brisbane emissions at the two monitoring sites was a 99th percentile concentration of about 4 ppb, whereas the Toowoomba impact was less than 0.1 ppb. These impacts are small and would occur relatively infrequently, as seen by the wind roses in Figure 6.2, which show a low frequency of south-easterly winds.

The above plots show the modelled concentration across the Surat region. Information about what sources the monitoring sites 'see' is given in Figures 6.10 and 6.11. These show the upwind footprints for each of the monitoring sites. The coloured shading shows the relative contribution of the various sources to the annual average concentration at the monitoring site. At Ironbark, the sources to the east and north-east make the largest contributions but there is some impact from sources up to 100 km away. The upwind footprint is different at GHG Site #2 with a slightly different group of sources making the largest contribution to the annual averages. The footprints show that some potential seepage areas may also be monitored by Ironbark and Site #2. These figures indicate the potential of the proposed inverse modelling techniques using information about measured methane concentrations, winds, atmospheric conditions and back trajectories to infer methane emission rates across the CSG areas.



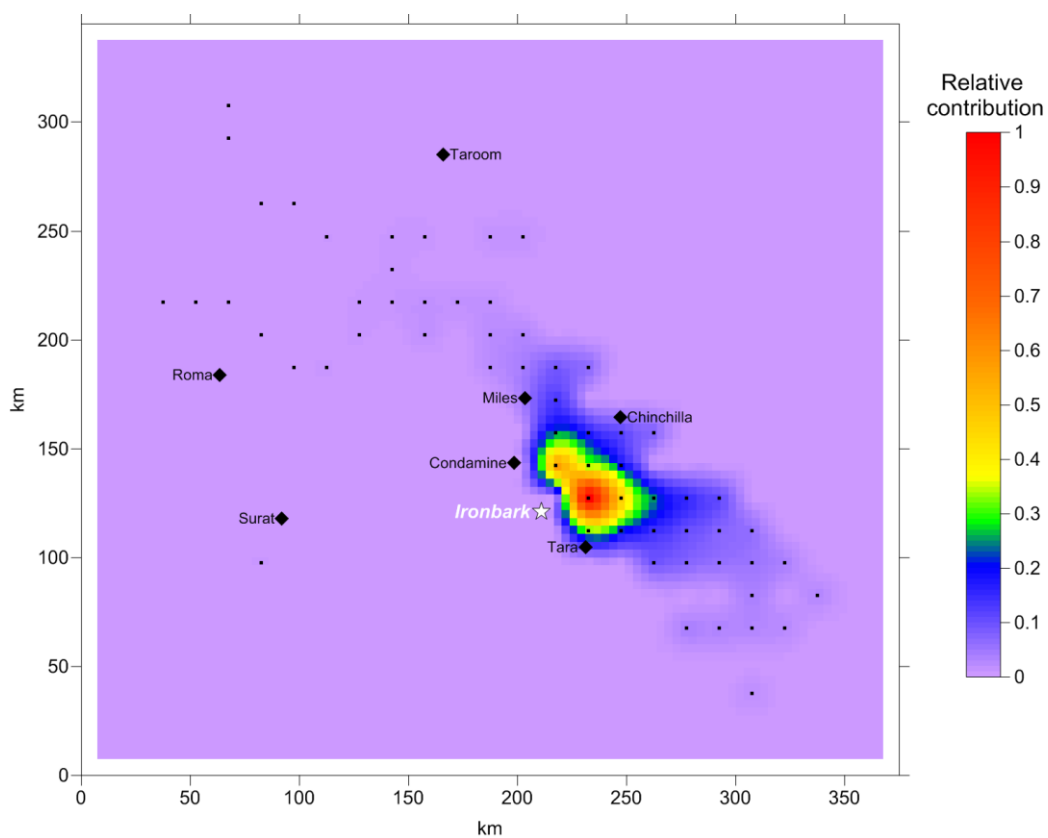


**Figure 6.10. Relative contribution of potential emissions (upwind footprint) from current and projected CSG areas to annual average concentrations at Ironbark site.**

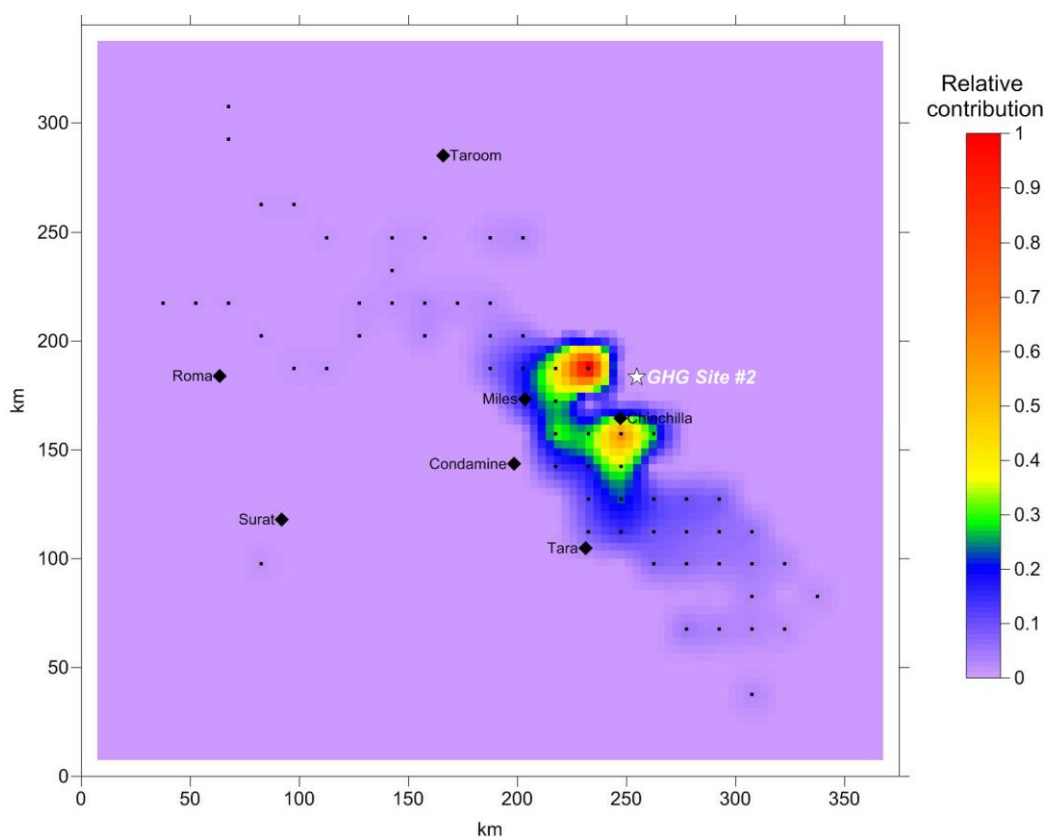


**Figure 6.11. Relative contribution of potential emissions (upwind footprint) from current and projected CSG areas to annual average concentrations at GHG Site #2.**

### 6.3 Installation of Ironbark Greenhouse Gas Monitoring Facility

The Ironbark site is 57 km southwest of Chinchilla and about 15 km from the edge of a zone of CSG activity, including wells, plants, produced water bodies, and a high potential of seepage. The monitoring facility is located within the Ironbark property, owned by Origin Energy. It was previously a grazing farm (Greenlea) and still runs a small number of livestock. CSG development is unlikely to proceed on the property for several years and there are presently few industrial gas sources. A camp comprising several offices and accommodation buildings was recently installed 250 metres southwest of the site but is not currently occupied. A gas pilot (Duke) is 3.5 km to the northwest, consisting of about 5 wells producing gas which is flared. Produced water from the pilot is fed to a dam about 2.5 km west of the monitoring container.

Before committing to the site, the property was surveyed for nearby methane sources using the mobile Picarro analyser (Figure 6.12). High concentrations were found near the dam and the pipeline from the Duke pilot so winds from that direction should be treated with caution. However, because the sources are not within the key southwest-northeast direction they are unlikely to affect the 2 point monitoring strategy. Small methane elevations above background were found in the vicinity of livestock, which may need to be fenced away from key zones near the monitoring container. Otherwise CH<sub>4</sub> concentrations in the area were at the background level for that time of year. A generator for the camp about 200 metres west of the monitoring container may also emit gases, including CO<sub>2</sub> and CH<sub>4</sub>, but it only operates in the event of a power outage. The monitoring facility power is backed up by this generator. A temporary generator 70 metres west of the monitoring site was used to power the facility while awaiting connection to mains power from the camp and it is possible that its emissions were measured during the first four months of monitoring.

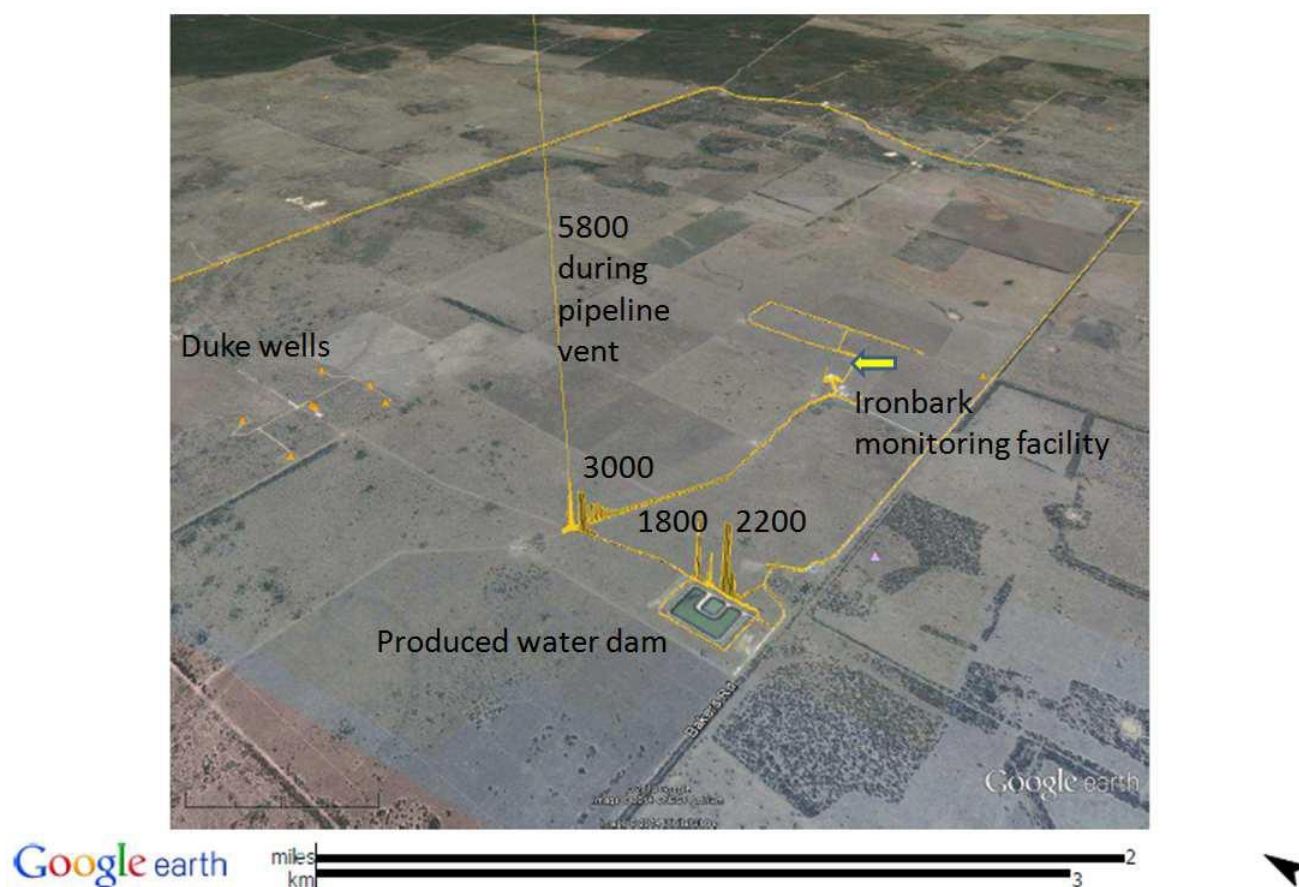


**Figure 6.12. Methane concentrations in the vicinity of the Ironbark monitoring facility. Measurements were made at about 11 am on 9 July 2014. The yellow line shows the route travelled and its height reflects the concentration. Peak concentrations at the point sources are given in ppb. The distance scale applies at the bottom of the image.**

The monitoring facility comprised a container with a gas concentration analyser, tower, meteorological instruments, computer for logging and control, and communications modem. An eddy covariance flux station was installed about 150 metres northeast of the container. Both were previously used at the Arcturus CSIRO/Geoscience Australia site near Emerald in Queensland (Berko et al., 2012). The coordinates of their new locations at Ironbark are given in Table 6.1.

**Table 6.1. Location of Ironbark monitoring facilities**

	Zone	Easting	Northing	Latitude	Longitude
Container	56	0226806	6995596	-27° 08' 06.57270"	150° 14' 37.577729"
Flux Tower	56	0226913	6995689	-27° 08' 3.62976"	150° 14' 41.53397"

### 6.3.1 CONCENTRATIONS

Atmospheric concentrations of CO<sub>2</sub> and CH<sub>4</sub> are a result of the fluxes between land and atmosphere and their subsequent dispersion in the atmosphere. Therefore measurements of concentrations and meteorology are needed to be able to detect, attribute and quantify emissions.

The concentrations of CO<sub>2</sub>, CH<sub>4</sub> and H<sub>2</sub>O in air are measured by a Picarro cavity ring down spectrometer (model G2301; number CFAD2324) from a 10 metre inlet on the tower adjacent to the container (Figure 6.13). This height extends above the extreme vertical gradients at the surface and corresponds to the

lowest level of the TAPM modelling software. Measurement frequency is every few seconds, from which means over a range of periods from a minute to an hour are calculated. Measurements of a reference gas are made for 20 minutes every 2 days, and of calibration gases nominally every month. Concentrations of CO<sub>2</sub> and CH<sub>4</sub> are calibrated to these gases and corrected for H<sub>2</sub>O volumes to give dry-air concentrations. Data are stored on the computer at the site and downloaded daily by internet to CSIRO servers for processing by GCWerks software (GC Soft Inc., California). Concentrations are reported on internationally recognised mole fraction scales (WMOx2007 for CO<sub>2</sub> and NOAA04 for CH<sub>4</sub>), which are adopted by the World Meteorological Organisation's Global Atmosphere Watch (WMO GAW) program. This ensures certainty in trends over time and allows precise intercomparison between measurement sites in CSIRO and WMO networks and with the mobile Picarro surveys. Measurement accuracy is better than ±0.1 ppm for CO<sub>2</sub> and ±1 ppb for CH<sub>4</sub>.

Meteorological instruments are fitted to the inlet mast to measure wind speed and direction, solar radiation, relative humidity, temperature, pressure and rainfall.



**Figure 6.13.** Ironbark monitoring container and inlet tower shortly after installation. Inset: Picarro analyser, inlet pump, reference and calibration gas cylinders and regulators, air conditioner.

### 6.3.2 METEOROLOGY, TURBULENCE AND FLUXES

The spatial extent of the area contributing to the measured CO<sub>2</sub> and CH<sub>4</sub> concentrations at a fixed location (the footprint of CO<sub>2</sub> and CH<sub>4</sub>) depends on the wind direction, wind speed, turbulence and the resulting height of the atmospheric boundary layer.

The atmospheric boundary layer (ABL) comprises the bottom 200 m to 2 km of the atmosphere. It undergoes large daily variations of temperature, wind, static stability and turbulence. These variations are driven by the diurnal cycle of solar heating during the day and emission of thermal infrared radiation at night. It is to a large extent the height of the ABL that determines the volume of air available to mix atmospheric constituents.

On a sunny day the surface is heated and the boundary layer becomes unstable, promoting convective plumes and turbulent mixing. On a clear night the surface is cooled and the boundary layer becomes stable, suppressing vertical movement of air. Turbulence can also be created by shear. During very windy days the development of large convective cells is usually suppressed and smaller shear produced eddies will dominate the flow. On windy nights turbulence produced by wind shear can overcome buoyant consumption of turbulence leading to neutrally stratified flows.

Quantification of energy fluxes, radiation components as well as shear and buoyant production (or consumption) of turbulence are critical for modelling CO<sub>2</sub> and CH<sub>4</sub> emissions. These are measured at the flux tower, located 140 m northeast of the concentration measurements (Figure 6.14). Energy fluxes and turbulence are measured using measured using Eddy Covariance (EC) instrumentation. Three -dimensional wind speed and direction is measured using a CSAT3 sonic anemometer (Campbell Scientific Inc.) which transmits and receives ultrasonic signals to sense wind speeds and directions, and measures the speed of sound through an air volume to measure air density (e.g. temperature and humidity). Gas sensor measurements are coupled with 3D wind measurements to calculate a flux of gas towards (negative flux) or away from (positive flux) the land surface. The LI-7500A, manufactured by LI-COR Biosciences, uses non-dispersive infrared detection to measure H<sub>2</sub>O and CO<sub>2</sub> in the atmosphere with precision accuracies of 4.7 ppm and 0.11 ppm respectively. Radiation components (long and shortwave incoming and outgoing radiation) are measured with a CNR4 manufactured by Kipp and Zonen.

Several other variables are measured which feed into the overall energy flux calculation equations or are used for quality control. These include wind speed and direction (Gill 2D sonic anemometer), temperature and humidity (HMP45; Vaisala temperature and relative humidity probe). Soil property measurements are also required and include soil temperature (TCAV; Campbell type E thermocouple averaging soil temperature probes), soil heat flux (CN3; Middleton soil heat flux plates), and soil moisture (CS616; Campbell water content reflectometer).





**Figure 6.14.** Flux tower instrumented to measure wind field, turbulence and energy fluxes. Inset: EC instruments including sonic anemometer, temperature and humidity probes, gas sensor, radiometers.

### 6.3.3 PRELIMINARY RESULTS

Concentration measurements began at Ironbark on 12 November 2014. The flux tower became fully operational on 17 November 2014.

Figure 6.15 shows a time series of some key variables measured in the first 20 days of operation.

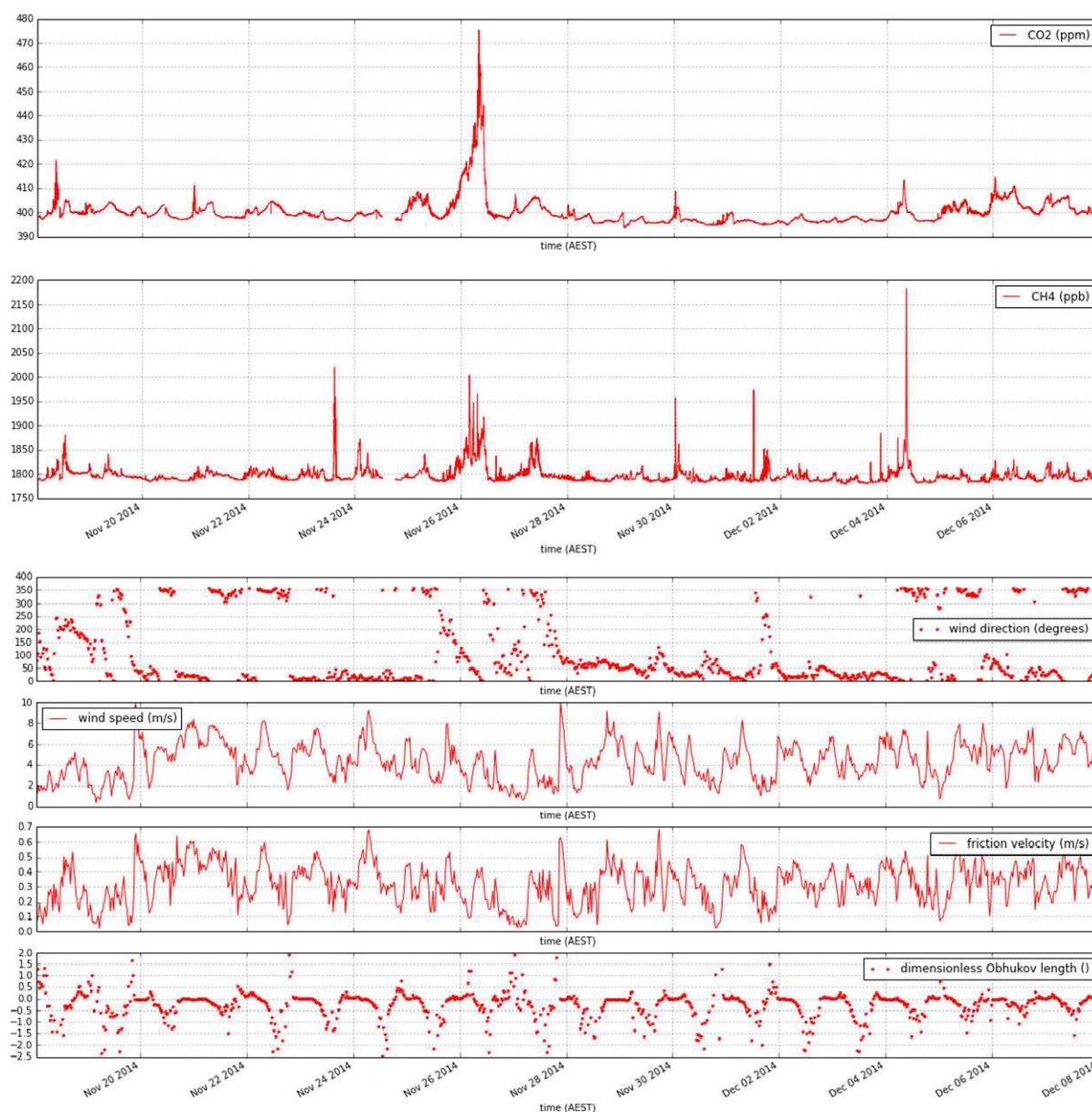


**Figure 6.15. Measurements over the period 18/11/2014 to 08/12/2014 of CO<sub>2</sub> and CH<sub>4</sub> concentrations from the Ironbark container, and wind direction, wind speed, friction velocity and dimensionless Obukhov length at the flux tower.**

Diurnal variations are apparent in the concentrations of both gases as a result of varying dispersion, with strong mixing during the day and stable conditions at night. The CO<sub>2</sub> diurnal cycle is further enhanced by daytime photosynthetic uptake and nighttime respiration.

For comparison, mean CO<sub>2</sub> and CH<sub>4</sub> concentrations in November 2014 were 396.6 ppm and 1789.4 ppb at Cape Ferguson, Queensland and 395.9 ppm and 1789.4 ppb at Cape Grim Tasmania, respectively. These represent the concentrations of the clean marine atmosphere for the corresponding latitudes.

Several narrow peaks in CH<sub>4</sub> concentration are evident and indicate point source emissions. Some of these are accompanied by CO<sub>2</sub> peaks which suggest combustion as the source. Wind measurements and back trajectories computed using an atmospheric transport model (HYSPLIT; Draxler and Rolph) show that CH<sub>4</sub> peaks above 1900 ppb occur in winds from the north which pass over large facilities such as gas or power plants tens of kilometres away.

Wind direction for the time period was mainly from the north and maximum wind speeds of 10 m s<sup>-1</sup> were reached. Shear or friction velocity is closely linked to wind speed and high shear production of turbulence was frequently observed. The Obukhov length is the height at which the buoyant production of turbulent

kinetic energy is equal to that produced by shear and therefore is a good indicator of atmospheric stability. Figure 6.15 (bottom trace) indicates that during nighttime conditions were often close to neutral or slightly stable (note that a normalised inverse Obukhov length is given) but daytimes were characterised by unstable conditions.

On November 26, peak concentrations of CO<sub>2</sub> and CH<sub>4</sub> were observed - on December 4 even higher CH<sub>4</sub> concentrations were observed. In both cases wind direction was from N (30° and 355° respectively), and wind speeds and friction velocities were moderate. While on November 26 the boundary layer stratification was unstable, relatively higher friction velocities on December 4 indicate more shear production that led to neutral stability conditions.

Turbulence measurements carried out at the flux tower allow the measured concentrations to be related to the area they were emitted from. Given that the landscape is flat and homogeneous inverse modelling techniques can be used to determine the footprint of the measured CO<sub>2</sub> and CH<sub>4</sub> concentrations (see also Figure 6.10). For example, in the event of November 26 the source area lies to the ENE from Ironbark and is smaller than on December 4 when winds were more northerly and the source area is larger but narrower.

These early results and model simulations suggest that the Ironbark facility, combined with the proposed Site #2 facility to the north, will be well suited to monitoring potential emissions from CSG activities in their present state and as they are projected to grow. The combined concentration, meteorology and turbulence data will be used as input to test the ability of inverse modelling to infer sources across the CSG area in the next phase of the project.

## 7 Discussion

Mobile ground surveys have been demonstrated as a viable method for locating CH<sub>4</sub> seeps and other emission sources. Modern instrumentation now has the sensitivity, stability and response time, which when combined with accurate positional data, provides a rapid means for covering large areas of landscape within a reasonable period of time. During this project a number of ground seeps of varying emission intensities with no apparent surface manifestations were located successfully using mobile surveys. Other groups have also recently used vehicle surveys to locate CH<sub>4</sub> emission sources (Maher, et al., 2014; Iverach et al., 2014). However, one of the main limitations of this approach is that surveys are generally confined to formed roads. Off road surveys are feasible when vehicle access is available; however, given the scale of the Surat Basin, which covers approximately 300,000 km<sup>2</sup>, it is unlikely that the entire region can be surveyed in detail by mobile surveys alone. Mobile ground based surveys are also highly dependent upon prevailing wind conditions such that the vehicle must pass through the source plume. If the wind is from the wrong direction, sources may not be detected.

Remote sensing potentially overcomes many of the limitations associated with ground based surveys because these methods allow access to larger areas and in less time, provided the sensors have sufficient sensitivity and spatial resolution for the purpose. Phase 1 of this project identified and recommended the SIGIS-FTIR and CHARM®-DIAL technologies for further investigation during Phase 2. Unfortunately, these systems were not available in Australia during the timeframe of Phase 2 so instead, the ALMA G2 pipeline inspection system, which had recently been made commercially available, was examined. The survey conducted with the ALMA G2 during this project is the first time that this system has been tested for use for baseline CH<sub>4</sub> values.

The ALMA G2 system demonstrated the ability of such systems to locate CH<sub>4</sub> sources and preliminary results show that it had sufficient sensitivity to locate even small emission sources. However, the detection limit is inversely proportional to the flying speed of the aircraft, hence relatively slow speeds and low altitude are required to achieve the necessary detection limits required for low level seeps. Further, unlike the CHARM® system, it is a profiling system (similar to geophysics) where one pixel of approximately 1 m footprint is recorded along a path rather than an imaging system where a number of pixels are acquired along track. Therefore, a large number of flight lines are required to provide a spatially comprehensive coverage over an area. While the method shows some promise for locating seeps and other CH<sub>4</sub> sources at the local scale, the limitations in the speed of data acquisition and footprint places the application of this technology to discreet local scale surveys (such as surface infrastructure) rather than regional scale basin wide assessments. Imaging systems may provide a better method of rapidly surveying large areas but the instrumentation required is of very limited availability in Australia, although it proposed to investigate this further during Phase 3 of the project.

The determination of an appropriate remote sensing method is important because it is the only method where spatially comprehensive data can be efficiently acquired over large areas such as the Surat Basin. Besides providing a baseline of the spatial distribution and locating the source of anomalies, with appropriate data complemented with other independent corroborative observations, remote sensing could become an important component of routine monitoring. Additionally, remote sensing is complementary to the atmospheric methods discussed in this report. For example, remote sensing may be useful for validating and verifying the model(s) developed, and possibly as a source of input data for the model(s).

Satellite based remote sensing data such as SCIAMACHY has potential for providing regional scale trends of gas production regions. The investigation of SCIAMACHY satellite data indicates that this technology was able to provide an indication of the trends over time at a regional scale. The statistics show that the average trends across the entire Surat Basin were close to the average trends across the rest of Australia for the time period analysed (2003-2009). This provides a regional scale trend of the column CH<sub>4</sub> level close to before the establishment of the CSG industry. It is important to track regional scale trends and impacts

after the establishment of the CSG industry, it may be useful to acquire longer term data of this nature. However, it must be noted that these data only yield broad scale information and will not provide the ability to identify and separate local scale impacts such as the contributions from the feedlots compared to a gas well.

Although our analysis of the satellite data acquired over the Surat Basin did not show significantly higher CH<sub>4</sub> levels within the CSG production region, it is worth noting that two independent studies also using SCIAMACHY data have found elevated CH<sub>4</sub> concentrations in some U.S. gas production regions (Schneising et al., 2014; Kort et al., 2014). These studies examined satellite-derived column CH<sub>4</sub> measurements near the San Juan coal seam gas production region (near the junction of the borders of Arizona, New Mexico, Colorado and Utah; Kort et al., 2014) and near the shale oil and gas production fields of Eagle Ford in Texas and Bakken in North Dakota (Schneising et al., 2014).

Based on the calculated fluxes, these three regions alone appear to account for 2.11 Tg yr<sup>-1</sup> of the 7.7 Tg yr<sup>-1</sup> (2008) of CH<sub>4</sub> emissions from natural gas when compared with the US-EPA Greenhouse Gas Reporting Program (i.e. approximately 27 % of national gas emissions), suggesting a disproportionately large contribution from these regions. In addition, the leakage to production ratios for the Eagle Ford and Bakken regions are more than 10±7 % and 9±6 %, respectively. Such values are higher than the 3% threshold in fugitive emissions ratios that would eliminate any potential 'climate benefit' derived from substituting gas for coal (Alvarez et al., 2012). These two studies based on SCIAMACHY data have added to the intense debate in the U.S. on the magnitude of fugitive emissions from onshore gas development and recent top-down versus bottom-up studies (Pétron et al., 2012; Howarth et al., 2011; Howarth et al., 2012; Cathles, 2012; Cathles et al., 2012). These studies highlighted differences between the different types of measurements which warrant further investigations. However, the two studies of Schneising et al (2014) and Kort et al (2014) also introduce their own uncertainties and so do not provide a definitive conclusion regarding fugitive emissions from unconventional gas in the United States.

While some of the recent studies of emissions from unconventional gas production in the United States have reported high levels of emissions, there is a wide range of reported emission rates, highlighting the large uncertainties associated with these estimates. When using atmospheric CH<sub>4</sub> concentration data derived from SCIAMACHY observations to determine fugitive emissions, there are four important uncertainties that must be considered when interpreting the results:

#### **1. Different column methane maps.**

While both studies (Kort et al., 2014; Schneising et al., 2014) use the same data from the SCIAMACHY sensor, each study uses different algorithms for determining atmospheric column methane concentrations. Kort et al. (2014) use the IMAP-DOAS algorithm (see Section 4.2) which uses the CO<sub>2</sub> concentrations as a proxy for air column in the computation of methane mole fractions. In contrast, Schneising et al. (2014) uses the WFM-DOAS algorithm (see Section 4.2) consisting of a simplified radiative transfer model and atmospheric column normalised weighting functions to determine total column CH<sub>4</sub> concentration. "The differences between the algorithms are fairly distinct. Obvious is the far larger scatter in the WFM-DOAS data (overall 76 ppb compared to 50 ppb for IMAP)" Dils, et al., 2014. As a consequence, these two algorithms produce different 'raw' column methane maps for North America. For example the San Juan CH<sub>4</sub> 'raw' column methane map (Kort et al., 2014) doesn't appear in the equivalent maps of Schneising et al. (2014). It is necessary to harmonise the CH<sub>4</sub> concentration anomalies across the continental United States before accurate fluxes can be determined.

#### **2. Sensor degradation and observation uncertainties.**

Since November 2005, SCIAMACHY's channel 6+, which is used for the methane column retrievals, suffered from an increasing number of dead and bad detector pixels including so-called random telegraph detector pixels, which unpredictably jump between at least two quasi-stable dark signal levels (Lichtenberg et al., 2006; Frankenberg et al., 2011; Schneising et al., 2011). Thus, retrievals of atmospheric methane concentration from both algorithms are of reduced quality and suffer increased noise after this date compared to retrievals made pre-November 2005. Additional errors



also arise from random excursions from the dark standard that have appeared during specific orbits since 2005.

Measurements of regional relative precision for column methane using the WFM-DOAS algorithm (Schneising et al., 2012) based on direct comparisons with instantaneous ground observations were 12 ppb prior to November 2005 (relative accuracy approximately 3 ppb) and 17 ppb after November 2005 (relative accuracy 10-20 ppb) for monthly averages at a spatial scale of ~500 km (Schneising et al., 2012). The methane concentration anomalies reported for the Eagle Ford and Bakken production fields are less than 10 ppb. The similarity in magnitude of anomaly and uncertainty suggest that this could potentially translate to large uncertainties associated with flux calculations (see below).

### **3. Methane flux estimation uncertainties.**

The increase in detector noise associated with the SCIAMACHY has resulted in higher uncertainties with the associated methane fluxes for each of the Eagle Ford and Bakken production fields (Schneising et al., 2014). This yields a coefficient of variance of over 60 % on the estimated fluxes. On the other hand, Kort et al. (2014) report lower uncertainties with estimated fluxes for the San Juan basin vicinity (coefficient of variance ~14 %). This is most likely to be related to the differences in the algorithms used to derive the column methane values (Dils, et al., 2014) but further evidence is required to determine this.

### **4. Methane flux attribution.**

Each of the studies (Kort et al., 2014; Schneising et al., 2014) report on fluxes calculated from model simulations constrained by observed atmospheric column methane concentrations and taking into account lower troposphere meteorology. In both cases, all modelled fluxes are attributed to gas industry sources based on the time evolution of atmospheric concentration anomalies. While this approach provides circumstantial evidence for gas industry methane sources (notwithstanding the above uncertainties), corroborative evidence needs to be collected (e.g. isotopic or other tracer measurements) to correctly and accurately attribute methane sources. This is particularly important because of correlated increases in methane fluxes from other northern hemisphere land based sources unrelated to the gas industry. The magnitude of these sources, which are dispersed throughout landscapes, is unknown at this stage but, locally, may be an important contributor to enhanced methane emissions. Furthermore, in regions where significant natural background methane seeps occur (such as in the Surat Basin in Queensland) these fluxes may be important sources of methane flux to the atmosphere.

Until the above uncertainties are addressed, no definitive statement on fugitive emissions can be made using the SCIAMACHY data alone. Further research is required particularly in harmonising satellite, airborne and ground based observations in order to get a full understanding of the fluxes attributed to natural background seeps, other methane sources and fugitive emissions. The present project in the Surat Basin seeks to address these issues. Such a comprehensive approach is necessary as input to life-cycle analyses required to accurately determine the climate impacts/benefits of substituting gas for coal in energy production. Therefore, it would be fruitful to undertake further investigations to help ascertain the optimal information retrieval method to obtain the best estimate for column methane and the uncertainties associated with their usage. Further, there are uncertainties related to the ground composition, land use, seasonal variations, sampling resolution, topography and other interferences such as atmospheric water vapour which need to be accounted for as well.

Detection of CH<sub>4</sub> sources, either by mobile surveys or remote sensing methods, is obviously an important aspect of developing a comprehensive emissions inventory of the Surat Basin or any other region. However, concentration data collected during these surveys, in isolation, provide limited information on the emission rates, which are essential for assessing the impact of activities on the overall CH<sub>4</sub> budget. In some cases, emission rate estimates may be derived from concentration data measured during ground level surveys when combined with local meteorological data. However, these estimates may be subject to large uncertainties, especially if attempting to measure emissions from spatially large or distant sources. Other techniques based on downwind traverses using controlled releases of tracer gases may yield more accurate

emission data and this is being investigated further within CSIRO. More sophisticated atmospheric methods based on continuous monitoring at fixed stations such as those discussed in Section 6 are likely to yield more reliable and continuous emission flux data for the broader region than periodic measurements of downwind plume concentrations made by vehicle traverses. However, it is apparent that top-down atmospheric methods will require a detailed understanding of the location and relative sizes of the CH<sub>4</sub> sources within the monitoring field if individual sources are to be quantified. Mobile surveys are likely to be able to provide much of this prior 'initialisation' data required to properly set up inverse models and potentially provide high resolution data needed to resolve closely spaced sources of CH<sub>4</sub>.

Surface flux chambers are an effective and reliable method for directly measuring emissions flux from many terrestrial sources. In particular, localised sources such as legacy boreholes, natural soil respiration and river seeps are amenable to this method. The primary drawback however, is that many individual measurements are required to accurately map and quantify emission sources and hence for large areas, the method may not be practical. Nevertheless, the simplicity of the technique means that it has considerable application for any detailed survey of surface emission points, particularly when information such as the location of abandoned boreholes or geological faults is available.

One of the challenges that will be faced during Phase 3 will be developing a detailed map and emission inventory of the CH<sub>4</sub> sources in the region covered by the monitoring network. It is clear for the results obtained to date that there are many sources or potential sources of CH<sub>4</sub> that will be detected by the fixed monitoring stations. Many of these are associated with CSG production infrastructure; wells, gas processing plants pipelines etc. and initial monitoring data from the Ironbark site confirm that emissions from CSG processing facilities to the northeast are contributing to the CH<sub>4</sub> signal. Agriculture is also an important source of CH<sub>4</sub>. Cattle feedlots, which are widespread throughout the study region, are significant emitters of CH<sub>4</sub>. Irrigation may also contribute to CH<sub>4</sub> emissions, either through microbial activity in dams and other wetlands but also potentially from CH<sub>4</sub> reaching the surface via groundwater wells. This latter aspect has not been widely considered but given the large number of irrigation bores across Queensland is an important area for further research. If the known source locations and strengths (many of which are independently quantified) are included in the inverse modelling, the top down monitoring may be able to provide information on these lesser known sources.

Another, as yet unquantified, CH<sub>4</sub> source contributing to regional emissions was from leaking legacy coal exploration boreholes. A recent study in the U.S. concluded that leaking abandoned oil and gas boreholes are contributing between 4 and 7 % of anthropogenic CH<sub>4</sub> emissions in Pennsylvania (Kang et al., 2014). This is a significant finding as it may account for some of the discrepancies between high emissions rates reported in most top-down studies and the usually lower rates top-down estimates of current gas production facilities (Allen et al., 2013). In the Australian context, recent reports indicate that abandoned exploration boreholes, some of which are more than 60 years old, are widespread throughout Queensland (Gasfields Commission, 2013b). Methane emission rates from 10 such boreholes located during this project were found to be significant, ranging from about 0.1 to more than 100 kg CH<sub>4</sub> day<sup>-1</sup>. One of these leaking boreholes was subsequently filled with concrete which reduced the emission rate to about one quarter of the original leak rate. While this was effective at reducing any fire safety hazard associated with high levels of CH<sub>4</sub> leakage, greenhouse mitigation may require alternative approaches if surrounding strata have high permeability.

Although some of the boreholes located during this study had high CH<sub>4</sub> emission rates, it is important to recognise that these results are very much preliminary and are not representative of emissions from legacy boreholes more generally. Consequently it is not valid to extrapolate these results to estimate regional CH<sub>4</sub> for the Surat Basin using the approach of Kang et al. (2014). It is clear that considerably more work is required to properly assess the contribution from legacy boreholes. However, locating many of these legacy boreholes may present somewhat of a challenge given that probably all predate current GPS technology and hence records, if they still exist, may not provide an accurate location. For wells with appreciable CH<sub>4</sub> emissions, mobile surveys such as those used during this project can be used to find leaking wells, provided access to the area is possible. Remote sensing technologies, especially those with imaging capability may also have application to locating leaking boreholes. Surface flux chamber measurements can then be used to accurately determine emission rates from these leaking abandoned wells.

While detecting and quantifying CH<sub>4</sub> emitting legacy boreholes is important, it is equally important to determine the numbers of non-emitting boreholes to be able to gauge what proportion are leaking. However, this is generally more difficult than locating leaking boreholes (which have elevated CH<sub>4</sub> levels in the vicinity) since there is often little evidence of the borehole remaining on site and as already noted, existing records may not provide accurate locations.

## 8 Future Work

Phase 2 of the project was primarily aimed at developing and trialling techniques to locate and quantify emissions within the Surat Basin. Phase 3 is intended to extend this work by deploying the most promising of these methods at selected locations to provide the basis for an ongoing baseline monitoring programme.

Originally, it had been proposed that Phase 3 would run for one year. However, the LNG facilities currently under construction in Gladstone are scheduled to commence operation during 2015 and it is anticipated that CSG production in the Surat gas fields will progressively increase to meet demand from these plants. Hence a unique opportunity exists to measure methane emissions from the Surat Basin during the initial stages of one of Australia's largest gas development projects. To take advantage of this opportunity, it is proposed that Phase 3 be conducted over three years, rather than one, to provide baseline monitoring of emissions from the Surat gas fields during the period of increasing gas production that will occur over the next few years. Longer term monitoring is also more likely to reveal any seasonal variability in emissions that would be difficult to discern from a 12-month monitoring campaign.

The main components of Phase 3 will be:

1. Operation of the two fixed methane monitoring stations at two locations within the Surat Basin and estimation of regional emissions. The first of these stations is now operational (Section 6) while the second is expected to commence operation during the second half of 2015 provided Phase 3 proceeds.
2. Periodic field surveys using an instrumented vehicle.
3. A trial of an imaging remote sensing system for locating terrestrial seeps.

Previous work by CSIRO has shown the potential of inverse modelling to monitor dispersed emission sources; however, the technique has not been applied at the scale proposed for Phase 3. Consequently, a significant effort will be directed at developing suitable models for monitoring at the regional scale and including them in an inverse framework to infer source locations and strengths from concentration and wind measurements.

Given that there are a number of significant CH<sub>4</sub> sources such as cattle feedlots and coal mines, etc. throughout the region, source attribution will be an important aspect of Phase 3. This will be attempted by including the locations and inventory emissions estimates in the dispersion modelling. A flask sampling system will also be installed at one of the sites to collect ambient air samples for offline analyses at the CSIRO Aspendale and North Ryde laboratories for chemical and isotopic composition to compare with the source compositions found from sampling during Phase 2. Further ground surveys will also be made from time to time to provide positive identification of sources that contribute to the methane signals detected by the monitoring stations.

During Phase 3 of the project it is also intended to examine other remote sensing instrumentation. While the ALMA G2 system trialled during Phase 2 demonstrated a high level of sensitivity that is sufficient to locate even small CH<sub>4</sub> sources, the relatively low speed of the surveys and the narrow footprint of the beam limit the system to local surveys rather than regional scale operation. Accordingly, during Phase 3 it is proposed to conduct further remote sensing trials using an imaging system based on Fourier transform infrared spectroscopy (FTIR) as recommended as part of Phase 1 of this project. Such a system, which was not available during Phase 2, may potentially provide spatially comprehensive data which was lacking in the airborne ALMA G2 system. We have now secured the use of the Bruker HI90 and potentially SIGIS systems for a trial. An experiment will be designed to evaluate the feasibility of such a system for determining the spatial distribution of CH<sub>4</sub> emissions. The location of the field trial is likely to be in the Chinchilla region with preliminary testing conducted on the CSIRO site at Newcastle.

The initial trial will be limited to deployment from a fixed ground platform (rather than an aircraft) and will consist of:

1. A controlled release where different flow rates and instrument heights will be tested to determine the detection limits of the instrument.
2. Deployment of the instrument to a known site where leakage has been previously detected, such as near Chinchilla.

At the end of Phase 3, it is anticipated that a robust method for continuously monitoring regional CH<sub>4</sub> emissions in the Surat Basin will be available. Phase 3 will also provide an initial set of data on baseline CH<sub>4</sub> emissions for the region.



# References

- Allen, D.T. Torres, V.M., Thomas, J., Sullivan, D.W., Harrison, M., Hendler, A., Herndon, S.C., Kolb, C.E., Fraser, M.P., A. Daniel Hill, A.D., Lamb, B.K., Miskimins, J., Sawyer, R.F., Seinfeld, J.H., 2013. Measurements of methane emissions at natural gas production sites in the United States. *Proceedings of the National Academy of Science* 110, 18023–18024.
- Alvarez, A.A., Pacala, S.W., Winebrake, J.J., Chameides, W.L., Hamburg, S.P., 2012. Greater focus needed on methane leakage from natural gas infrastructure. *Proceedings of the National Academy of Science*, 109, 6435-6440.
- Berko, H., Etheridge, D., Loh, Z., Kuske, T., Allison, C., Gregory, R., Spencer, D., Law, R., Zegelin, S. and Feitz, A., 2012. Installation Report for Arcturus (ARA): An inland baseline station for the continuous measurement of atmospheric greenhouse gases. Record 2012/54. Geoscience Australia: Canberra.
- Berner, U., Faber, E., 1996. Empirical carbon isotope/maturity relationships for gases from algal kerogens and terrigenous organic matter, based on dry, open-system pyrolysis. *Organic Geochemistry* 24, 947–955.
- Bruzzi, S., Louet, J., Pfeiffer, B., 1995. ENVISAT-1 system and missions. *Space Technology and Commercial Applications* 15, 145-155.
- Buchwitz, M., De Beek, R., Burrows, J.P., Bovensmann, H., Warneke, T., Notholt, J. et al., 2005. Atmospheric methane and carbon dioxide retrieved from SCIAMACHY satellite data: initial comparison with chemistry and transport models. *Atmospheric Chemistry and Physics* 5, 941-962.
- Buchwitz, M., De Beek, R., Noël, S., Burrows, J.P., Bovensmann, H., Scheising, O., et al., 2006. Atmospheric carbon gases retrieved from SCIAMACHY by WFM-DOAS: version 0.5 CO and CH<sub>4</sub> and impact of calibration improvements on CO<sub>2</sub> retrieval. *Atmospheric Chemistry and Physics* 6, 2727-2751.
- Buchwitz, M., Rozanov, V.V., Burrows, J.P., 2000. A near infrared optimized DOAS method for the fast global retrieval of atmospheric CH<sub>4</sub>, CO, CO<sub>2</sub> H<sub>2</sub>O and N<sub>2</sub>O total column amounts from SCIAMACHY ENVISAT-1 nadir radiances. *Journal of Geophysical Research – Atmospheres*. 105, 15231-15245.
- Burrows, J.P., Holzle, E., Goede, A.P.H., Visser, H., Fricke, W., 1995. SCIAMACHY – scanning imaging absorption spectrometer for atmospheric cartography. *Acta Astronautica* 35, 445-451.
- Burruss, R.C. and Laughrey, C.D., 2010. Carbon and hydrogen isotopic reversals in deep basin gas: evidence for limits to the stability of hydrocarbons. *Organic Geochemistry* 41, 1285-1296.
- Campbell, J.B., 2002. *Introduction to Remote Sensing*. Taylor and Francis.
- Cathles, L., Brown, L., Taam, M., Hunter, A. 2012. A commentary on ‘The greenhouse-gas footprint of natural gas in shale formations’ by R.W. Howarth, R. Santoro, and Anthony Ingraffea. *Climatic Change*, 113, 525-535.
- Cathles, L.M., 2012. Assessing the greenhouse impact of natural gas. *Geochemistry, Geophysics, Geosystems* 13, Q06013.
- Chung, H.M., Sackett, W.M., 1979. Use of stable carbon isotope compositions of pyrolytically derived methane as maturity indices for carbonaceous materials as well as degradation, resulting in depletion of. *Geochimica et Cosmochimica Acta* 43, 1979–1988.
- Clark-Thorne, S.T., Yapp, C.J., 2003. Stable carbon isotope constraints on mixing and mass balance of CO<sub>2</sub> in an urban atmosphere: Dallas metropolitan area, Texas, USA. *Applied Geochemistry* 18(1), 75–95. doi:10.1016/S0883-2927(02)00054-9.

- Clayton, J.L., 1998. Geochemistry of coalbed gas – A review. *International Journal of Coal Geology* 35(1-4), 159–173. doi:10.1016/S0166-5162(97)00017-7.
- Clearstone Engineering, 2002. Identification and evaluation of opportunities to reduce methane losses at four gas processing plants. Gas Research Institute, Des Plaines IL.  
([http://epa.gov/gasstar/documents/four\\_plants.pdf](http://epa.gov/gasstar/documents/four_plants.pdf), accessed 1 June 2014).
- Connan, J., Cassou, A., 1980. Properties of gases and petroleum liquids derived from terrestrial kerogen at various maturation levels. *Geochimica et Cosmochimica Acta* 44, 1–23.
- Conrad, R., 2005. Quantification of methanogenic pathways using stable carbon isotopic signatures: a review and a proposal. *Organic Geochemistry* 36(5), 739–752.
- Crill, P.M., 1991. Season patterns of methane uptake and carbon dioxide release by a temperate woodland soil. *Global Biogeochemical Cycles* 5, 319–334.
- Crosson, E.R., 2008. A cavity ring-down analyzer for measuring atmospheric levels of methane, carbon dioxide, and water vapor. *Applied Physics B* 92, 403–408.
- Dai, J., Qi, H., 1989. Relationship of  $^{13}\text{C}$ -R<sub>o</sub> of coal-derived gas in China. *Chinese Science Bulletin* 34, 690–692.
- Dalal, R.C., Allen, D.E., Livesley, S.J., 2008. Magnitude and biophysical regulators of methane emission and consumption in the Australian agricultural, forest and submerged landscapes: a review. *Plant Soil* 309, 43–76.
- Day, S., Etheridge, D., Connell, N., Norgate, T. (2012). Fugitive greenhouse gas emissions from coal seam gas production in Australia. CSIRO Report EP128173. 28 pp.
- Day, S., Dell’Amico, M., Ong, C., Rodger, A., Sherman, B., Barrett, D., 2013. Characterisation of regional fluxes of methane in the Surat Basin, Queensland – Phase 1: A review and analysis of literature on methane detection and flux determination. 32pp, CSIRO Australia.
- Day, S., Dell’Amico, M., Fry, R., Javanmard Tousi, H., 2014. Field measurements of fugitive emissions from equipment and well casings in Australian coal seam gas production facilities. 41 pp, CSIRO Australia.
- Denmead, O.T., 2008. Approaches to measuring fluxes of methane and nitrous oxide between landscapes and the atmosphere, *Plant Soil* 309, 5–24.
- Dils, B., Buchwitz, M., Reuter, M., Schneising, O., Boesch, H., Parker, R., Guerlet, S., Aben, I., Blumenstock, T., Burrows, J.P., Butz, A., Deutscher, N.M., Frankenberg, C., Hase, F., Hasekamp, O.P., Heymann, J., De Mazière, M., Notholt, J., Sussmann, R., Warneke, T., Griffith, D., Sherlock, V., Wunch, D., (2014). The Greenhouse Gas Climate Change Initiative (GHG-CCI): comparative validation of GHG-CCI SCIAMACHY/ENVISAT and TANSO-FTS/GOSAT CO<sub>2</sub> and CH<sub>4</sub> retrieval algorithm products with measurements from the TCCON. *Atmospheric Measurement Techniques*, 7, 1723–1744.
- DNRM, 2013. Protocol for managing uncontrolled gas emissions from legacy boreholes. Queensland Department of Natural Resources and Mines, Brisbane,  
(<http://mines.industry.qld.gov.au/assets/legislation-pdf/legacy-borehole-protocol.pdf>, accessed 11 December 2014).
- DNRM (2014). Queensland’s coal seam gas overview, January 2014, prepared by Queensland Department of natural Resources and Mines. <http://mines.industry.qld.gov.au/assets/qld-mining-update/csg.pdf>, accessed 18 Dec 2014.
- Draxler, R.R., Rolph, G.D., HYSPLIT (HYbrid Single-Particle Lagrangian Integrated Trajectory) Model access via NOAA ARL READY Website <http://www.arl.noaa.gov/HYSPLIT.php>). NOAA Air Resources Laboratory, College Park, MD.
- Emery, D., Robinson, A. G., Aplin, A., Smalley, C., 1993. *Inorganic geochemistry: applications to petroleum geology* (p. 254). Oxford, Boston: Blackwell Scientific. Retrieved from  
<http://csiro.summon.serialssolutions.com/document/show?id=FETCHMERGED->

- Etiope G., Zwalen C., Aselmetti F.S., Kipfer R., Schubert C.J., 2010. Origin and flux of a gas seep in the Northern Alps (Giswil, Switzerland), *Geofluids* 10, 476-485.
- Etiope, G., Drobnia, A., Schimmelmann, A., 2013. Natural seepage of shale gas and the origin of the 'eternal flames' in the Northern Appalachian Basin, USA. *Marine and Petroleum Geology* 43, 178-186.
- Frankenberg, C., Platt, U., Wagner, T., 2005. Iterative maximum a posterior (IMAP) DOAS for retrieval of strongly absorbing trace gases: model studies for CH<sub>4</sub> and CO<sub>2</sub> retrieval from near infrared spectra of SCIAMACHY onboard ENVISAT. *Atmospheric Chemistry and Physics* 5, 9-22.
- Games, L.M., Hayes, J.M., Gunsalus, R. P., 1978. Methane-producing bacteria: natural fractionations of the stable carbon isotopes. *Geochimica et Cosmochimica Acta* 42, 1295-1297.
- GasFields Commission Queensland, 2013a. Historic landscape gas seeps data search (<http://www.gasfieldscommissionqld.org.au/key-issues/historic-landscape-gas-seeps-data-search.html>, accessed 2 August 2013).
- GasFields Commission Queensland, 2013b. (<http://www.gasfieldscommissionqld.org.au/whats-happening/legacy-borehole-protocol-a-step-forward.html>, accessed 16 December 2013).
- Gloudemans, A.M.S., Schrivner, H., Kleipool, Q., Van Den Broek, M.M.P., Straume, A.G., Lichtenberg, G., et al., 2005. The impact of SCIAMACHY near infrared instrument calibration on CH<sub>4</sub>, and CO total columns. *Atmospheric Chemistry and Physics* 5, 2369-2383.
- Golding, S.D., Boreham, C.J., Esterle, J.S., 2013. Stable isotope geochemistry of coal bed and shale gas and related production waters: A review. *International Journal of Coal Geology* 120, 24-40.
- Gottwald, M., Bovensmann, H., 2013. SCIAMACHY product handbook (Eds Gottwald, M. and Bovensmann, H.) p 116. ESA, <https://earth.esa.int/web/guest/missions/esa-operational-eo-missions/envisat/instruments/sciamachy-handbook>.
- Gray, A.R.G., 1967. Natural Gas Occurrence in the Brigalow Area, March, 1967. Queensland Government Mining Journal 68, 394-395.
- Hamilton, S.K., Golding, S.D., Baublys, K.A., Esterle, J.S., 2014. Stable isotopic and molecular composition of desorbed coal seam gases from the Walloon Subgroup, eastern Surat Basin, Australia. *International Journal of Coal Geology* 122, 21-36.
- Hamilton, S.K., Golding, S.D., Baublys, K.A., Esterle, J.S., 2015. Conceptual exploration targeting for microbially enhanced coal bed methane (MECoM) in the Walloon Subgroup, eastern Surat Basin, Australia. *International Journal of Coal Geology* 138, 68-82.
- Hanna, S.R., Briggs, G.A., Hosker Jr., R.P., 1982. Handbook on atmospheric diffusion. U.S. Department of Energy, Technical Information Center (page 29).
- Hoefs, J., 1987. Stable Isotope Geochemistry (p. 63). Berlin: Springer-Verlag.
- Howarth, R., Santoro, R., Ingraffea, A., 2011. Methane and the greenhouse-gas footprint of natural gas from shale formations. *Climatic Change* 106, 679-690.
- Howarth, R., Santoro, R., Ingraffea, A., 2012. Venting and leaking of methane from shale gas development: response to Cathles et al. *Climatic Change* 113, 537-549.
- Humphries, R., Jenkins, C., Leuning, R., Zegelin, S., Griffith, D., Caldow, C., Berko, H., Feitz, A., 2012. Atmospheric tomography: a Bayesian inversion technique for determining the rate and location of fugitive emissions. *Environmental Science and Technology* 46, 739-746.
- Hunt, J., 1979. *Petroleum Geochemistry and Geology* (p. 617). San Francisco: W. H. Freeman.
- Hurley, P.J., Physick, W.L., Luhr, A.K., 2005. TAPM: a practical approach to prognostic meteorological and air pollution modelling. *Environmental Modelling and Software* 20, 737-752.

- Hutley, L.B., Leuning, R., Beringer, J., Cleugh, H.A., 2005. The utility of eddy covariance as a tool in carbon accounting: tropical savanna as a case study. *Australian Journal of Botany* 53, 663–675.
- Irwin, H., Curtis, C., Coleman, M., 1977. Isotopic evidence for source of diagenetic carbonates formed during burial of organic-rich sediments. *Nature* 269, 209–213.
- Iverach, C., Lowry, D., France, J., Fisher, R., Nisbet, E., Baker, A., Acworth, I., Loh, Z., Day, S., Dell’Amico, M., Kelly, B.F.J., 2014. The complexities of continuous air monitoring in attributing methane to sources of production. *Proceedings of the Australian Earth Sciences Convention, Newcastle, Australia July 7–10*. Geological Society of Australia.
- Javoy, M., Pineau, F., Delorme, H., 1986. Carbon and nitrogen isotopes in the mantle. *Chemical Geology* 57(1-2), 41–62. doi:10.1016/0009-2541(86)90093-8.
- JBS, 2014. JBS website <http://www.jbssa.com.au/OurFacilities/Feedlots/default.aspx>, accessed 10 Nov, 2014.
- Jenden, P.D., Hilton, D.R., Kaplan, I.R., 1993. Abiogenic hydrocarbons and mantle helium in oil and gas fields. In D.G. Howell (Ed.), *The Future of Energy Gases* (pp. 1570, 31–56). US Geological Survey, Professional paper.
- Jenden, P.D., Kaplan, I.R., Poreda, R.J., Craig, H., 1988. Origin of nitrogen-rich natural gases in the California Great Valley: Evidence from helium, carbon and nitrogen isotope ratios. *Geochimica et Cosmochimica Acta* 52, 851–861.
- Jenden, P.D., Kaplan, I.R., 1986. Comparison of microbial\* gases from the Middle America Trench and Scripps Submarine Canyon: implications for the origin of natural gas. *Applied Geochemistry* 1(6), 631–646.
- Kang, M., Kanno, C.M., Reid, M.C., Zhang, X., Mauzerall, D.L., Celia, M.A., Chen, Y., Onstott, T.C., 2014. Direct measurements of methane emissions from abandoned oil and gas wells in Pennsylvania. *Proceedings of the National Academy of Science Early Edition* [www.pnas.org/cgi/doi/10.1073/pnas.1408315111](http://www.pnas.org/cgi/doi/10.1073/pnas.1408315111).
- Kinnon, E.C.P., Golding, S.D., Boreham, C.J., Baublys, K.A., J.S. Esterle, J.S., 2010. Stable isotope and water quality analysis of coal bed methane production waters and gases from the Bowen Basin, Australia. *International Journal of Coal Geology* 82, 219–231.
- Kort, E.A., Frankenberg, C., Costigan, K.R., Lindenmaier, R., Dubey, M.K., Wunch, D., 2014. Four corners: The largest US methane anomaly viewed from space. *Geophysical Research Letters* 41, 6898–6903.
- Kotarba, M., Rice, D., 1995. Microbial methane and endogenic carbon dioxide in Lower Silesian Coal Basin, SW Poland. In R.D. Lama (Ed.), *Proceedings of the International Symposium-cum-workshop on Management and Control of High Gas Emissions and Outbursts in Underground Coal Mines* (p. 385). Wollongong, NSW, Australia.
- Kriese, R., Wochele, S., Butterbach-Bahl, K., 2008. Site specific and regional estimates of methane uptake by tropical rainforest soils in north eastern Australia. *Plant Soil* 309, 211–226.
- Lamb, B.K., McManus, J.B., Shorter, J.H., Kolb, C.E., Mosher, B., Harriss, R.C., Allwine, E., Blaha, D., Howard, T., Guenther, A., Lott, R.A., Siverson, R., Westberg, H., Zimmerman P., 1995. Development of atmospheric tracer methods to measure methane emissions from natural gas facilities and urban areas. *Environmental Science and Technology* 29, 1468–1479.
- Leuning, R., Etheridge, D., Luhr, A., Dunse, B., 2008. Atmospheric monitoring and verification technologies for CO<sub>2</sub> geosequestration. *International Journal of Greenhouse Gas Control* 2(3):401–414.
- Lilley, W., Day, S., Williams, D., Rae, M., Carras, J., 2012. A comparison of three methods for the quantification of greenhouse gas emissions from spontaneous combustion in open-cut coal mines. *Greenhouse Gas Measurement and Management*. 2, 93–105.

- Loh, Z., Leuning, R., Zegelin, S. J., Etheridge, D. M., Bai, M., Naylor, T., Griffith, D., 2009. Testing Lagrangian atmospheric dispersion modelling to monitor CO<sub>2</sub> and CH<sub>4</sub> leakage from Geosequestration. *Atmospheric Environment* 43(16), 2602–2611.
- Longinelli, A., Lenaz, R., Ori, C., Selmo, E., 2005. Concentrations and  $\delta^{13}\text{C}$  values of atmospheric CO<sub>2</sub> from oceanic atmosphere through time : polluted and non-polluted areas. *Tellus* 57B, 385–390.
- LTE, 2007. Phase II Raton Basin Gas Seep Investigation Las Animas and Huerfano Counties, Colorado, Project #1925 Oil and Gas Conservation Response Fund Characterisation of Regional Fluxes of Methane in the Surat Basin, Queensland (<http://cogcc.state.co.us/Library/RatonBasin/Phase%20II%20Seep%20Investigation%20Final%20Report.pdf>, accessed 4 August 2013).
- Luhar, A. K.; Etheridge, D. M.; Leuning, R.; Steele, L. P.; Spencer, D. A.; Hurley P. J., et al., 2009. Modelling carbon dioxide fluxes and concentrations around the CO<sub>2</sub>CRC Otway geological storage site. In: CASANZ 2009 Conference : 19th International Clean Air and Environment conference : 6th-9th September 2009, Perth Convention Exhibition Centre Perth, Western Australia; 2009; Perth, Australia. Clean Air Society of Australia and New Zealand; 2009.
- Maher, D.T., Santos, I.R., Tait, D.R., 2014. Mapping methane and carbon dioxide concentrations and  $\delta\text{C}^{13}$  values in the atmosphere of two Australian coal seam gas fields. *Water, Air and Soil Pollution* 225, 2216.
- McGinn, S.M., Chen, D., Loh, Z., Hill, J., Beauchemin, K.A., Denmead, O.T., Methane emissions from feedlot cattle in Australia and Canada. *Australian Journal of Experimental Agriculture* 2008, 48, 183–185.
- Nisbet, E.G., Dlugokencky, E.J., Bousquet, P., 2014. Methane on the Rise—Again. *Science*, 343, 493–495.
- NOHSC, 2001. Guidance note on the interpretation of exposure standards for atmospheric contaminants in the occupational environment NOHSC 3008(1995) 3<sup>rd</sup> Edition. ([http://www.safeworkaustralia.gov.au/sites/SWA/about/Publications/Documents/238/GuidanceNote\\_InterpretationOfExposureStandardsForAtmosphericContaminants\\_3rdEdition\\_NOHSC3008-1995\\_PDF.pdf](http://www.safeworkaustralia.gov.au/sites/SWA/about/Publications/Documents/238/GuidanceNote_InterpretationOfExposureStandardsForAtmosphericContaminants_3rdEdition_NOHSC3008-1995_PDF.pdf), accessed 8 May 2015).
- Pétron, G., Frost, G., Miller, B. R., Hirsch, A. I., Montzka, S. A., Karion, A., Trainer, M., Sweeney, C., Andrews, A. E., Miller, L., Kofler, J., Bar-Ilan, A., Dlugokencky, E.J., Patrick, L., Moore Jr., C.T., Ryerson, T.B., Siso, C., Kolodzey, W., Lang, P.M., Conway, T., Novelli, P., Masarie, K., Hall, B., Guenther, D., Kitzis, D., Miller, J., Welsh, D., Wolfe, D., Neff, W., Tans, P., 2012. Hydrocarbon emissions characterization in the Colorado Front Range: A pilot study. *Journal of Geophysical Research-Atmospheres*, 117, D04304.
- Phillips, N.G., Ackley, R., Crosson, E.R., Down, A., Hutrya, L., Brondfield, M., Karr, J.D., Zhao, K., Jackson, R.B., 2013. Mapping urban pipeline leaks: methane leaks across Boston. *Environmental Pollution* 173, 1–4.
- Queensland Department of Agriculture, Fisheries and Forestry, 2014. Web-based agricultural land information (WALI). <http://wali.daff.qld.gov.au/>, accessed 10 Nov 2014.
- Queensland EPA, 2004. Air Emissions Inventory: South-east Queensland region. <http://www.qld.gov.au/environment/library/>, accessed 18 Dec 2014.
- Reznikov, A.N., 1969. On the geochemical significance of the n-butane/iso-butane ratio in petroleum gases. *Geol. Nefti Gaza* 4, 43–47.
- Rice, D., 1993. Composition and origins of coalbed gas. In B. Law & D. Rice (Eds.), *Hydrocarbons from coal: AAPG Studies in Geology* (pp. 159–184).
- Rice, D.D., Clayton, J.L., Pawlewicz, M.J., 1989. Characterization of coal-derived hydrocarbons and source-rock potential of coal beds, San Juan Basin, New Mexico and Colorado, USA. *International Journal of Coal Geology* 13, 597–626.



- Scheepmaker, R., Frankenberg, C., 2007. SRON/JPL SCIAMACHY IMAP-DOAS V6 xCH<sub>4</sub>. In: Product specification document, p 6. Netherlands Institute for Space Research, [http://www.temis.nl/climate/docs/TEMIS\\_SCIA\\_CH4\\_IMAPv60\\_PSD\\_v2\\_6.pdf](http://www.temis.nl/climate/docs/TEMIS_SCIA_CH4_IMAPv60_PSD_v2_6.pdf), accessed 15 Dec 2014.
- Schneising, O., Buchwitz, M., Reuter, M., Heymann, J., Bovensmann, H., Burrows, J. P., 2011. Long-term analysis of carbon dioxide and methane column-averaged mole fractions retrieved from SCIAMACHY, *Atmospheric Chemistry and Physics* 11(6), 2863–2880, doi:10.5194/acp-11-2863-2011.
- Schneising, O., Heymann, J., 2012. SCIAMACHY WFM-DOAS (WFMD) carbon dioxide and methane dry air column-averaged mole fractions. Algorithm and product specification pp1-18. Institute for Environmental Physics, University of Bremen.
- Schneising, O., Buchwitz, M., Burrows, J.P., Bovensmann, H., Bergamaschi, P., Peters, W., 2009. Three years of greenhouse gas column-averaged dry air mole fractions retrieved from satellite – Part 2: methane. *Atmospheric Chemistry and Physics* 9, 443-465.
- Schneising, O., Bergamachi, P., Bovensmann, H., Buchwitz, M., Burrows, J.P., Deutscher, N.M., et al., 2012. Atmospheric greenhouse gases retrieved from SCIAMACHY: comparison to ground based FTS measurements and model results. *Atmospheric Chemistry and Physics* 12, 1527-1540.
- Schneising, O., Burrows, J. P., Dickerson, R. R., Buchwitz, M., Reuter, M., Bovensmann H., 2014. Remote sensing of fugitive methane emissions from oil and gas production in North American tight geologic formations. *Earth's Future* 2, 548–558, doi:10.1002/2014EF000265.
- Schoell, M., 1980. The hydrogen and carbon isotopic composition of methane from natural gases of various origins. *Geochimica et Cosmochimica Acta* 44(5), 649–661. doi:10.1016/0016-7037(80)90155-6.
- Schoell, M., 1988. Multiple origins of methane in the earth. *Chemical Geology* 71, 1–10.
- Scott, A.R., Kaiser, W.R., Ayers, W.B., 1994. Thermogenic and Secondary Biogenic Gases, San Juan Basin, Colorado and New Mexico — Implications for Coalbed Gas Producibility. *AAPG Bulletin* 78(8), 1186–1209.
- Sherman, B.S., Ford, P.W., Kernke, M., 2014. Condamine River coal seam gas emissions: final report. CSIRO Australia.
- Smith, J.W., Gould, K.W., Hart, G., Rigby, D., 1985. Isotopic studies of Australian natural and coal seam gases. *Proceedings of the Australasian Institute of Mining and Metallurgy*, 290(6), 42–51.
- Smith, J.W., Pallasser, R.J., 1996. Microbial origin of Australian coalbed methane. *AAPG Bulletin*, 80(6), 891–897. Retrieved from <http://aapgbull.geoscienceworld.org/content/80/6/891.abstract>.
- Stahl, W.J., 1974. Carbon isotope fractionations in natural gases. *Nature* 251, 134–135.
- Stahl, W.J., Carey, B., 1975. Source rock identification by isotope analyses of natural gases from fields in the Val Verde and Delaware basins, West Texas. *Chemical Geology*, 16, 257–267.
- Stahl, W.J., 1977. Carbon and nitrogen isotopes in hydrocarbon research and exploration. *Chemical Geology* 20, 121–149.
- Strapoc D., Mastalerz, M., Dawson, K., Macaladay, J., Callaghan, A.V., Wawrik, B., Turich, C., Ashby, M., 2011. Biogeochemistry of microbial coal-bed methane. *Annual Reviews in Earth and Planetary Science*, 39, 617-656.
- Stopler, D.A., Lawson, M., Davis, C.L., Ferreira, A.A., Santos Neto, E.V., Ellis, G.S., Lewan, M.D., Martini, A.M., Tang, Y., Schoell, M., Sessions, A.L. and Eiler, J.M., 2014. Formation temperatures of thermogenic and biogenic methane. *Science* 344, 15001503–149.
- Tsai, T., Rella, C., Crosson, E., 2013. Quantification of fugitive methane emissions with spatially correlated measurements collected with novel plume camera. *Geophysical Research Abstracts* Vol. 15, EGU2013-11020, 2013. EGU General Assembly 2013.

- Valentine, D.L., 2004. Emerging topics in marine methane biogeochemistry. *Annual Reviews in Marine Science*, 3, 147-171.
- Valentine, D.L., Chidthaisong, A., Rice, A., Reeburgh, W.S., Tyler, S.C., 2004. Carbon and hydrogen isotope fractionation by moderately thermophilic methanogens. *Geochimica et Cosmochimica Acta* 68(7), 1571–1590.
- Wang, Y-P., Bentley, S.T., 2002. Development of a spatially explicit inventory of methane emissions from Australia and its verification using atmospheric concentration data. *Atmospheric Environment* 36, 4965–4975.
- Whiticar, M.J., 1994. Correlation of natural gases with their sources. In L. Magoon & W. Dow (Eds.), *The Petroleum System — From Source to Trap* (pp. 261–284). AAPG.
- Whiticar, M.J., 1999. Carbon and hydrogen isotope systematics of bacterial formation and oxidation of methane. *Chemical Geology* 161, 291–314.
- Whiticar, M.J., Faber, E., Schoell, M., 1986. Biogenic methane formation in marine and freshwater environments: CO<sub>2</sub> reduction vs. acetate fermentation- isotope evidence. *Geochimica et Cosmochimica Acta*, 50, 693–709.
- Williams, D.J., Saghafi, A., Lange, A.L., Drummond, M.S., 1993. Methane emissions from open-cut mines and post-mining emissions from underground coal. CSIRO Investigation Report CET/IR173, CSIRO Australia.
- Wilson, P., Feitz, A., Jenkins, C., Berko, H., Loh, Z., Luhar, A., Hibberd, M., Spencer, D., and Etheridge, D., 2014. Sensitivity of CO<sub>2</sub> leak detection using a single atmospheric station, *Energy Procedia*, in press.
- World Data Center for Greenhouse Gases, 2015 <http://ds.data.jma.go.jp/gmd/wdcgg/cgi-bin/wdcgg/accessdata.cgi?index=CFA519S00-CSIRO&select=inventory>.

# Appendix

ALMA Airborne Methane Gas Detection Trial, July 2014. Report prepared by Skyline Sensing.

ALMA Survey  
Chinchilla QLD

Skyline Sensing Job 5681  
31/07/2014 Rev 1.0

## **ALMA Airborne Methane Gas Detection Trial**



**Chinchilla Queensland**

**Job 5681**

**for CSIRO**

**SKYLINE**  
S E N S I N G

Unit 4,339 Hillsborough Rd  
WARNERS BAY, NSW, 2282  
(0427) 01 4002  
[www.skylinesensing.com](http://www.skylinesensing.com)  
ACN: 169352381  
AOC: 528 994



#### CONTACT US

**t** 1300 363 400  
+61 3 9545 2176  
**e** [enquiries@csiro.au](mailto:enquiries@csiro.au)  
**w** [www.csiro.au](http://www.csiro.au)

#### YOUR CSIRO

Australia is founding its future on science and innovation. Its national science agency, CSIRO, is a powerhouse of ideas, technologies and skills for building prosperity, growth, health and sustainability. It serves governments, industries, business and communities across the nation.

#### FOR FURTHER INFORMATION

**Division/Unit Name**

Jonathan Bates

**t** +61 3 9123 4567

**e** [jonathan.bates@csiro.au](mailto:jonathan.bates@csiro.au)

**w** [www.csiro.au/businessunit-flagshipname](http://www.csiro.au/businessunit-flagshipname)